Optical Tweezers on Nanostructures

Onofrio M. MARAGÒ

CNR-IPCF, Istituto per i Processi Chimico-Fisici, Messina, Italy

onofrio.marago@cnr.it

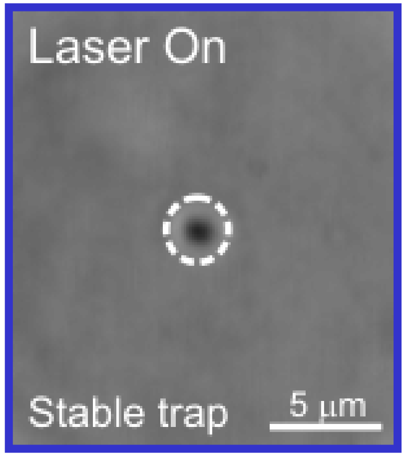

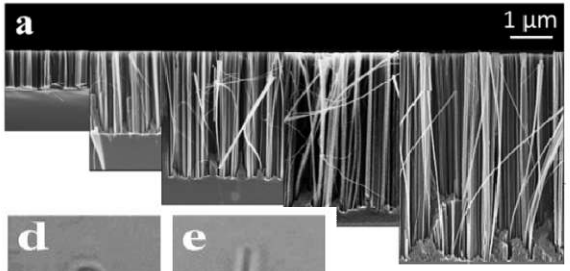

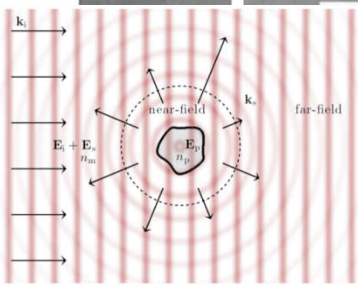

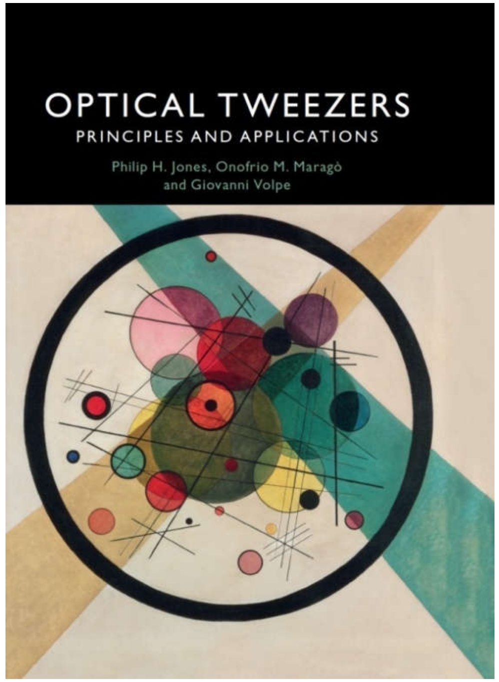


CNR-IPCF Messina

Optical Tweezers People – Messina 2018

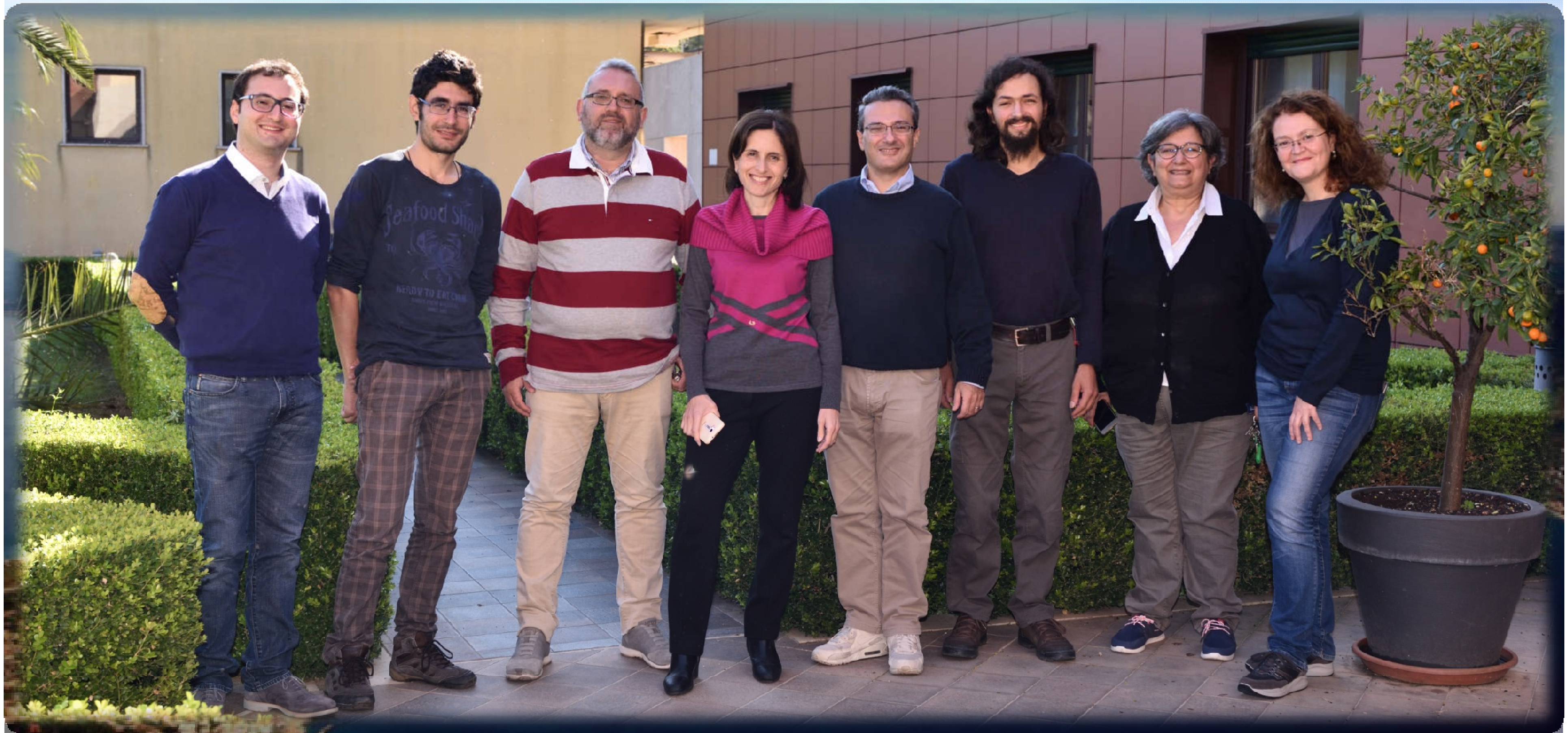

P. Polimeno (PhD Student), **F. Patti** (PhD Student), **P. G. Gucciardi** (CNR), **M. A. Iatì** (CNR), **O. M. Maragò** (CNR), **R. Gillibert** (Post-Doc), **R. Saija** (UniMe), **M.G. Donato** (CNR)

Past members: A. Magazzù, A. Foti, D. Spadaro, S. Vasi, E. Messina, C. D'Andrea, R. Sayed, M. Monaca

Acknowledgements

COLLABORATIONS

P. H. Jones (UCL)

Giovanni Volpe (Uni.Gothenbourg)

B. Fazio (CNR-IPCF.)

A. Irrera (CNR-IPCF)

A. Camposeo (CNR-NANO)

L. Persano (CNR-NANO)

D. Pisignano (Univ. Pisa)

A. C. Ferrari (Univ. Cambridge)

V. Amendola (Univ. Padova)

J. J. Saenz (DIPC, San Sebastian)

P. Zemanek (ISI-CAS, Brno)

G. Strangi (CASE Univ., Cleveland)

G. Cipparrone (Univ. Calabria)

A. Neves (Univ. ABC, Brasil)

G. Pesce (Univ. Napoli)

A. Veltri (USFQ, Quito)

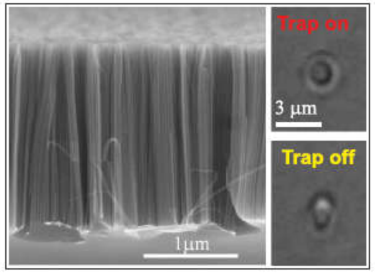

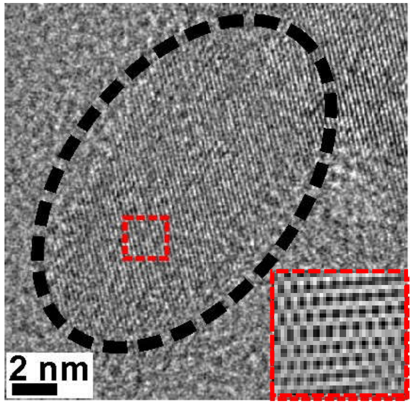

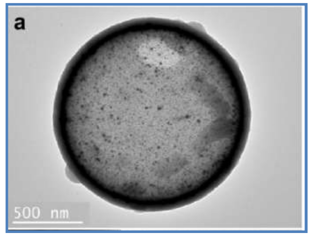

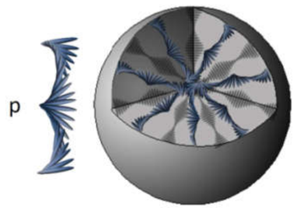

PON Ricerca e Competitività 2007-2013

Ifremer

THE ROYAL SOCIETY

nanoantenna

cost

Outline

- **General introduction**

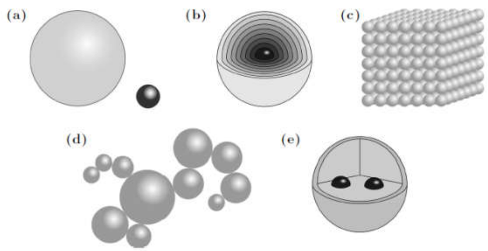

- **Theory background**
  - *T-matrix methods*

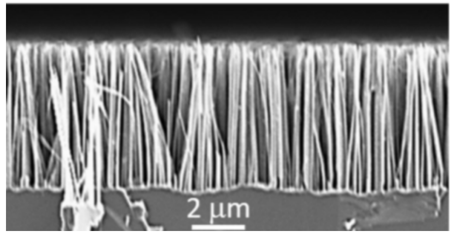

- **Experimental practice**

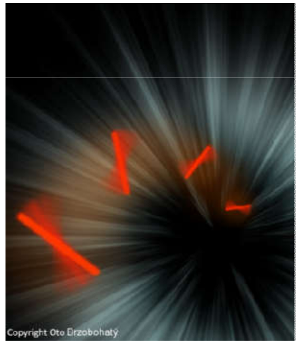

- **Linear nanostructures**
  - *Scaling, Binding & rotational dynamics*
  - *Air and vacuum*

- **Layered materials**
- **SERS Tweezers**

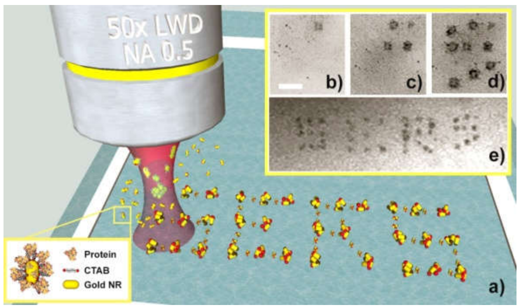

Light Moves Matter

- **J Kepler (1610)**
  comet tails are the result of light pressure

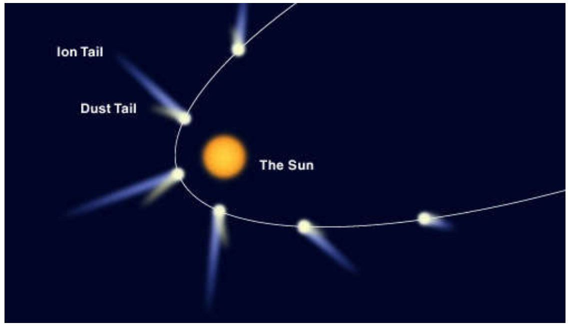

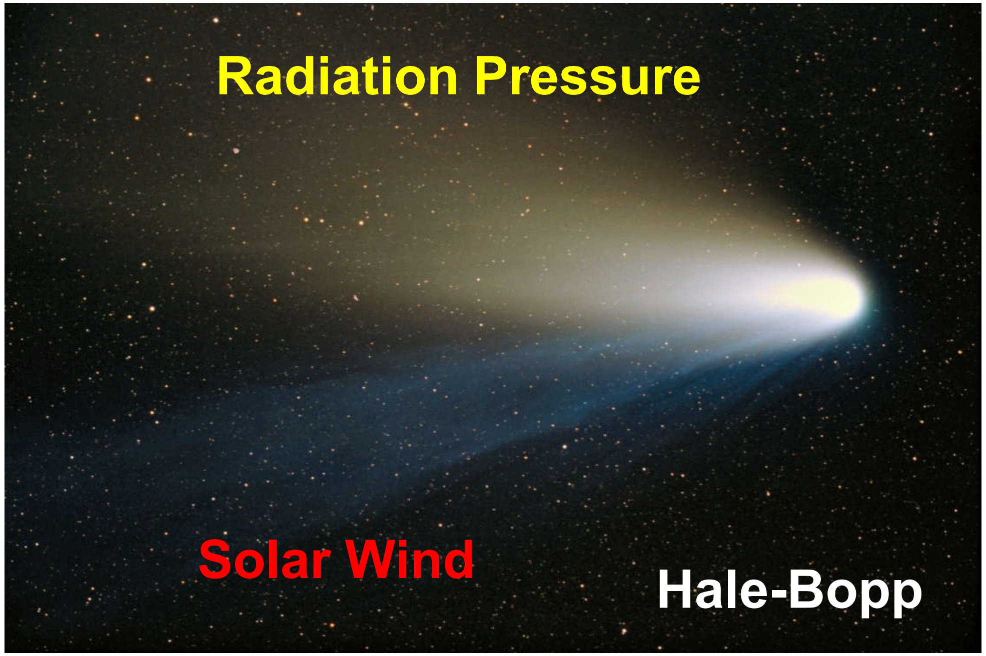

- **J C Maxwell (1864)**
  light pressure is explained in electromagnetic theory
- **P Lebedev (1901) and Nichols & Hull (1901)**
  measures light pressure for the first time
- **A Ashkin, T Haensch & A Schawlow, V Lethokov (1970s)**
  first proposals to manipulate atoms and microparticles, laser cooling
- **A Ashkin & S Chu (1986)**
  at Bell Laboratories moves and traps latex spheres suspended in water using a focused laser beam. Optical Tweezers are born!

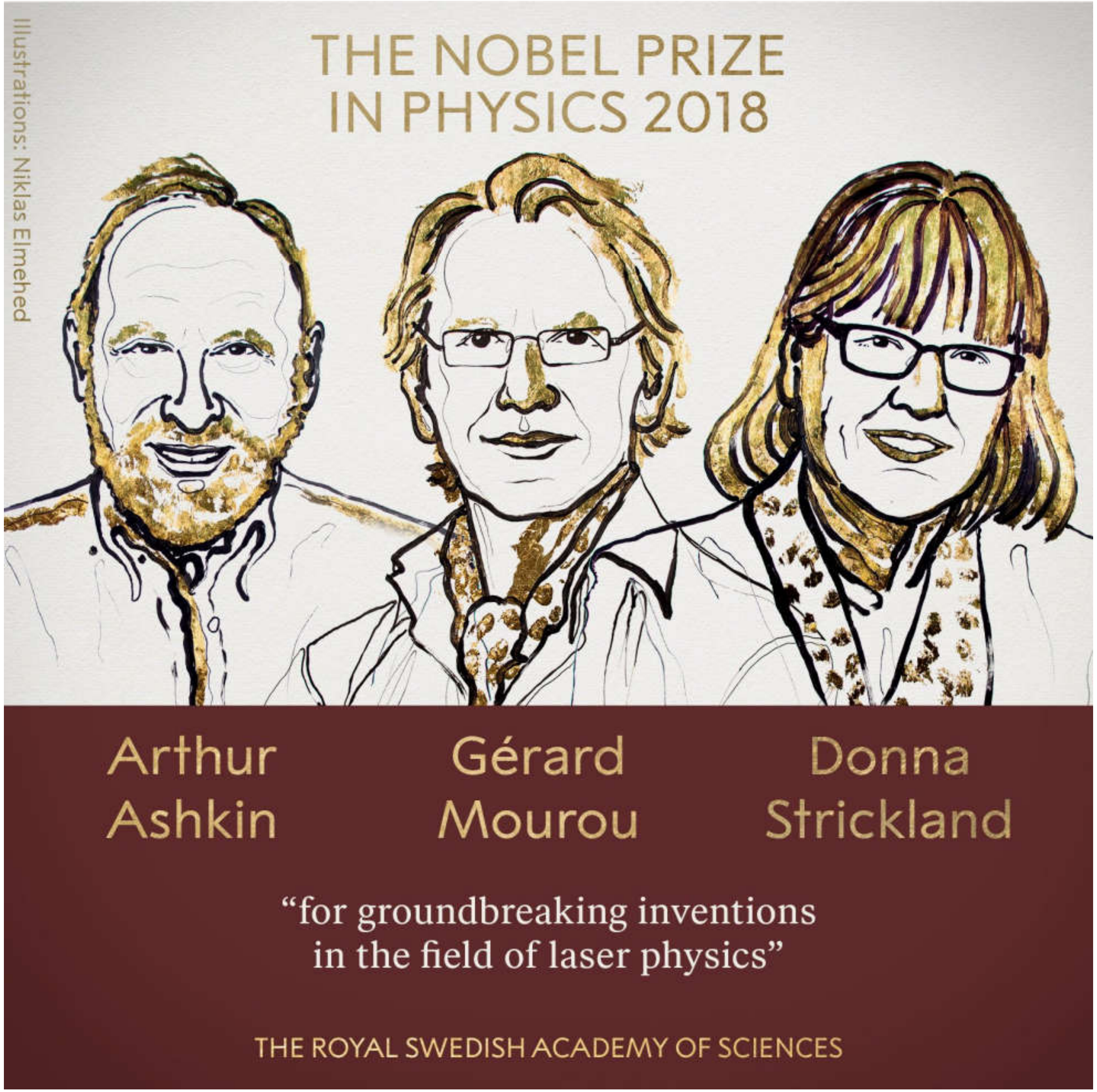
Illustrations: Niklas Elmehed
THE NOBEL PRIZE
IN PHYSICS 2018
Arthur
Ashkin
Gérard
Mourou
Donna
Strickland
“for groundbreaking inventions
in the field of laser physics”
THE ROYAL SWEDISH ACADEMY OF SCIENCES

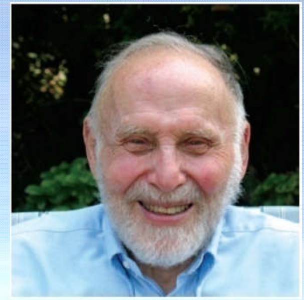

Celebrations for Arthur Ashkin's Nobel prize 2018

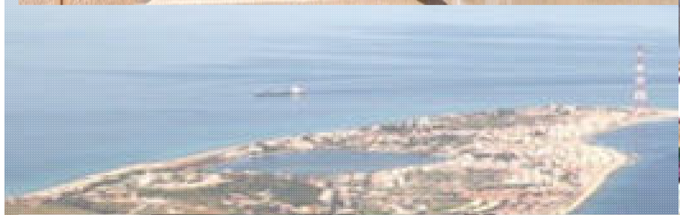

Optical Trapping at the Nanoscale

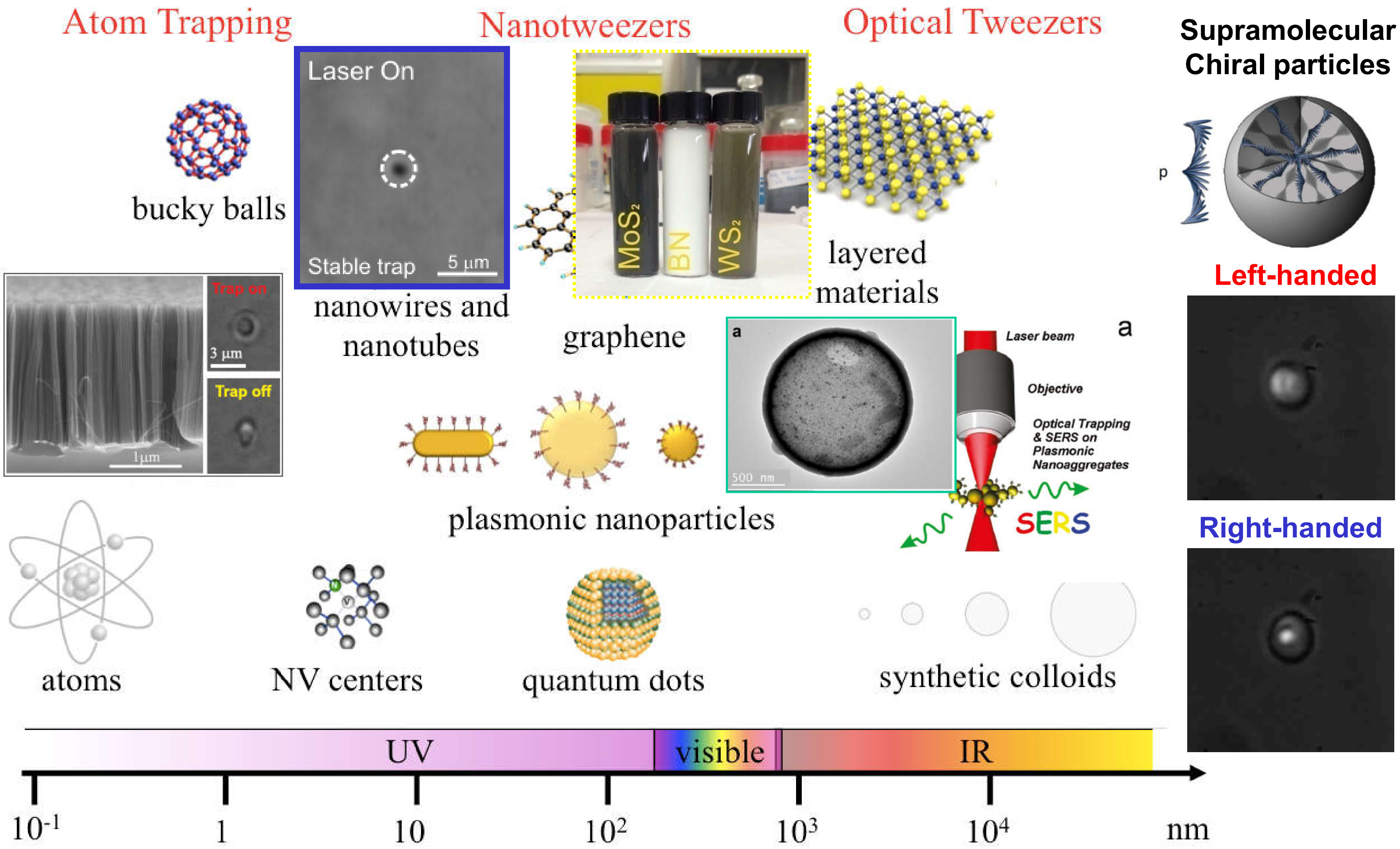

Maragò, Jones, Gucciardi, Volpe, Ferrari. *Nature Nanotechnology* **8**, 807–819 (2013)

Optical Trapping Theory

Optical trapping of particles is a consequence of the radiation force that stems from the **conservation of electromagnetic momentum in light scattering**.

Ray Optics, d/λ >> 1

- Trapping forces from **reflection and refraction** of rays
- Forces proportional to gradient of intensity
  (Ashkin, Biophys. J. 61, 569, 1992)

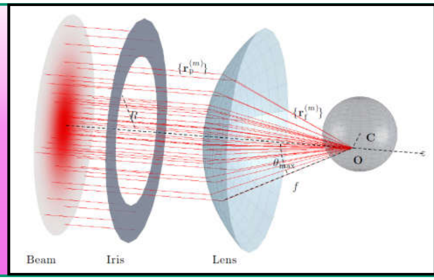

Dipole Approximation, d/λ << 1

- Three parts: **gradient force**, scattering force
  (Ashkin, et al. Optics Lett. 11, 288, 1986)

$$U_{\mathrm{dip}} = -\underline{p} \cdot \underline{E}$$
$$\underline{F}_{\mathrm{grad}} = -\underline{\nabla} U_{\mathrm{dip}}$$
$$\propto \underline{\nabla} I(\underline{r}) = -\kappa_i x_i$$

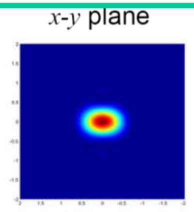

Complex Region, d/λ ≈ 1

- Full electromagnetic Theory (**Maxwell ST**)
- Make use of **T-Matrix methods** for force & torque
- **Angular spectrum representation**

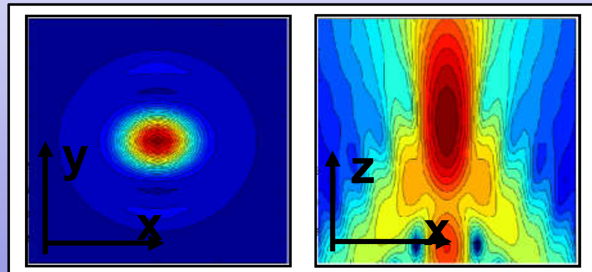

Extension to complex non-spherical particles

$$\mathbf{F}_{\mathrm{Rad}} = r'^2 \int_{\Omega'} \hat{\mathbf{r}}' \cdot \langle \mathsf{T}_{\mathrm{M}} \rangle \, d\Omega'$$

Borghese, Denti, Saija, Springer (2007)
Borghese et al., Optics Express (2007)
Borghese et al., Phys Rev Lett (2008)
Saija et al., Opt. Express (2009) …

Nieminen&Rubinsztein-Dunlop,Gousbet,Neves,Hanna,Zemanek,…

Optical Tweezers - Ray Optics

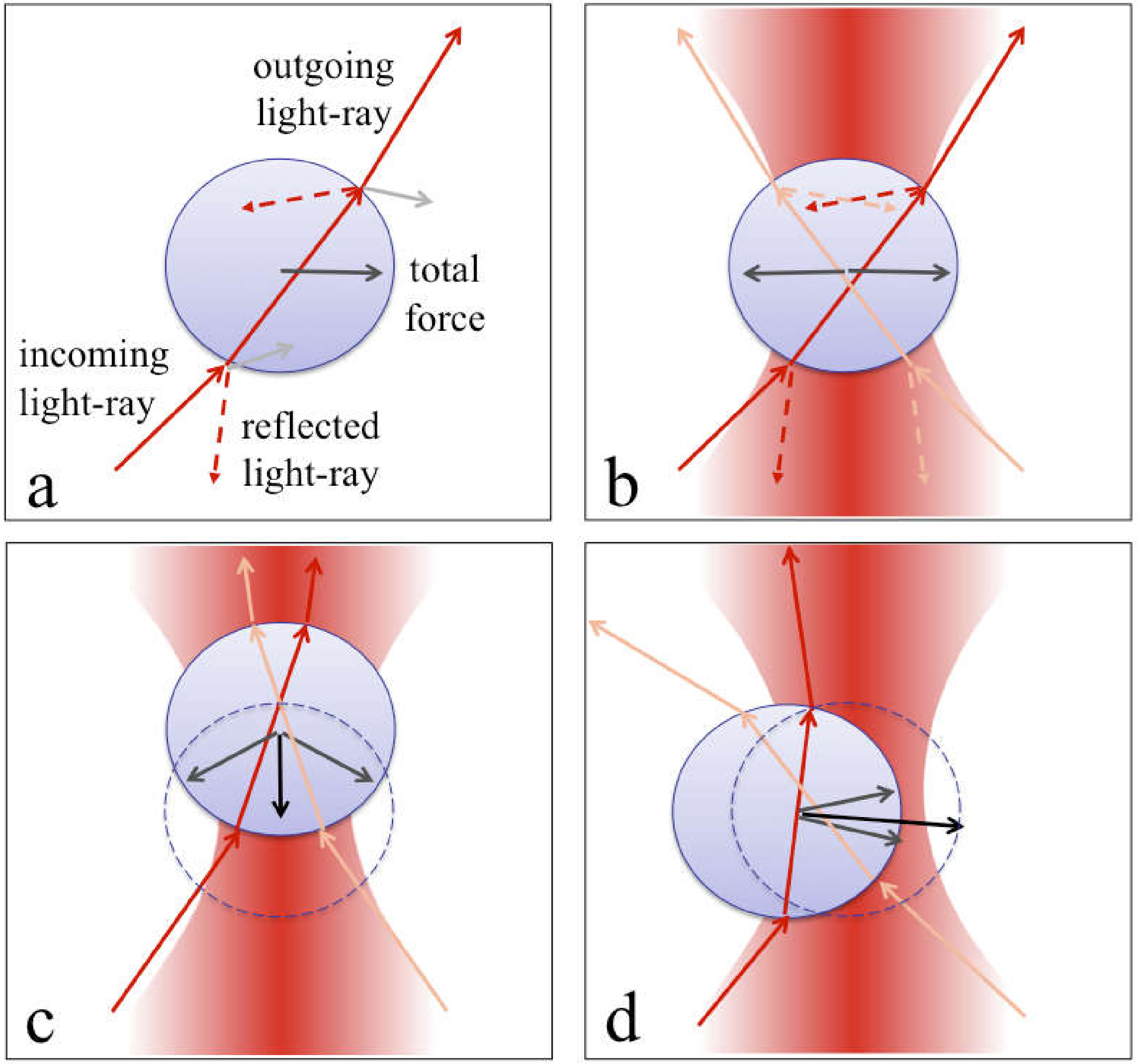

Microsphere acts as a lens for the refracted and reflected rays

Linear momentum exchange from light to particle, push towards beam center ($n_p > n_m$)

Trapping Force is proportional to the <u>gradient of light intensity</u>

Scattering force is proportional to light intensity and <u>directed as the Poynting vector</u>

$$\mathbf{F} = \sum_m \mathbf{F}^{(m)} = \sum_m \left[\frac{P_{\mathrm{i}}^{(m)}}{c_{\mathrm{i}}} \hat{\mathbf{u}}_{\mathrm{i}}^{(m)} - \frac{P_{\mathrm{r}}^{(m)}}{c_{\mathrm{i}}} \hat{\mathbf{u}}_{\mathrm{r},0}^{(m)} - \sum_{n=1}^{+\infty} \frac{P_{\mathrm{t},n}^{(m)}}{c_{\mathrm{i}}} \hat{\mathbf{u}}_{\mathrm{t},n}^{(m)} \right]$$

Dynamics of a spheroid in a double trap

G. Volpe

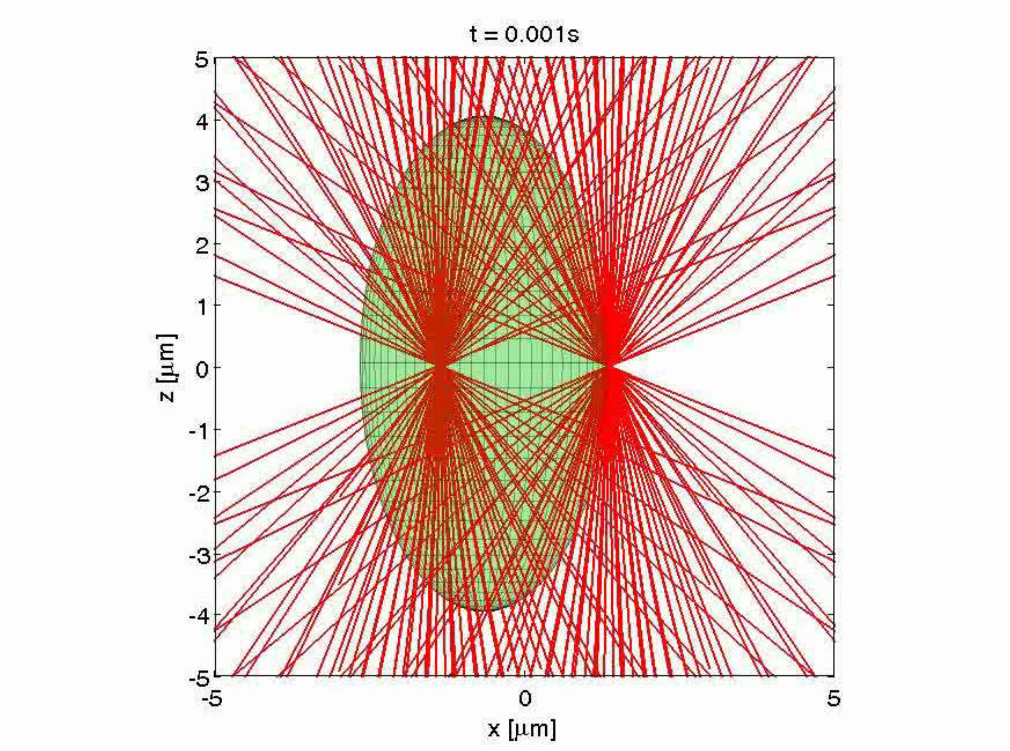

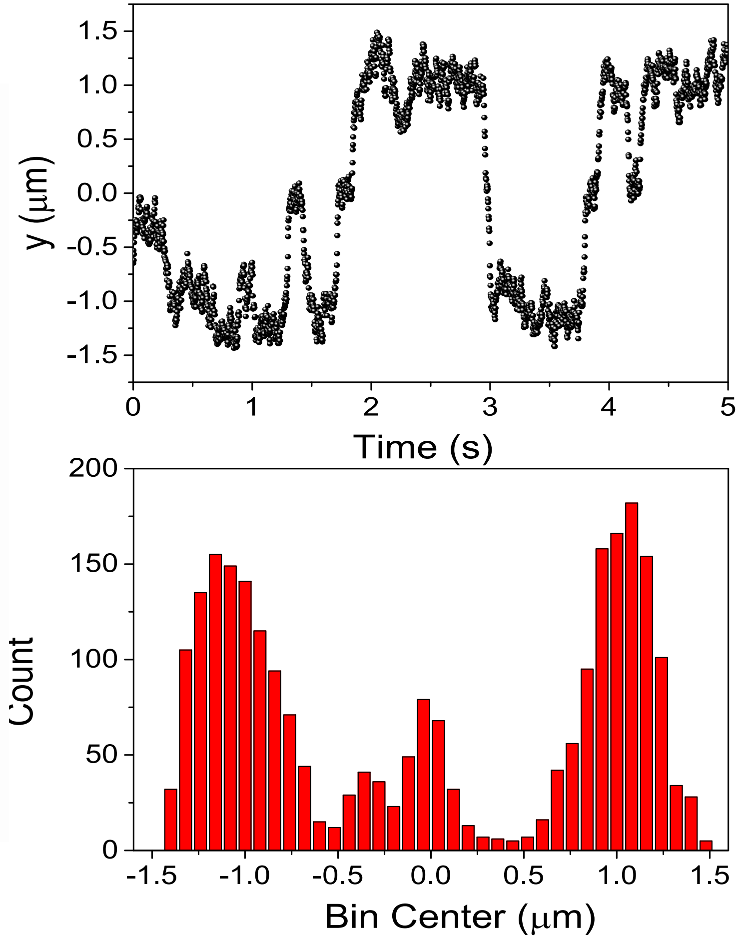

Diffusion Matrix Modeling for complex particles using Hydro++

G. Volpe & G. Volpe American Journal of Physics **81**, 224 (2013).
A. Callegari, M. Mijalkov, et al. JOSA B **32**, B11-B19 (2015)
A. Stilgoe et al., Phys. Rev. Lett. **107**, 248101 (2011).

By Magazzù, Callegari

Optical Tweezers – Dipole

Interaction of electric field of laser with induced dipole in dielectric $U = -\underline{p} \cdot \underline{E} = -\alpha |E|^2$

Average force on particle $\langle \mathbf{F} \rangle = \frac{1}{2} \mathrm{Re} \left(\sum_i \alpha E_i \nabla E_i^* \right)$

For a Gaussian beam breaks in two contributions

$$F_{\text{scatt}} = \hbar k \frac{\Gamma}{2} \frac{I/I_{\text{sat}}}{1 + I/I_{\text{sat}} + 4\delta^2/\Gamma^2}$$

$$F_{\text{dipole}} = -\frac{\hbar\delta}{2} \frac{\nabla(I/I_{\text{sat}})}{1 + I/I_{\text{sat}} + 4\delta^2/\Gamma^2}$$

$$F_{scat}(r) = \frac{n\sigma_{ext}}{c} I(r)$$

$$F_{grad}(r) = \frac{n\,\mathrm{Re}\{\alpha(\omega)\}}{2c\varepsilon} \nabla I(r)$$

The (harmonic) trapping potential is defined by the incident light intensity

BEC

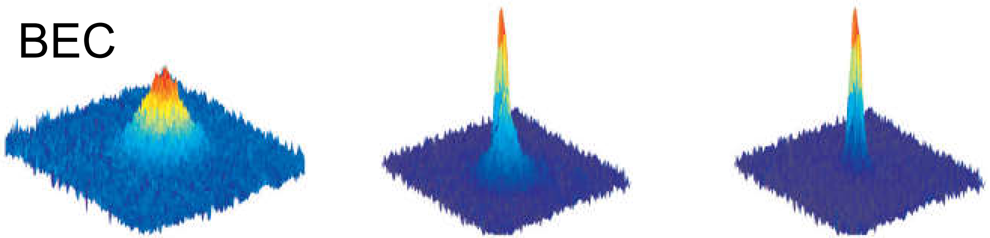

O. M. Maragò, Dphil Thesis, Oxford (2001)

$$U_{\text{dip}} = -\underline{p} \cdot \underline{E}$$
$$\underline{F}_{\text{grad}} = -\underline{\nabla} U_{\text{dip}}$$
$$\propto \underline{\nabla} I(\underline{r}) = -\kappa_i x_i$$

x-*y* plane

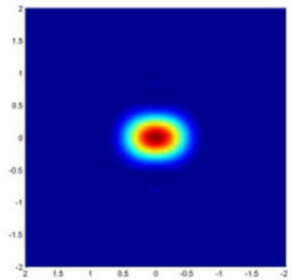

Optical response of colloidal metal nanoparticles

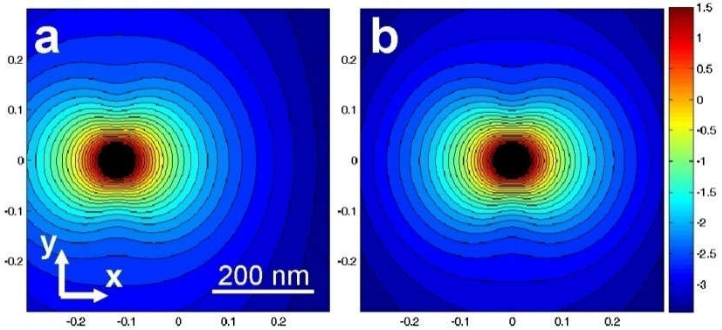

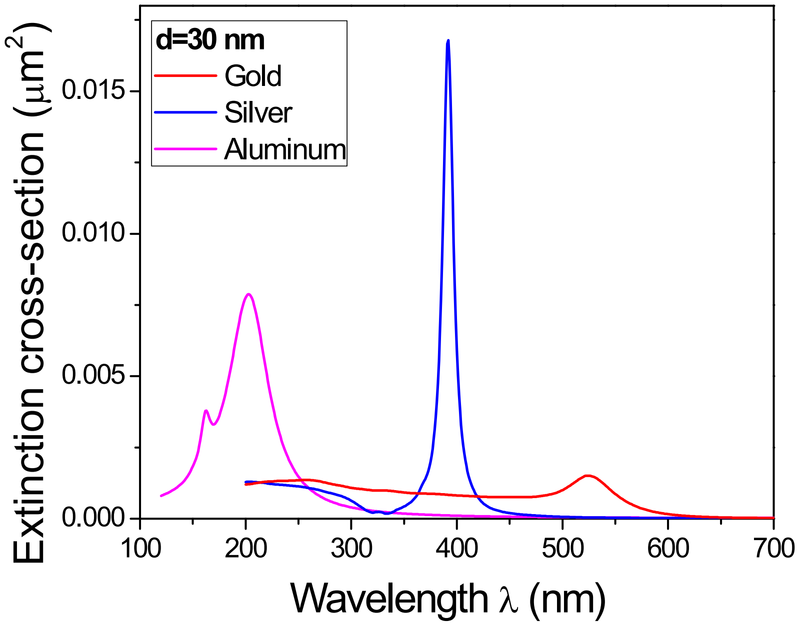

Amendola, V., et al. (2017). Surface plasmon resonance in gold nanoparticles: a review. *J. Phys.: Cond. Matt.*, ***29***, 203002.

For **metal nanoparticles**, the presence of **plasmon resonances** leads to their optical trapping with a wavelength in the **red side** of the spectrum.

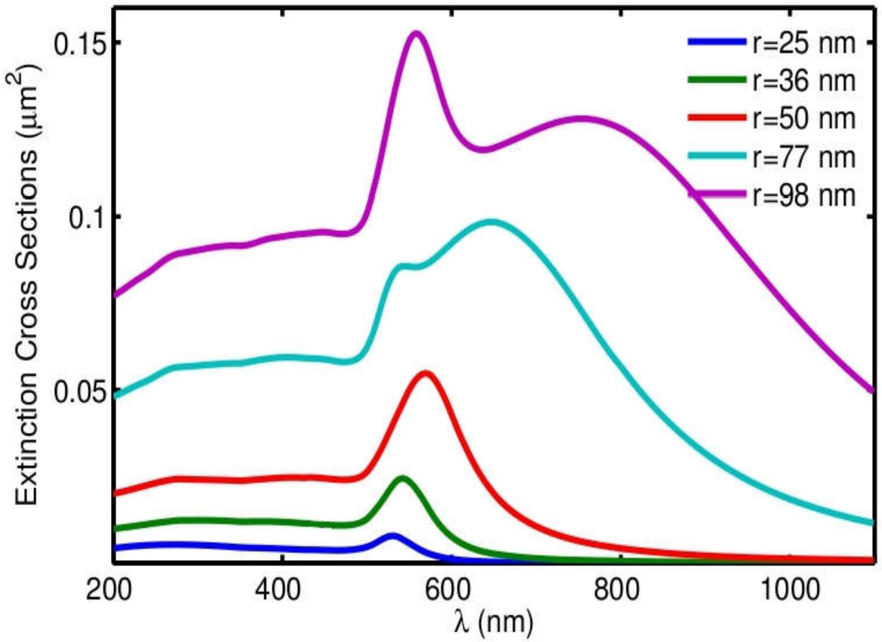

Saija R et al. Optics Express (2009)

Jones et al., ACS Nano (2009) – **Au Nanorods**

Messina et al., Optics Express (2015) – **Ag Platelets**

Optical trapping of plasmonic particles (dipole picture)

Lorentz-Drude model for dielectric constant using tabulated fit parameters that agrees well with experimental data and exploit plasmon resonance to enhance optical forces

$$\varepsilon(\omega) = \varepsilon_\infty + \sum_{k=1}^{K} \frac{f_k \omega_p^2}{\omega_k^2 - \omega^2 + i\omega\Gamma_k}$$

$$\boxed{\alpha(\omega) = 4\pi\varepsilon_0 a^3 \frac{\varepsilon_1(\omega) - \varepsilon_2}{\varepsilon_1(\omega) + 2\varepsilon_2}}$$

$$\sigma_{abs} = \frac{k}{\varepsilon_0} \operatorname{Im}\{\alpha(\omega)\}; \quad \sigma_{scat} = \frac{k^4}{6\pi\varepsilon_0^2} |\alpha(\omega)|^2$$

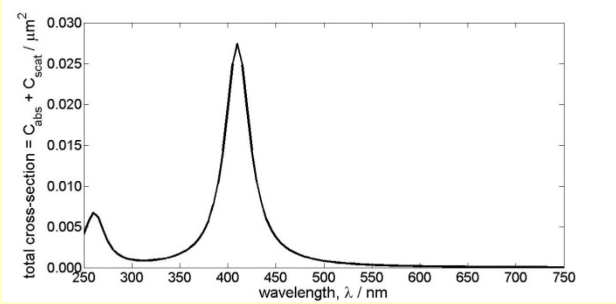

$$F_{scat}(r) = \frac{n\sigma_{ext}}{c} I(r)$$

$$F_{grad} = \frac{n}{2} \frac{\operatorname{Re}\{\alpha(\omega)\}}{c\varepsilon_0} \nabla I(r)$$

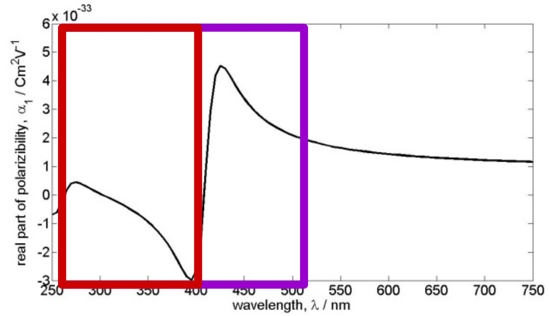

Trap Stiffness proportional to Re{$\alpha(\omega)$}

Trapped resonant gain metal/dielectric nanoshell

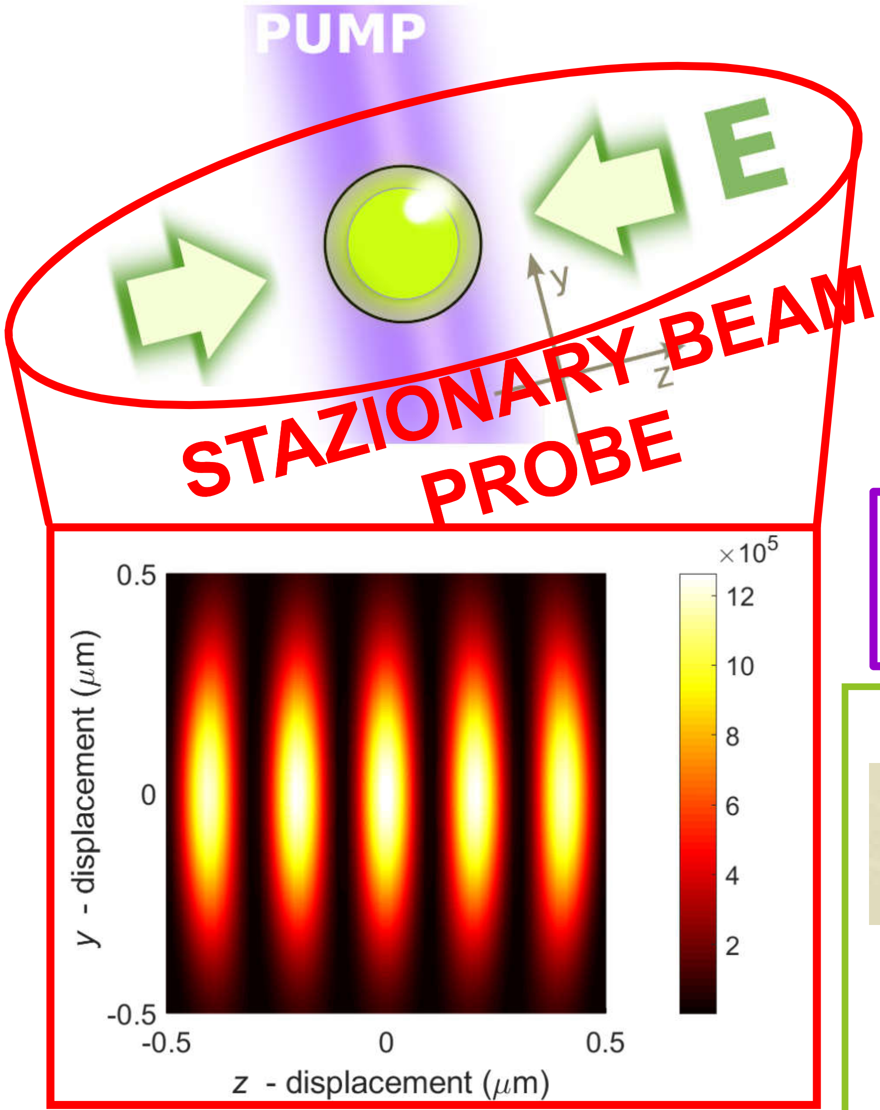

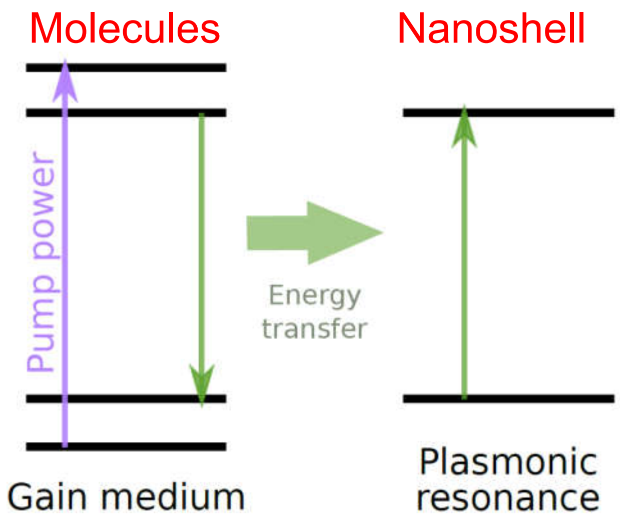

Silver nanoshell with externally **pumped optical gain material** on its core excited by an external electric field.

Steady State Gain dielectric permittivity

$$\varepsilon_1 = \varepsilon_b - \frac{G\Delta}{2(\omega - \omega_{21}) + i\Delta} \qquad \Delta = \frac{2}{\tau_2}$$

ε_b dielectric host permittivity

$$G = \Im[\varepsilon_1(\omega_{21})] = -\frac{n\mu^2\tau_2}{3\hbar\varepsilon_0}\tilde{N}$$

P. Polimeno, A. Veltri, submitted

Brownian Dynamics Simulation

G. Volpe and G. Volpe,
Am. J. Phys. (2013)

$$\frac{d}{dt}r(t) = -\frac{1}{\gamma}\frac{d}{dr}U(r) + \xi(t)$$

Overdamped Langevin equation

Integrating

$$\begin{cases} x_i = x_{i-1} - \dfrac{\kappa_x}{\gamma} x_{i-1}\Delta t + \sqrt{2D\Delta t}\, w_{x,i} \\ y_i = y_{i-1} - \dfrac{\kappa_y}{\gamma} y_{i-1}\Delta t + \sqrt{2D\Delta t}\, w_{y,i} \\ z_i = z_{i-1} - \dfrac{\kappa_z}{\gamma} z_{i-1}\Delta t + \sqrt{2D\Delta t}\, w_{z,i} \end{cases}$$

***P* = 20 mW**
***t* = 1 ms**
***Δt* = 2 ns**

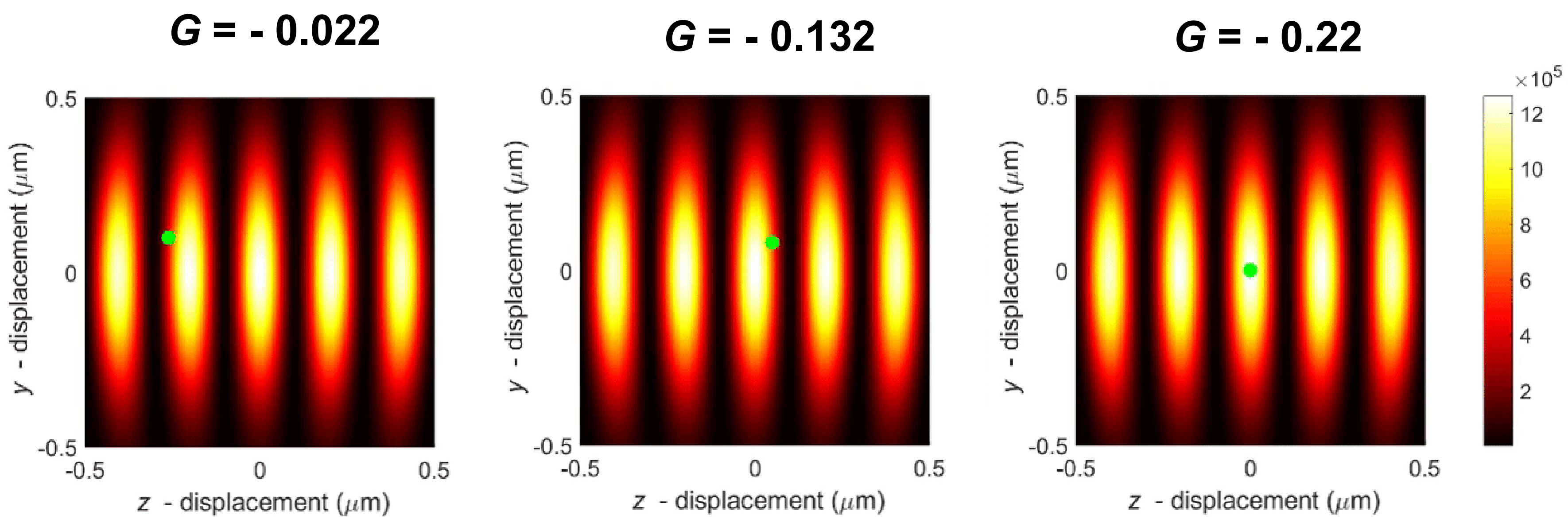

P. Polimeno, A. Veltri, submitted

Optomechanical Position Locking and Channelling

G = - 0,22
P = 20 mW
t = 1 ms
Δt = 2 ns

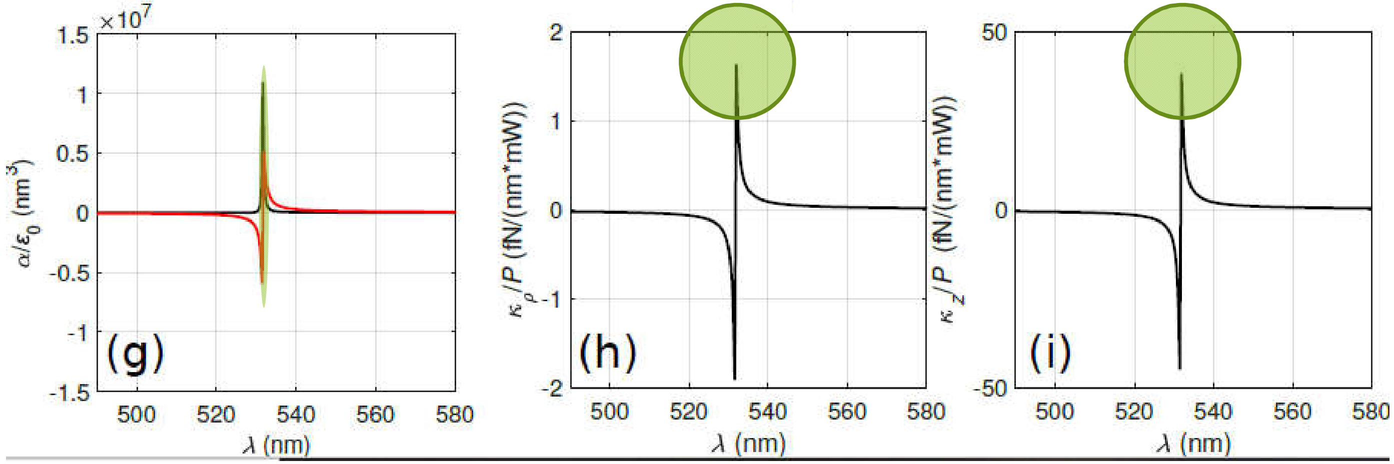

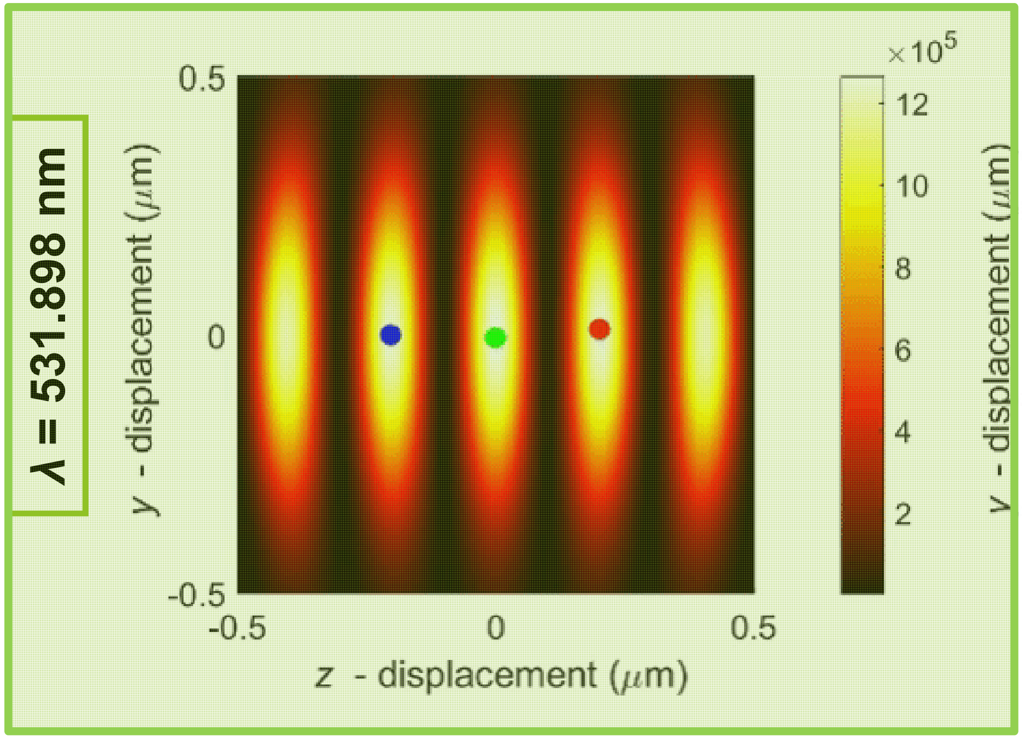

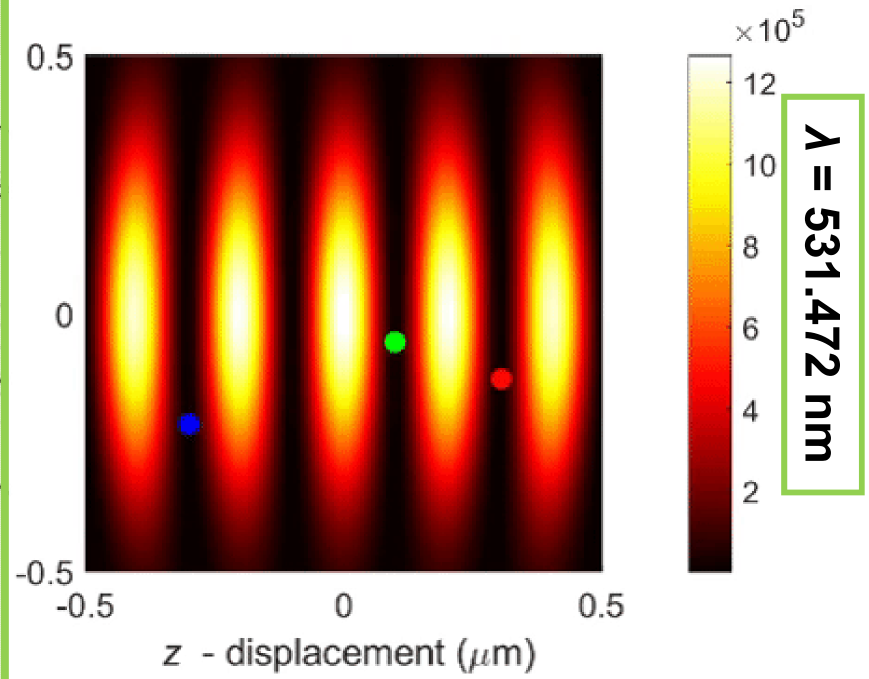

P. Polimeno, A. Veltri, submitted

OT & Light Scattering Theory

Optical trapping of particles is a consequence of the **conservation of electromagnetic momentum** and the **spatial redistribution of photons** in light scattering.

Mesoscopic Region, d/λ ≈ 1

- Full electromagnetic Theory
- Vector character of laser field
- Make use of Transition-Matrix approach
- Extension to non-spherical particles!

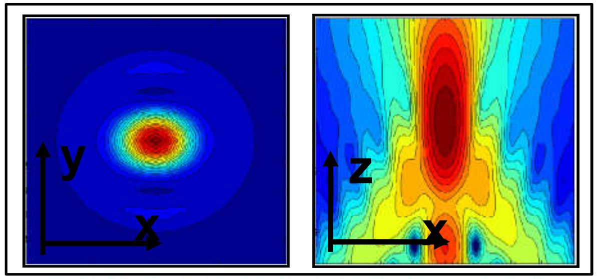

d/λ ≈ 1

Incident field E_i (plane wave)

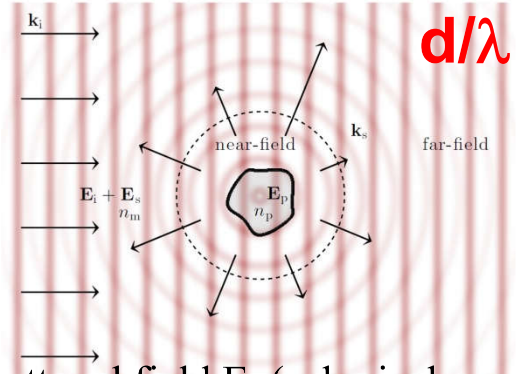

Scattered field E_s (spherical wave)

$\mathbf{E}_t = \mathbf{E}_i + \mathbf{E}_s$

Conservation of linear momentum

$$\left\langle \frac{d\mathbf{P}_{Mech}}{dt} \right\rangle = \mathbf{F}_{Rad} = \oint_S \hat{\mathbf{n}} \cdot \langle T_M \rangle dS$$

Conservation of angular momentum

$$\left\langle \frac{d\mathrm{L}_{Mech}}{dt} \right\rangle = \Gamma_{Rad} = -\oint_S \hat{\mathrm{n}} \cdot \langle T_M \rangle \times \hat{\mathrm{n}} dS$$

Averaged Maxwell stress tensor

$$\langle T_M \rangle = \frac{1}{2} \varepsilon_m \Re \left\{ \mathbf{E}_t \otimes \mathbf{E}_t^* + \frac{c^2}{n_m^2} \mathbf{B}_t \otimes \mathbf{B}_t^* - \frac{1}{2} \left(|\mathbf{E}_t|^2 + \frac{c^2}{n_m^2} |\mathbf{B}_t|^2 \right) \mathbf{I} \right\}$$

Nieminen, JQSRT (2003-2016); Singer et al., PR E (2006); Borghese, Opt. Express (2007); Borghese, Phys Rev Lett (2008); Saija,et al., Opt. Express (2009); Bareil & Sheng, Opt. Express (2010); Simpson & Hanna, PR E (2010); Simpson, JQSRT (2016);...

Special case: Mie Scattering

$$\begin{cases} a_l = -\dfrac{A^{(2)}_{\mathrm{s},lm}}{W^{(2)}_{\mathrm{i},lm}} \\[2ex] b_l = -\dfrac{A^{(1)}_{\mathrm{s},lm}}{W^{(1)}_{\mathrm{i},lm}} \end{cases}$$

Boundary conditions on a sphere
Only l-dependence
T-matrix is **diagonal**

Radiation pressure (plane wave)

$$\mathbf{F}^{\parallel}_{\mathrm{rad}} = \frac{n_{\mathrm{m}}}{c} I_{\mathrm{i}} \left[\sigma_{\mathrm{ext}} - g_{\mathrm{i}}\sigma_{\mathrm{scat}}\right] \hat{\mathbf{k}}_{\mathrm{i}}$$

Debye (1909), Mishchenko (2001)

$$\sigma_{\mathrm{ext}} = \frac{2\pi}{k_{\mathrm{m}}^2} \sum_{l=1}^{\infty} (2l+1) \mathrm{Re}\left\{a_l + b_l\right\}$$

$$\sigma_{\mathrm{scat}} = \frac{2\pi}{k_{\mathrm{m}}^2} \sum_{l=1}^{\infty} (2l+1) \left(|a_l|^2 + |b_l|^2\right)$$

$$g_{\mathrm{i}} = \frac{4\pi}{\sigma_{\mathrm{scat}} k_{\mathrm{m}}^2} \mathrm{Re}\left\{\sum_{l=1}^{+\infty}\left[\frac{l(l+2)}{l+1}(a_l a^*_{l+1} + b_l b^*_{l+1}) + \frac{2l+1}{l(l+1)} a_l b^*_l\right]\right\}$$

Observables can be obtained from the Mie coefficients

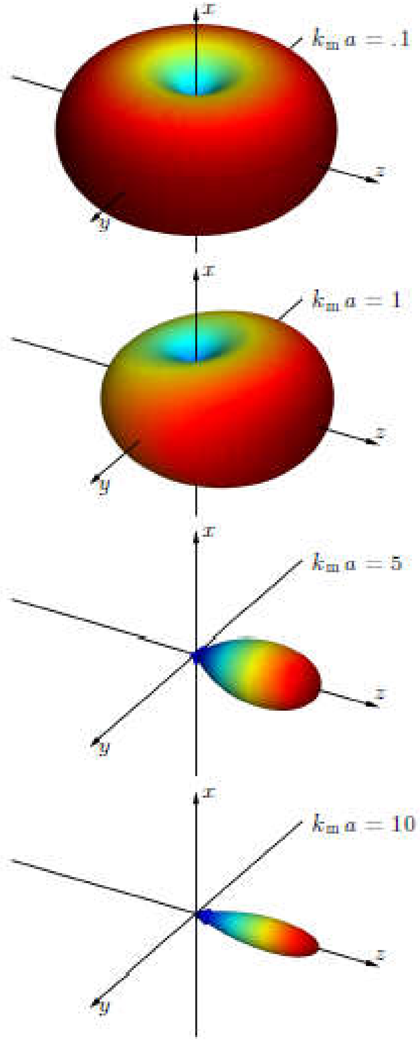

Jones, Maragò, Volpe, "Optical Tweezers", CUP (2015)

T-matrix & Brownian dynamics
Modelling feedback cooling

Cooling in phase-space (feedback on x)

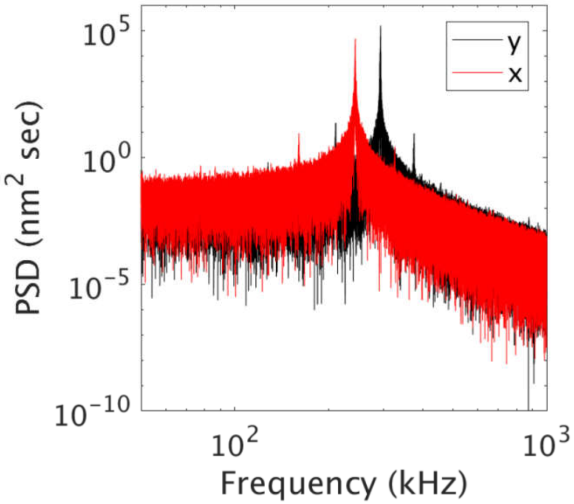

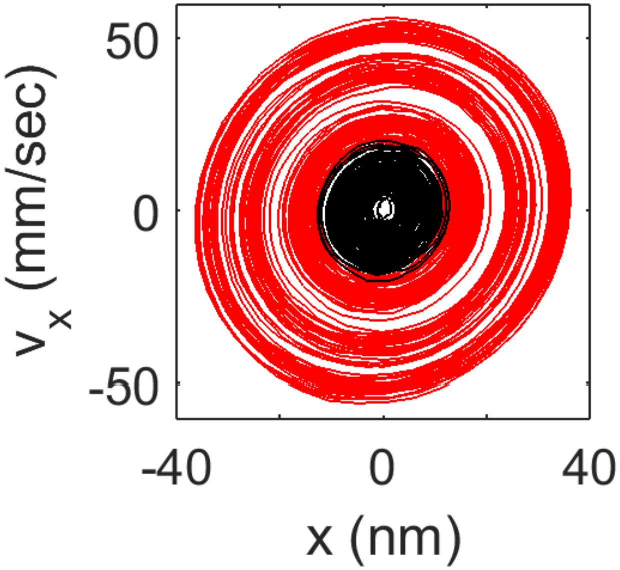

Feedback off-on

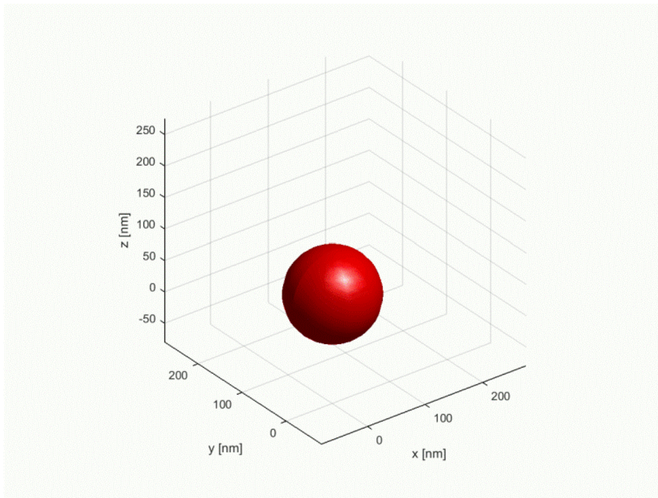

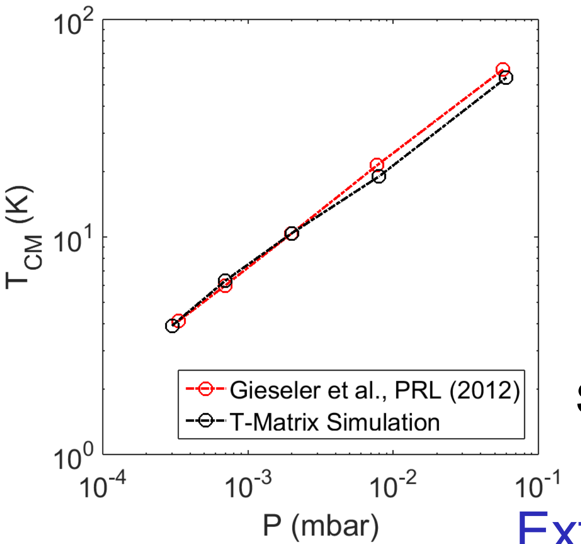

$$F_{FB} = \beta \frac{r v_r}{\langle r \rangle_{\beta=0} \langle v_r \rangle_{\beta=0}} F_x$$

See also Levi et al. Cont. Phys. (2014)

Extension to non-spherical particles

Mechanical effects on non-spherical particles

Radiation Pressure
Transverse Force

} Conservation of **linear momentum**

$$\mathbf{F}^{\parallel}_{\mathrm{rad}} = \frac{n_{\mathrm{m}}}{c} I_{\mathrm{i}} \left[\sigma_{\mathrm{ext}} - g_{\mathrm{i}}\sigma_{\mathrm{scat}}\right] \hat{\mathbf{k}}_{\mathrm{i}} = \frac{n_{\mathrm{m}}}{c} I_{\mathrm{i}} \sigma_{\mathrm{rad}} \hat{\mathbf{k}}_{\mathrm{i}}$$

$$\mathbf{F}^{\perp}_{\mathrm{rad}} = -\frac{n_{\mathrm{m}}}{c} I_{\mathrm{i}}\, g_1 \sigma_{\mathrm{scat}} \hat{\mathbf{u}}_1 - \frac{n_{\mathrm{m}}}{c} I_{\mathrm{i}}\, g_2\, \sigma_{\mathrm{scat}} \hat{\mathbf{u}}_2$$

$$g_{\mathrm{i}} = \frac{1}{\sigma_{\mathrm{scat}}} \oint_{\Omega} \frac{d\sigma_{\mathrm{scat}}}{d\Omega} \hat{\mathbf{r}} \cdot \hat{\mathbf{k}}_{\mathrm{i}}\, d\Omega$$

Radiation Torque $\longrightarrow$ Conservation of **angular momentum**

Saija et al, MNRAS, 2003

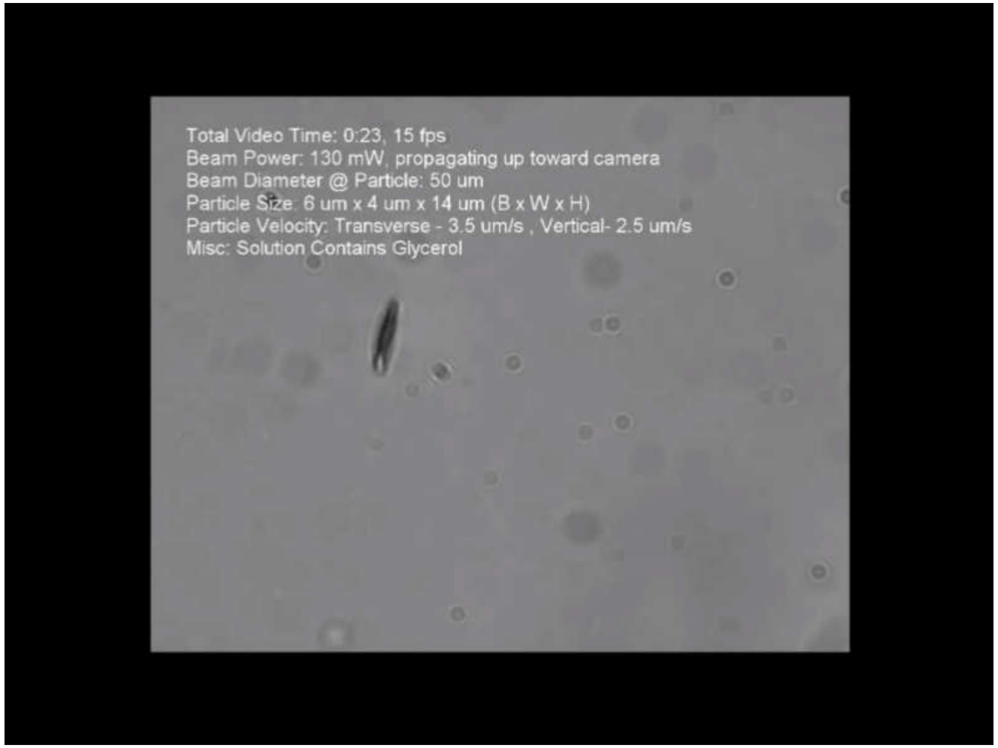

Swartzlander, Optical lift, Nature Photonics 2010
Simpson et al, Opt Lett **37**, 2012

Radiation cross-sections yield the mechanical effects of light on non-spherical particles

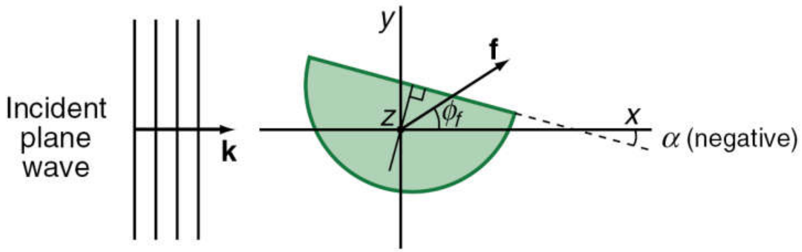

Wind sailing

Solar sailing

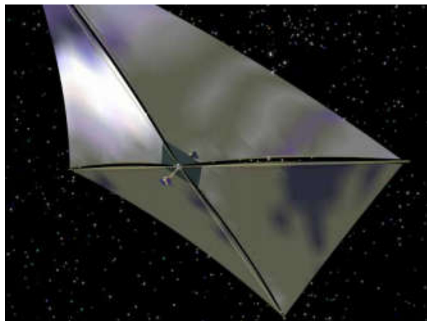

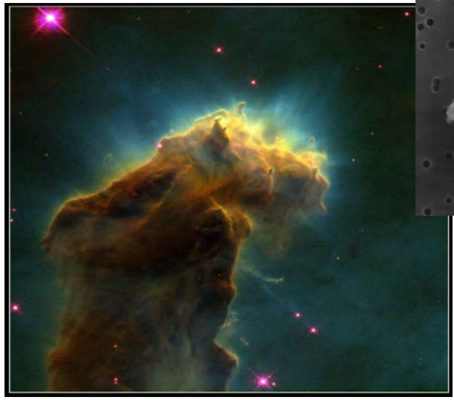

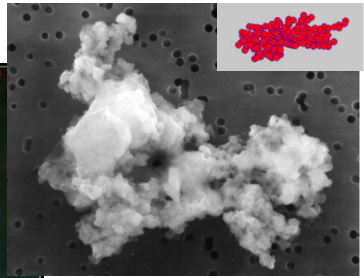

Astrophysics:
Interstellar dust

Iatì et al., MNRAS (2001)
Saija et al., MNRAS (2003)
Iatì et al., ApJ (2004)
Iatì et al., MNRAS (2008)

Fazio et al, Light: Science & Applications (2016)
Fazio et al. Nature Photonics (2017)

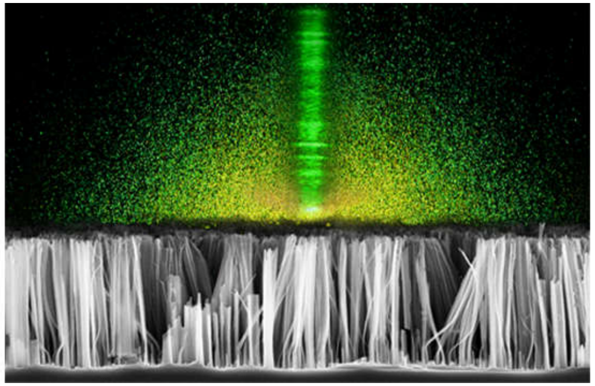

Scattering and light localization in disordered systems

T-Matrix Methods

Optical tweezers

Borghese et al., Optics Express (2007)

Borghese et al., PRL (2008)

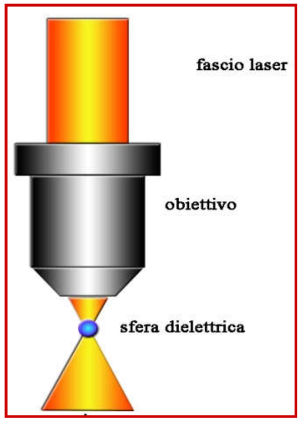

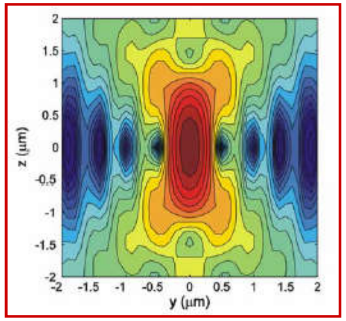

Plasmonics

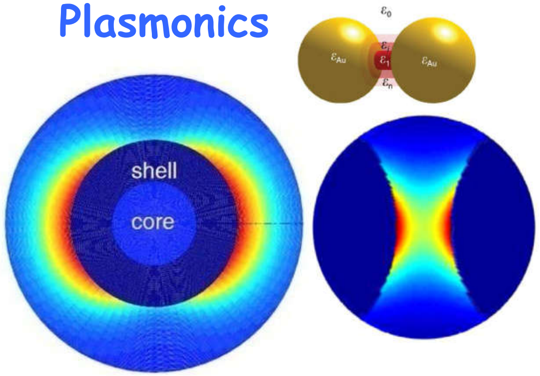

Review:Amendola et al. J Phys: Cond Matt (2017)

Cacciola et al., JQSRT (2017)

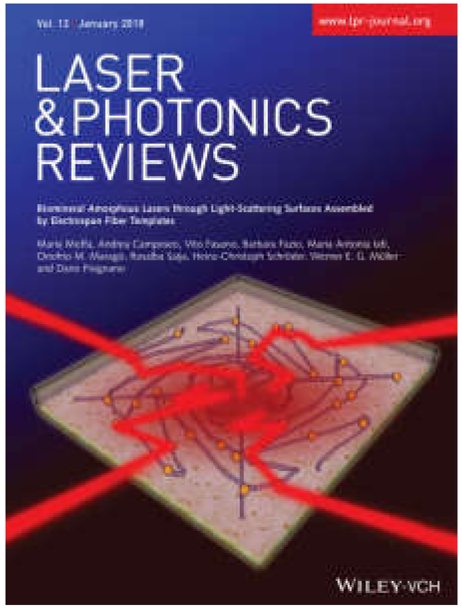

Moffa et al.,
Laser & Photonics Reviews (2018)

Force & Torque with T-matrix

Radiation force & torque from a general scattering process

Borghese equations

Generalize Mishchenko, JQSRT (2001)

$$F_{\mathrm{rad}}(\hat{\mathbf{u}}) = -\frac{\varepsilon_{\mathrm{m}} E_{\mathrm{i}}^2}{2k_{\mathrm{m}}^2}\mathrm{Re}\left\{\sum_{plm}\sum_{p'l'm'} i^{l-l'} I^{(pp')}_{lml'm'}(\hat{\mathbf{u}})\left[\overset{\text{scattering}}{A^{(p)*}_{\mathrm{s},lm}A^{(p')}_{\mathrm{s},l'm'}} + \overset{\text{extinction}}{W^{(p)*}_{\mathrm{i},lm}A^{(p')}_{\mathrm{s},l'm'}}\right]\right\}$$

$$T_{\mathrm{rad},z} = \underbrace{-\frac{\varepsilon_{\mathrm{m}} E_{\mathrm{i}}^2}{2k_{\mathrm{m}}^3}\sum_{plm} m\mathrm{Re}\left\{W^{(p)}_{\mathrm{i},lm}A^{(p)*}_{\mathrm{s},lm}\right\}}_{\text{extinction}} \underbrace{-\frac{\varepsilon_{\mathrm{m}} E_{\mathrm{i}}^2}{2k_{\mathrm{m}}^3}\sum_{plm} m|A^{(p)}_{\mathrm{s},lm}|^2}_{\text{scattering}}$$

Generalize Marston&Crichton PRA(1984)

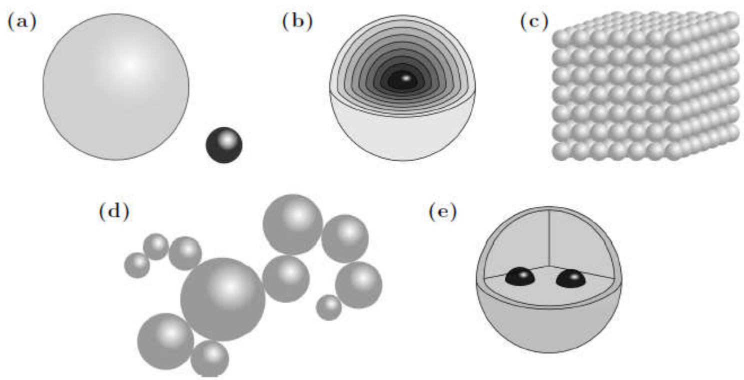

❖**Extension to chiral particles:** See Patti, et al., Sci. Rep. (2019).

❖**Extension to hybrid structures:** See Ridolfo et al. ACS Nano (2011)

❖**Extension to surfaces:** See Denti et al. JOSA A (1999).

See also Saija et al. (2005), Borghese et al. (2006), Borghese et al. (2007)

Size scaling for polystyrene spheres and nanowires

$$Q_i = F_i \frac{c}{n_m P_i}$$

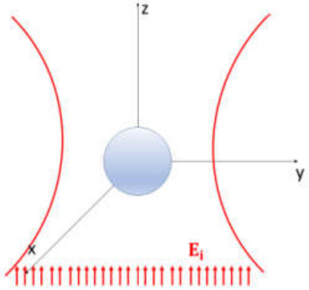

$\lambda = 830$ nm
NA $= 1.3$
$w_0 \approx 320$ nm

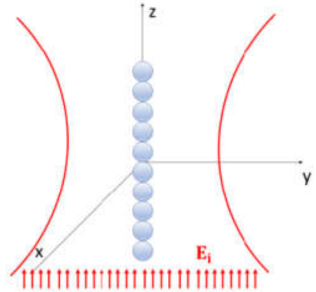

Sphere of radius
$a = 300$ nm

Nanowire of half-length
$L/2 = 300$ nm

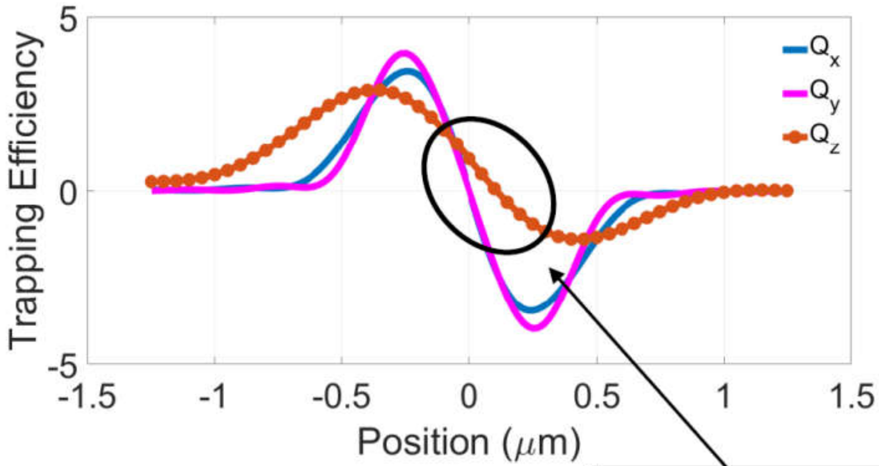

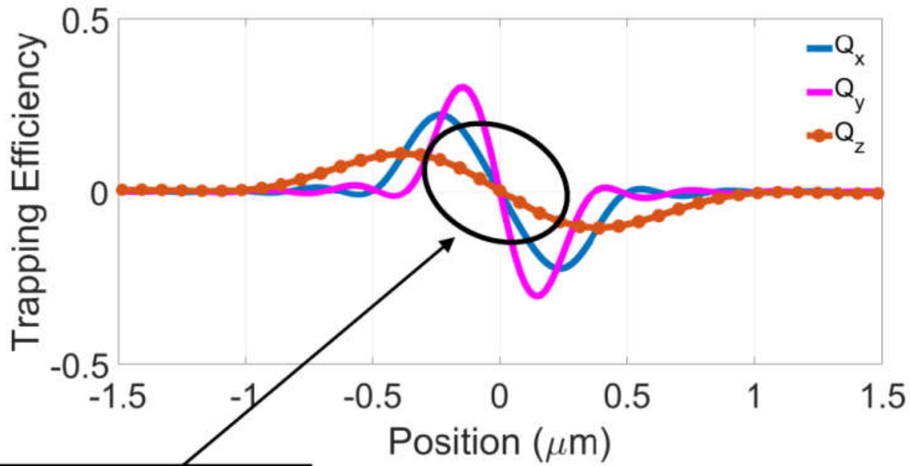

$$F_i = -\kappa_i x_i$$

Harmonic force trapping

By P. Polimeno, et al. JQSRT (2018)

Size scaling for a sphere

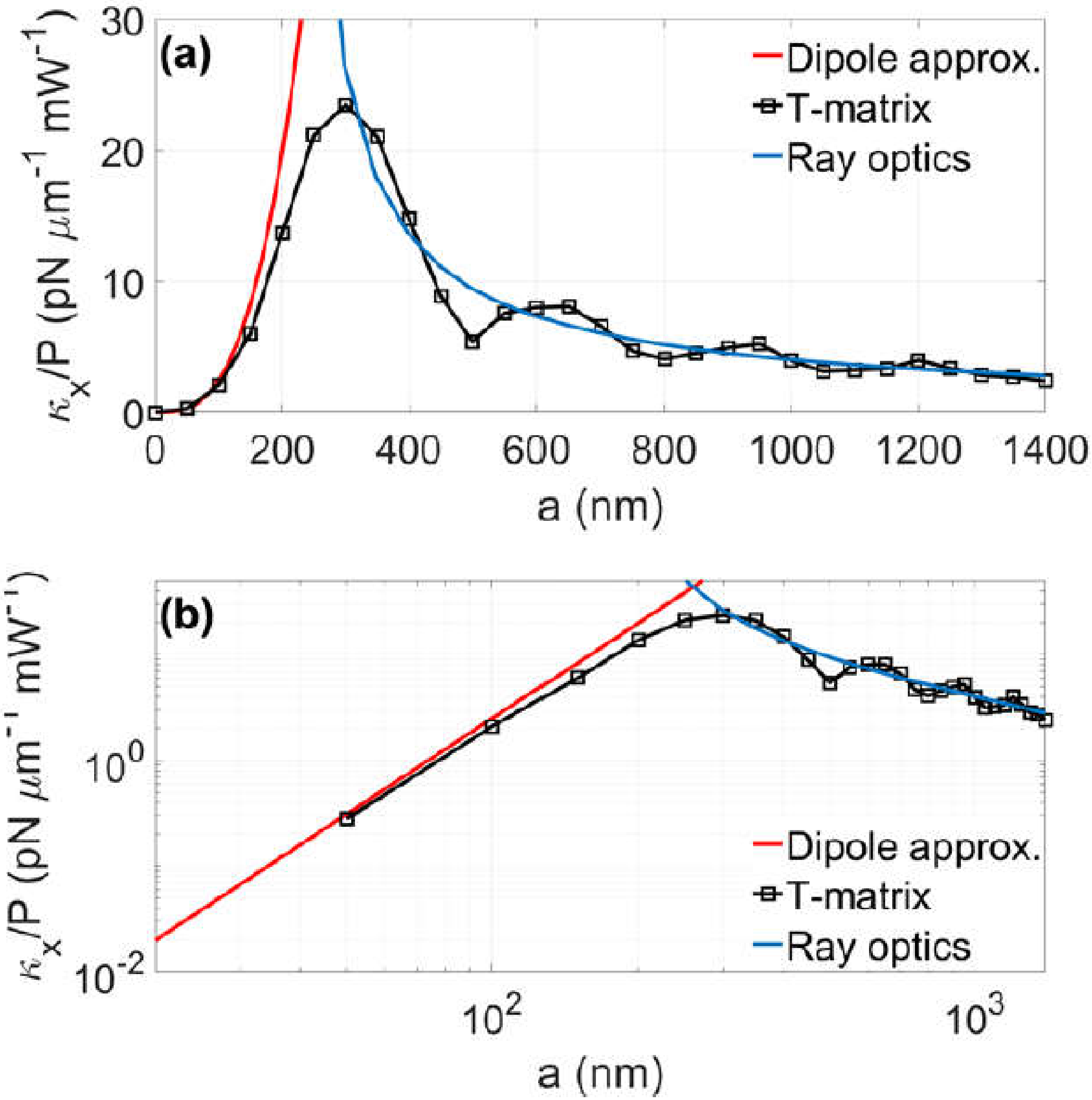

By P. Polimeno, A. Magazzù, et al. JQSRT (2018)

Size scaling for polystyrene spheres and nanowires

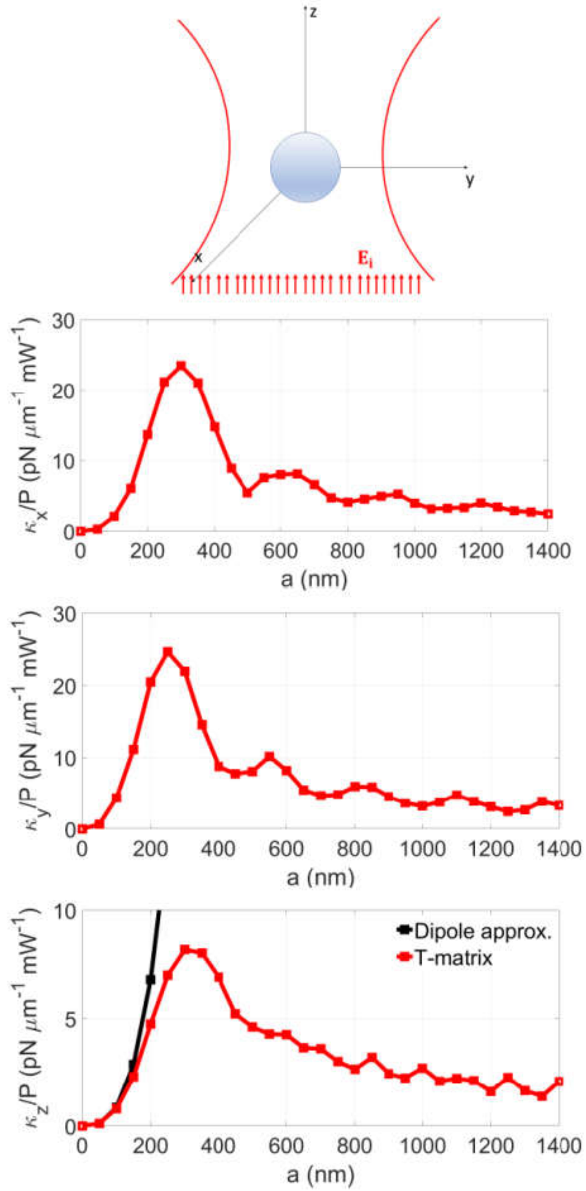

$\lambda = 830$ nm

NA $= 1.3$

$w_0 \approx 320$ nm

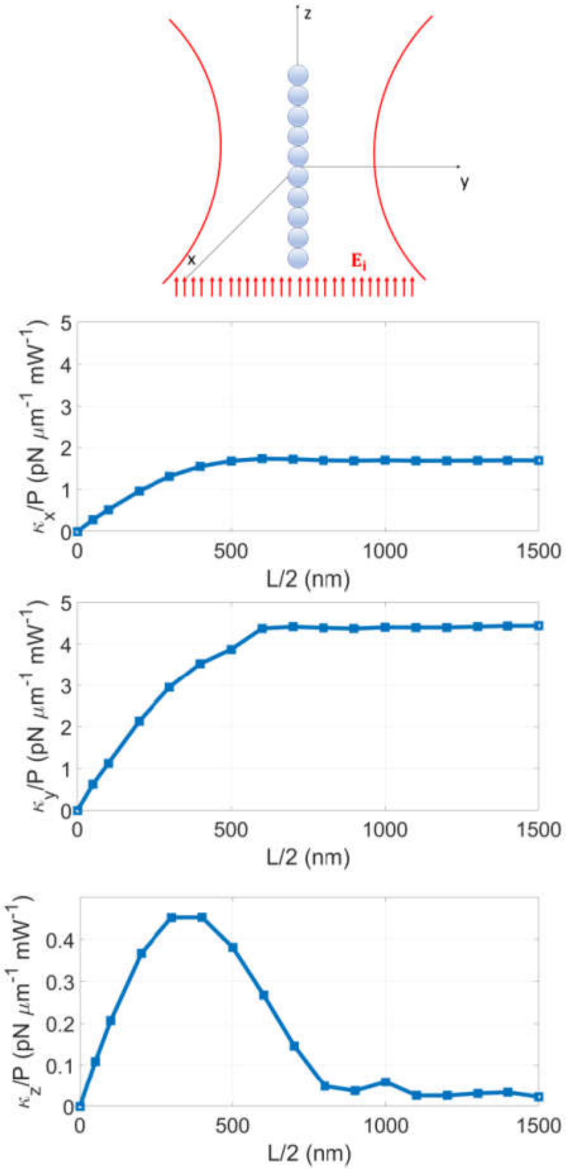

By P. Polimeno

Scaling of Force Constants

T-matrix calculations – Role of shape

By P. Polimeno

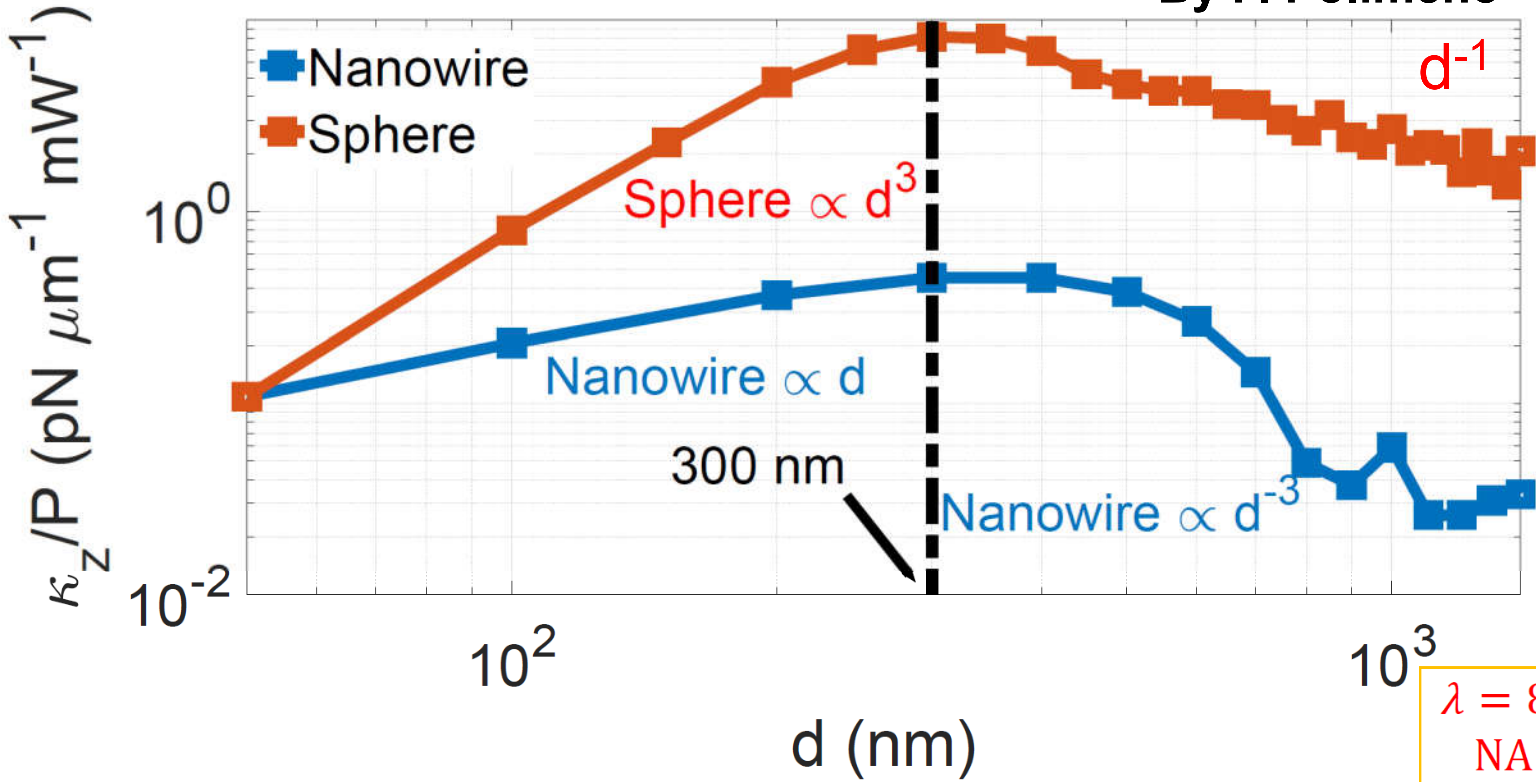

$\lambda = 830$ nm
NA $= 1.3$
$w_0 \approx 320$ nm

Maximum in the axial (z) force constant

Optimum overlap between wire and high intensity region (Rayleigh Range)

See also Simpson & Hanna, Nanotechnology (2012)

Experimental practice

Building an Optical Tweezers

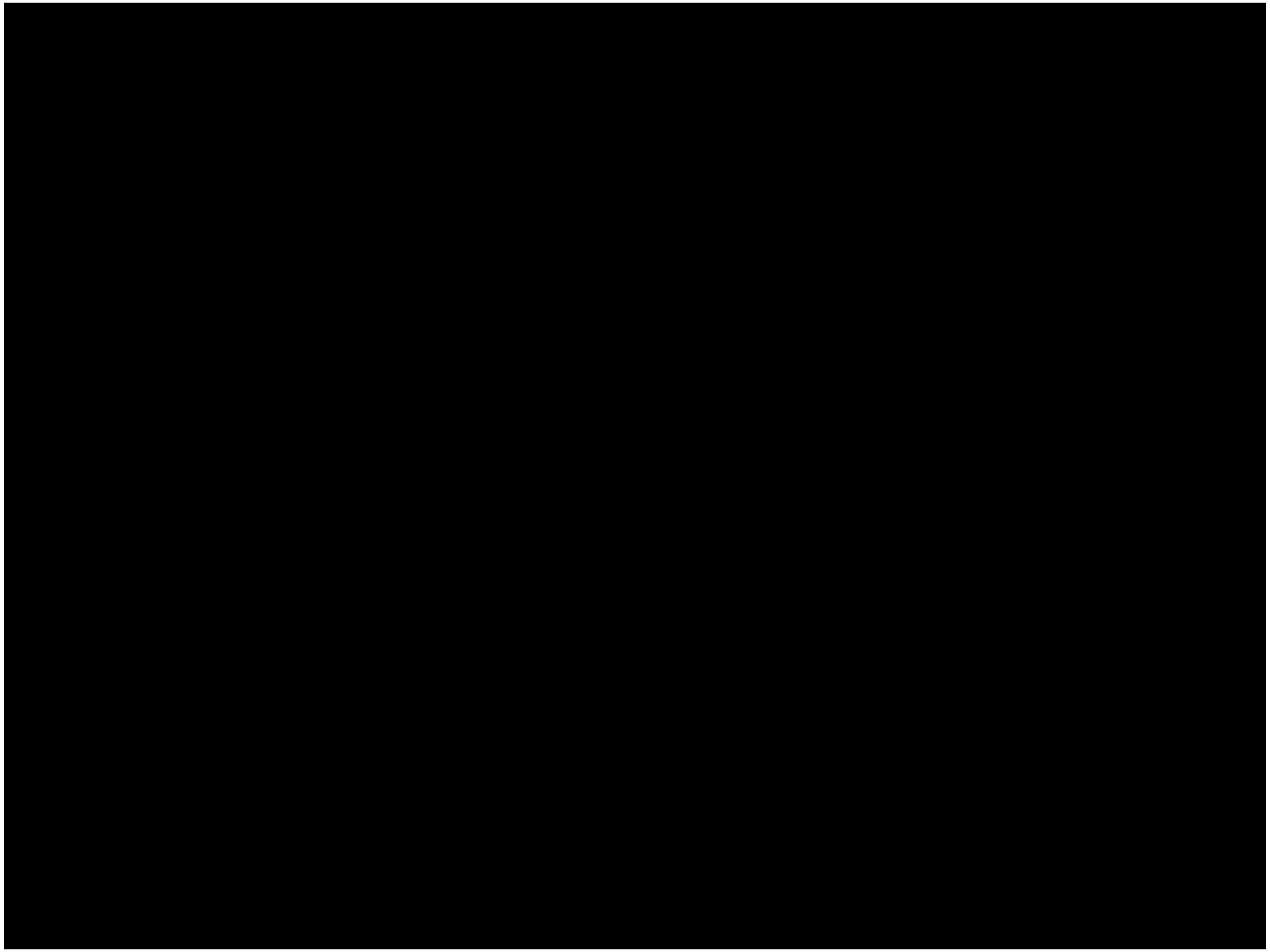

G. Pesce, et al, Step-by-step guide to the realization of advanced optical tweezers, *JOSA B* (2015)
Special Issue Opex & JOSA B on Optical Cooling & Trapping

Holographic Optical Tweezers

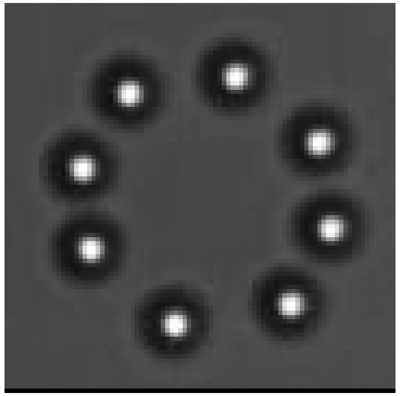

Laguerre-Gauss Beams can transfer Orbital Angular Momentum

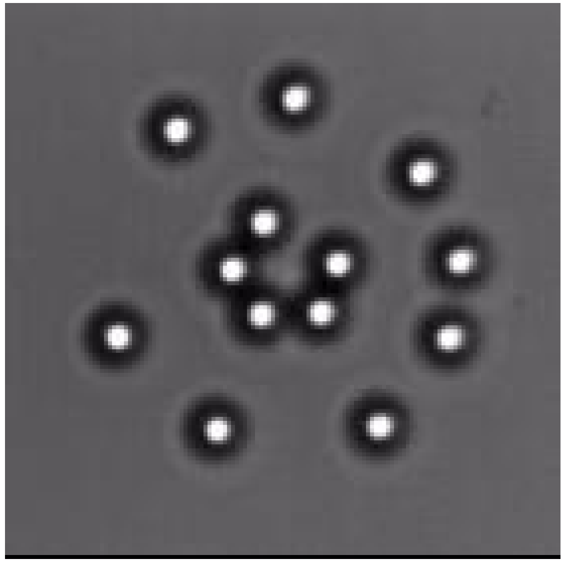

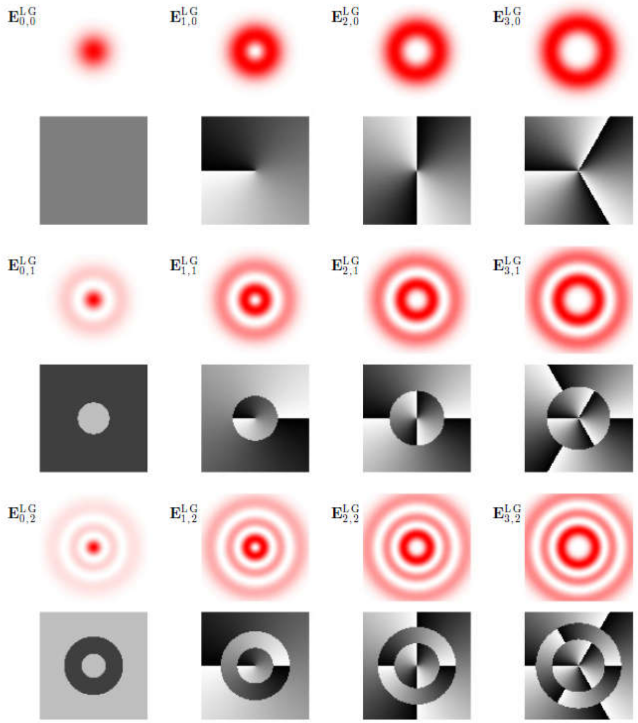

Phase Mask

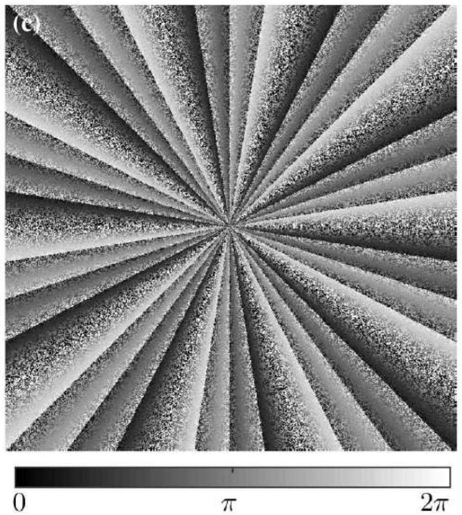

Trapped particles

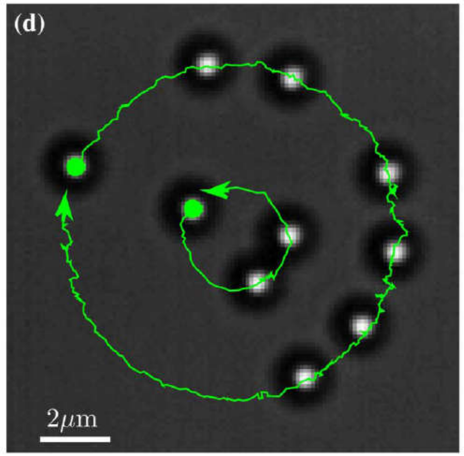

Jones, Maragò, Volpe, “Optical Tweezers”, CUP (2015)

G. Pesce, et al, JOSA B (2015)

Advanced Optical Tweezers (Speckle fields)

Optical sorting with speckle fields

High intensity traps large particles, while small particles move in the microfluidic flow

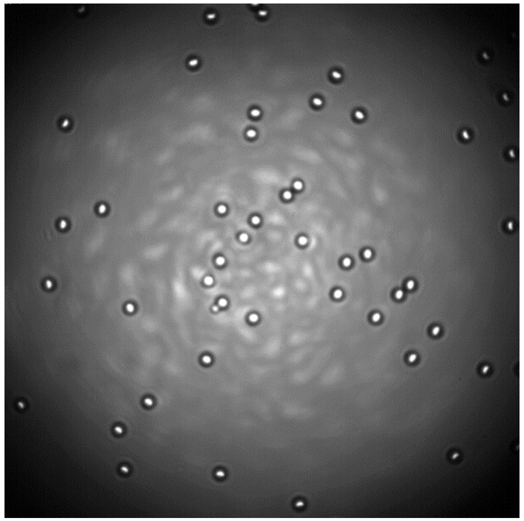

Jones, Maragò, Volpe, “Optical Tweezers”, CUP (2015) G. Pesce, et al, JOSA B (2015)

OT of Linear Nanostructures

Nature Nanotech (2013)

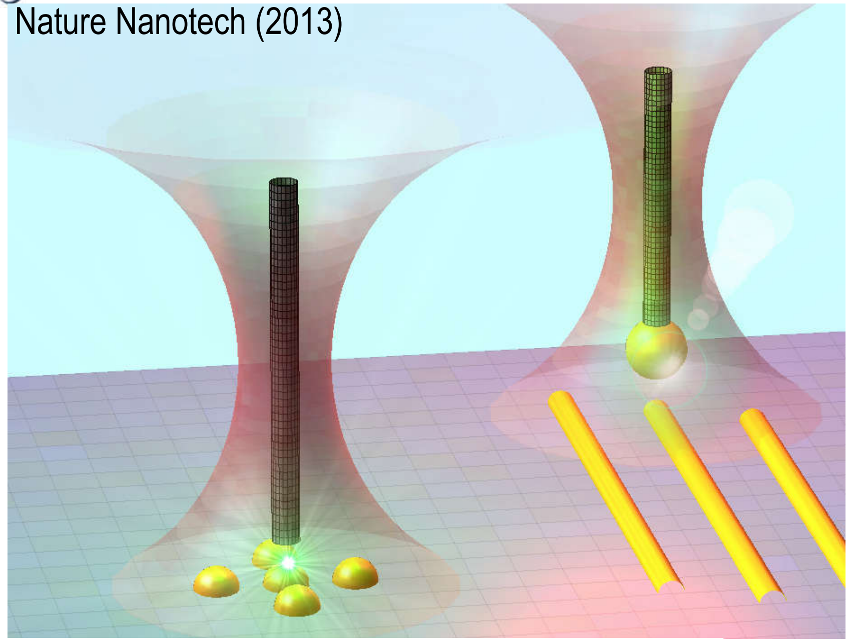

Nanowires:

Agarwal et al., Optics Express (2005)
Pauzauskie et al., Nat. Mat. (2006)
Nakayama et al., Nature (2007)
Borghese et al., Phys. Rev. Lett. (2008)
Carberry et al., Nanotech. (2010)
Simpson&Hanna, JOSA A (2010)
Simpson&Hanna, PR E (2010)
Reece et al., Nano Lett. (2011)
Dutta et al., Nano Lett. (2011)
Irrera et al., Nano Lett. (2011)
…

Nanotubes:

Tan et al., Nano Lett. (2004)
Plewa et al., Optics Express (2004)
Zhang et al., APL (2006)
O.M. Maragò et al., Physica E (2008)
O.M. Maragò et al., Nano Lett. (2008)
P.H. Jones, et al. ACS Nano (2009)
Pauzauskie et al, APL (2009)
Donato et al., Opt. Lett. (2012)

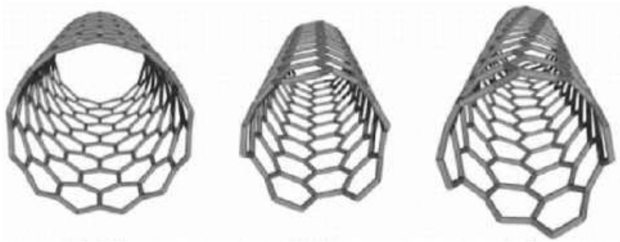

Nanofibers:

Neves et al., Optics Express (2010)

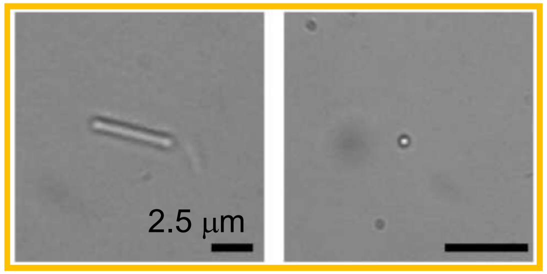

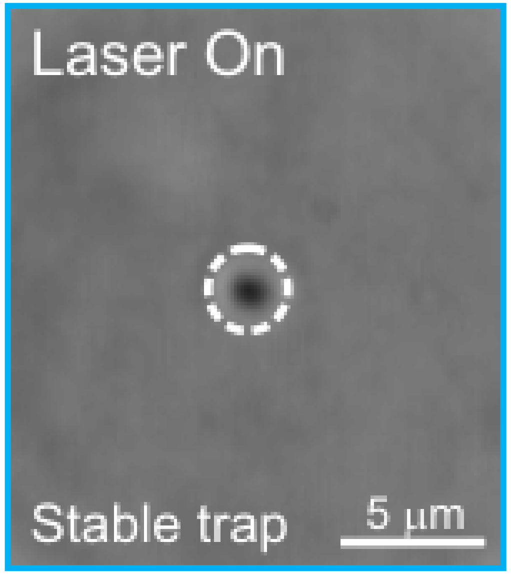

OT of Nanofibers

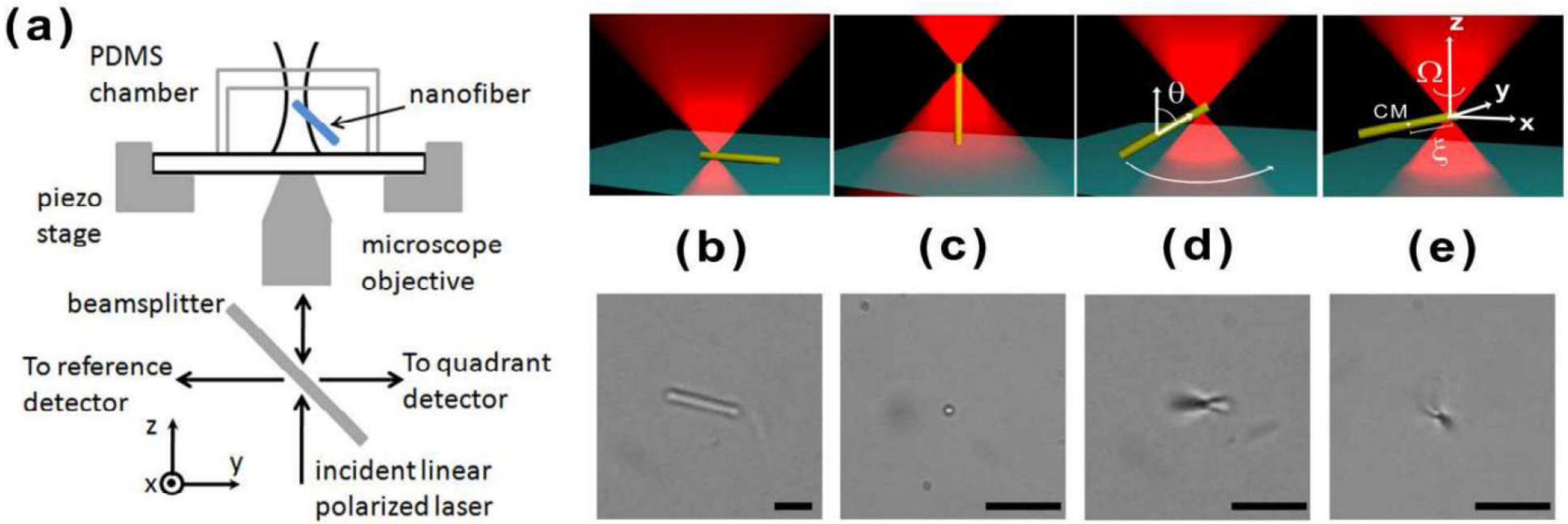

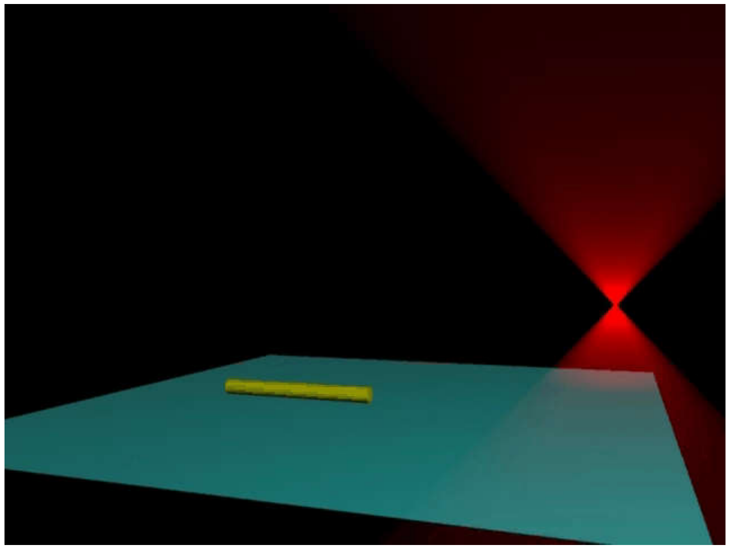

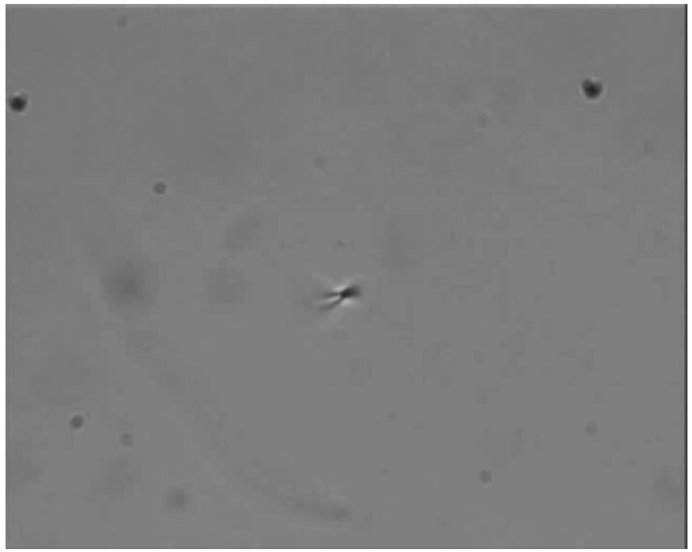

Neves, Camposeo, Pisignano - Opt. Express 18, 822 (2010)

Hydrodynamics

Broersma, J.Chem.Phys. (1981);
Tirado et al. J. Phys Chem C(1984)

Hydrodynamics of a rod-like nanostructure is anisotropic

$$\Gamma_{\perp} = \frac{\ln p + \delta_{\perp}}{4\pi\eta L}, \quad \Gamma_{||} = \frac{\ln p + \delta_{||}}{2\pi\eta L}$$

$$\Gamma_{\Theta} = \frac{3(\ln p + \delta_{\theta})}{\pi\eta L^3}$$

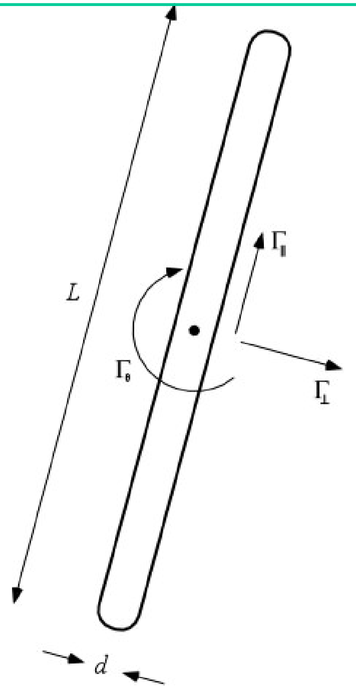

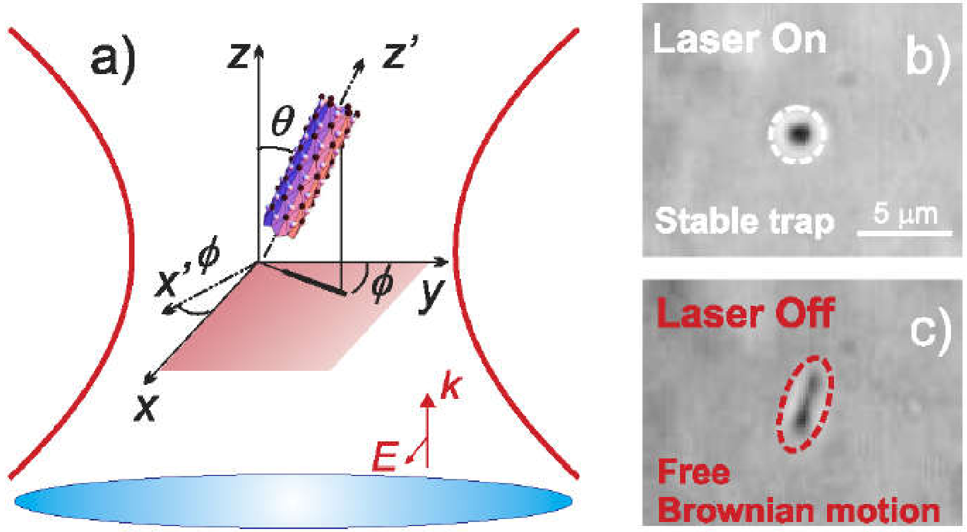

The signals from the QPD are a composition of center of mass Xi and angular motion Θi.

$$S_x \sim \beta_x (X + a\,\Theta_x)\,;\; S_y \sim \beta_y (Y + b\,\Theta_y)\,;\; S_z \sim \beta_z Z$$

Small angle approximation

Correlation Function Analysis

Correlation functions of the tracking signals give information on torque and force constants.

$$C_{ii}(\tau) = \langle S_i(t) S_i(t+\tau) \rangle$$
$$C_{xy}(\tau) = \langle S_x(t) S_y(t+\tau) \rangle$$

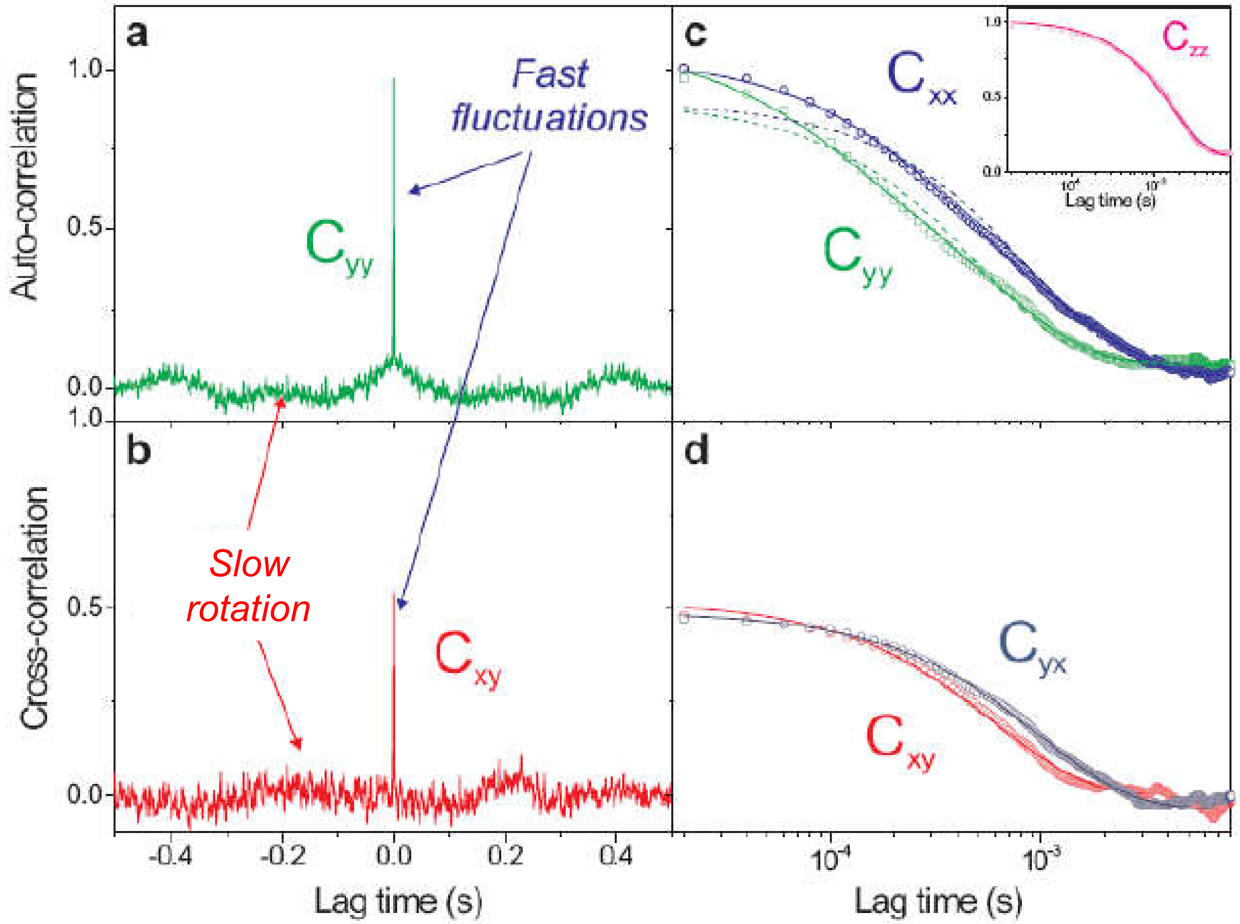

Double Exp for "fast" dynamics

Simple Exp for Z and Cross

Non-conservative forces:
Simpson&Hanna, PR E (2010)

Brownian Motion of Nanotubes/Nanowires

Shape determines the effective potential

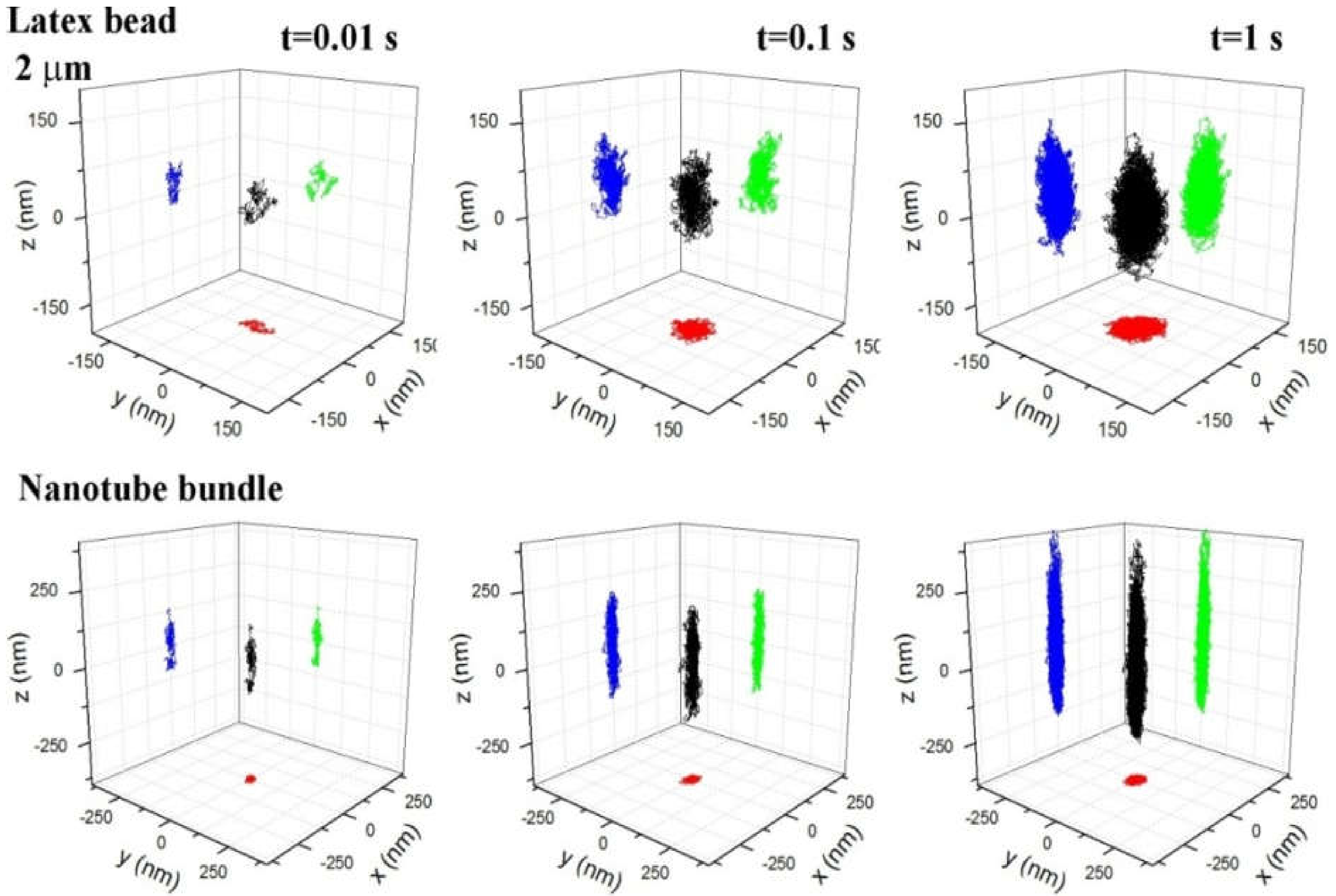

Transverse fluctuations in the 10 nm range

O. M. Maragò, Nano Letters 8, 3211–3216 (2008); A. Irrera, Nano Letters 11, 4879–4884 (2011).

OT of Silicon Nanowires

A. Irrera et al., *Nano Letters* **2011**, *11*, 4879
A. Irrera, A. Magazzù, et al., *Nano Letters* **2016**.

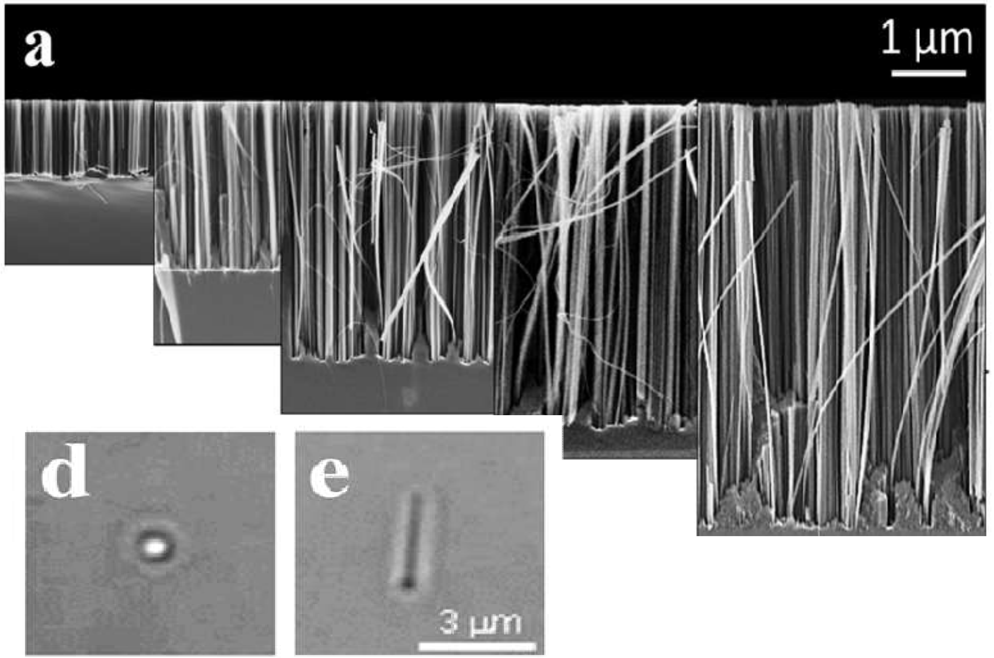

We can now control the length and the diameter

Length controls optical forces and torques

Size-scaling with the size parameter $x_L=\pi nL/\lambda$

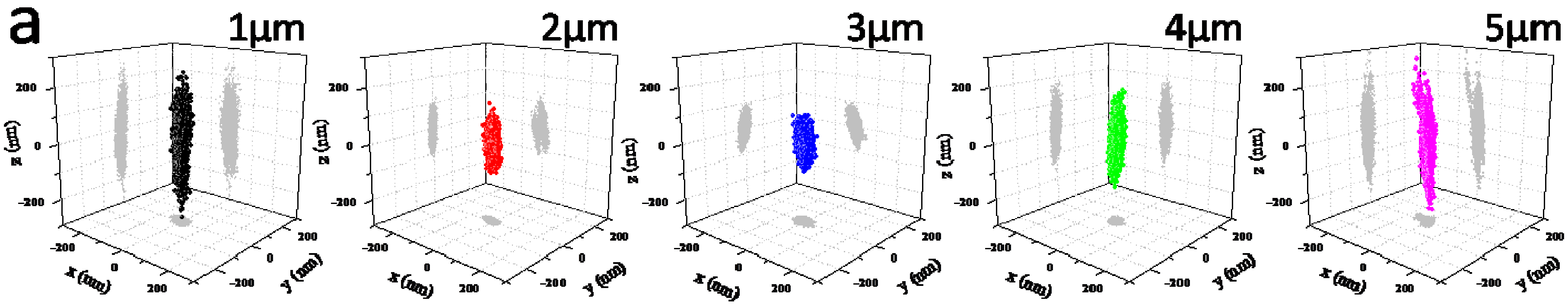

Optical trapping of SiNW with controlled size

Scaling of Force Constants

Experiment

Irrera et al., Nano Letters (2011)

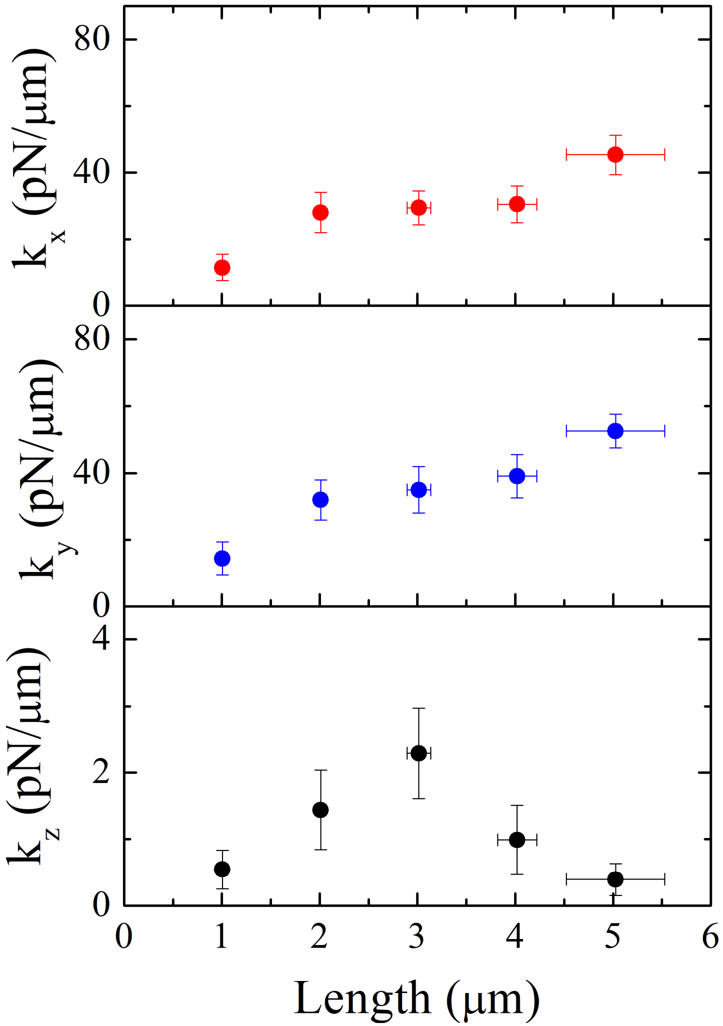

T-matrix

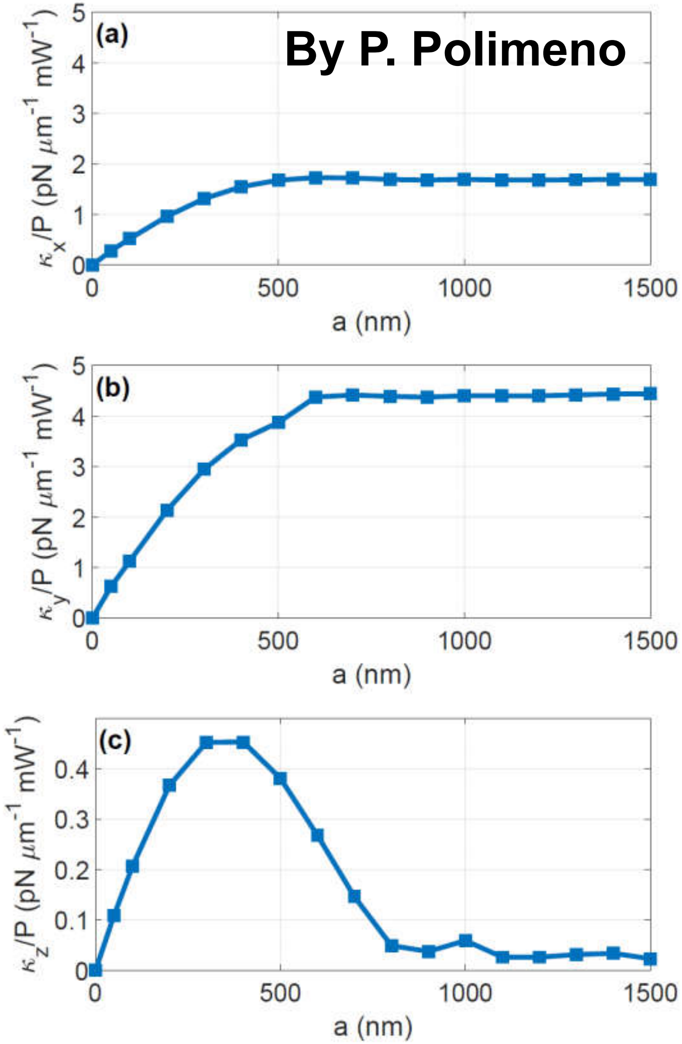

For long nanowires transverse force saturates, axial force drops.

High resolution photonic force microscopy
(F. Pedaci, CNRS, Montpellier)

Nanofabricated birifrengent particles with nanometric needles

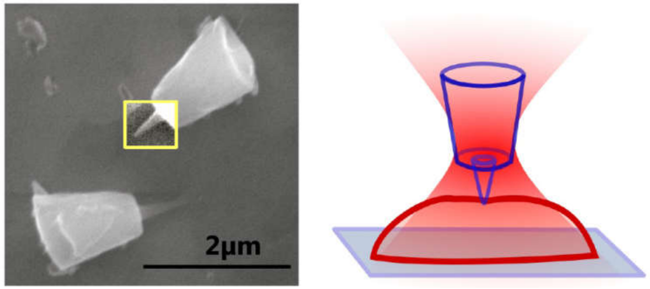

Accurate force calibration of non-spherical probes

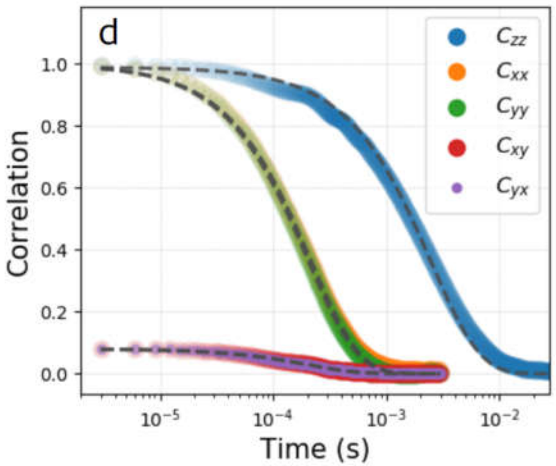

Topography of soft materials

Membrane of <u>living</u> malaria-infected red blood cells presenting knobs

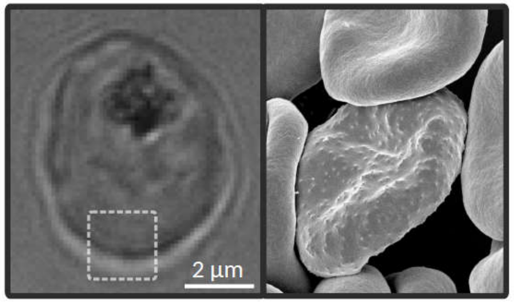

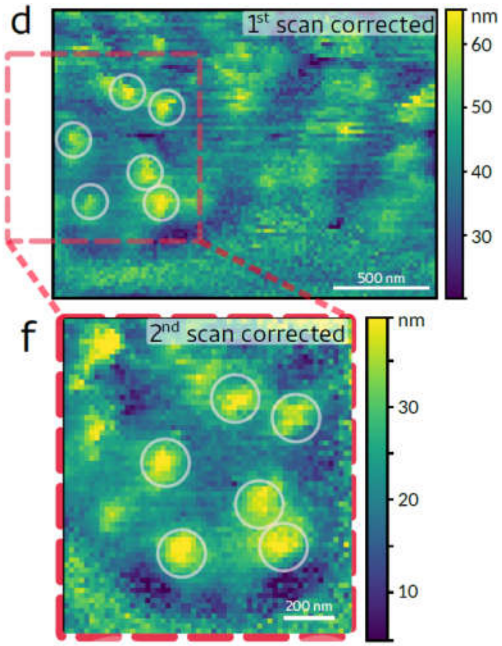

Pedaci et al. Nat. Phys (2010); Desgarceaux et al. arXiv:2002.01533 (2020)

Silicon nanowires in 2-beam traps

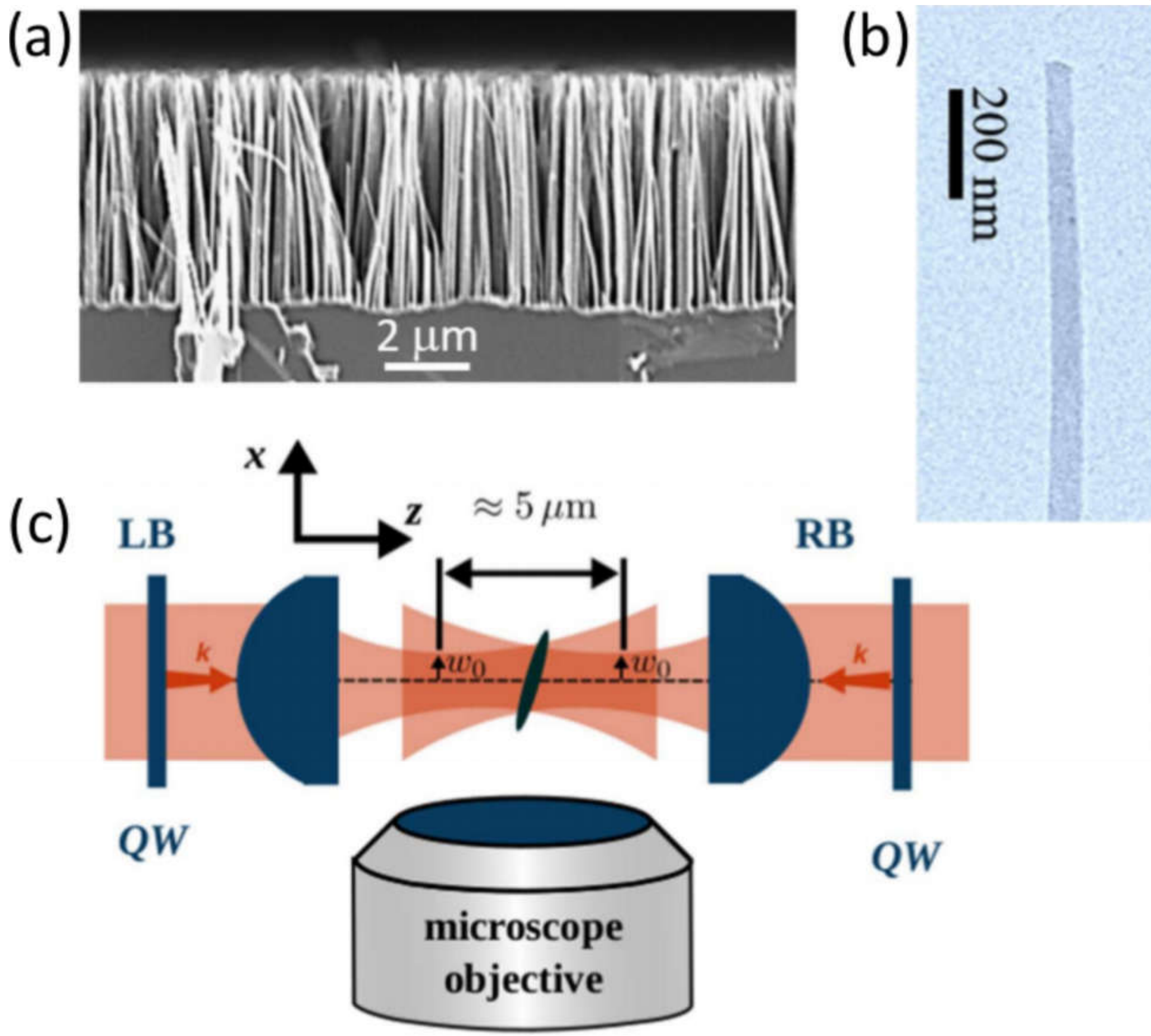

Donato, Brzobohaty, Simpson, et al. Nano Letters 19, 342 (2019)

Silicon nanowires in 2-beam traps

Rich scenario regulated by shape & polarization

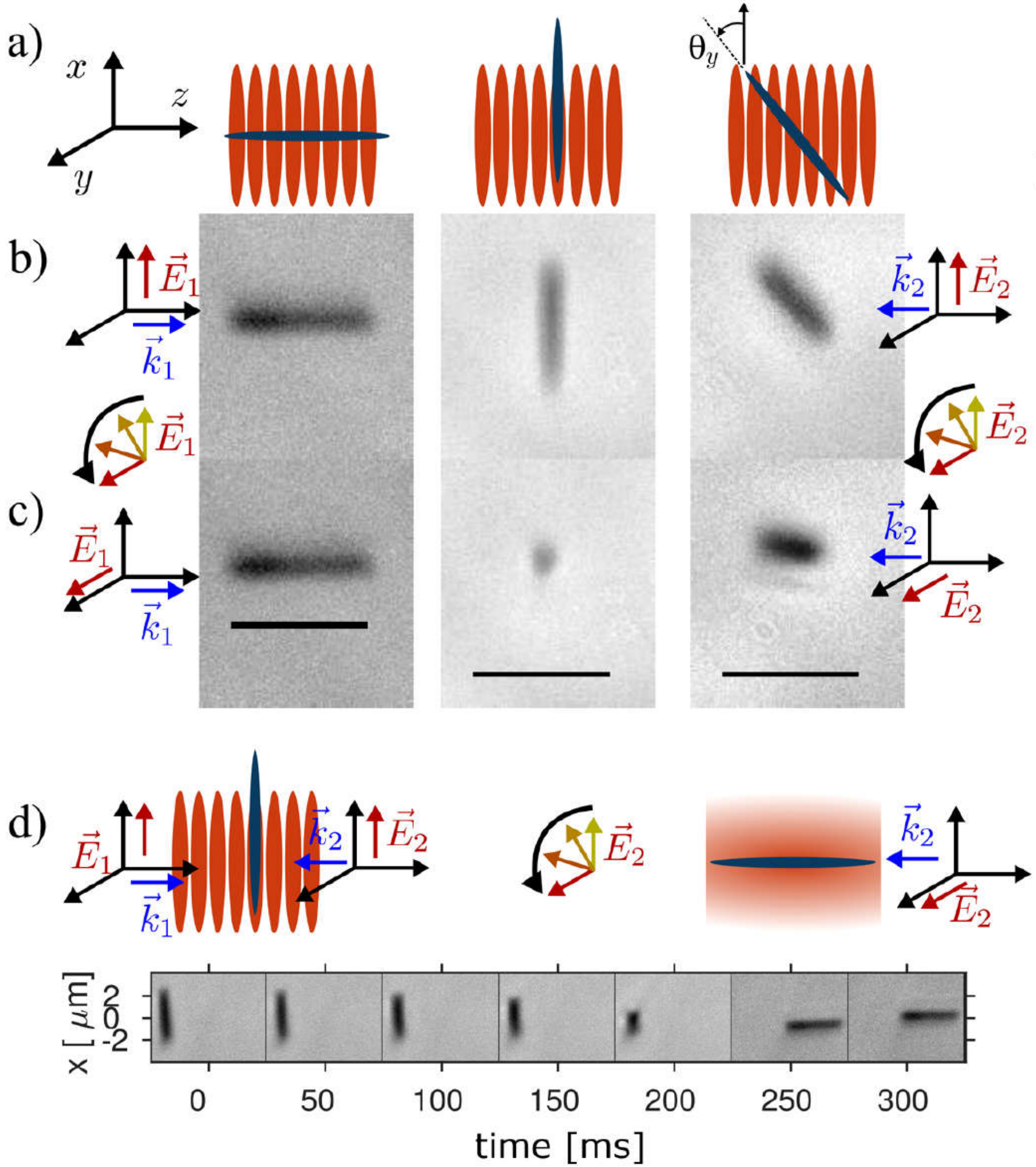

Parallel linear polarization (**PLP**) leads to **several equilibrium configuration** regulated by the **length** of the NWs

The NW scatters "mainly" from end-tips

Polarization can be used to control orientation

From PLP to XLP (fringes disappear) longitudinal torque wins over polarization torque

Optical binding of nanowires in cross linear polarization

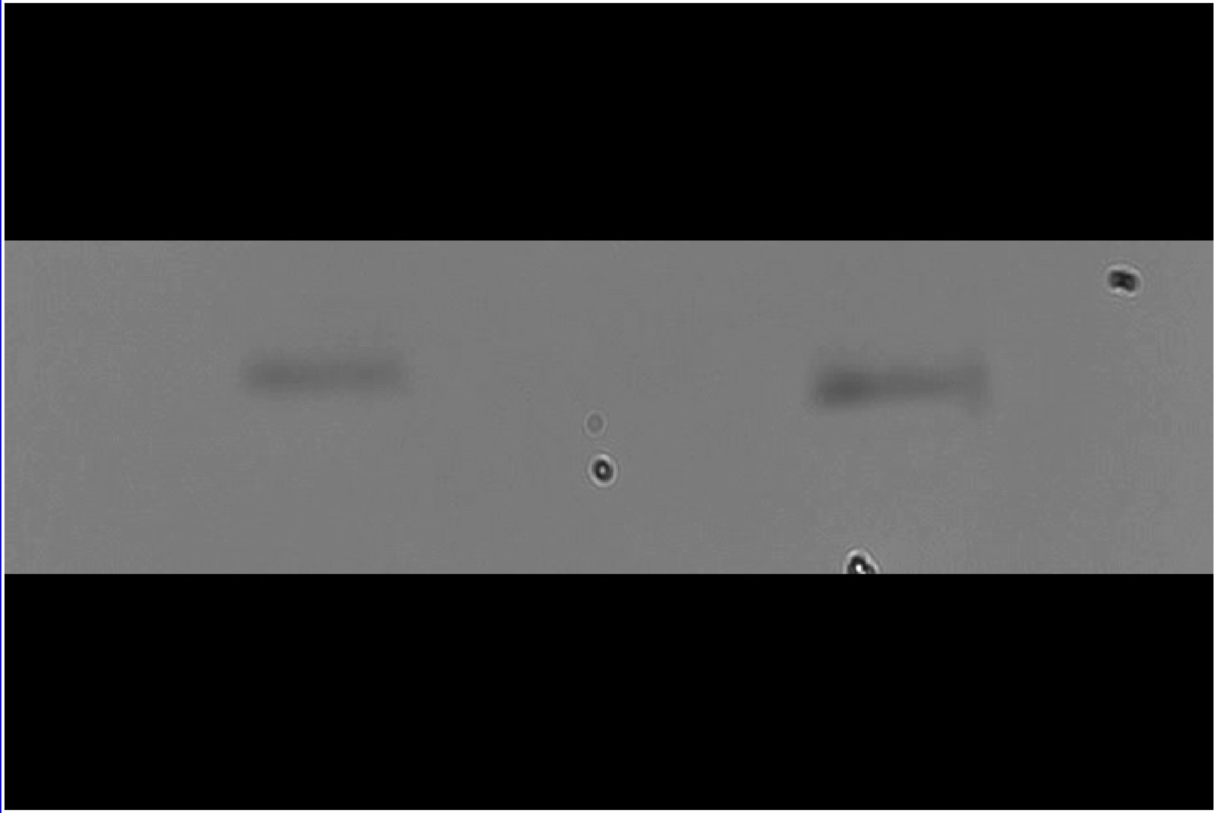

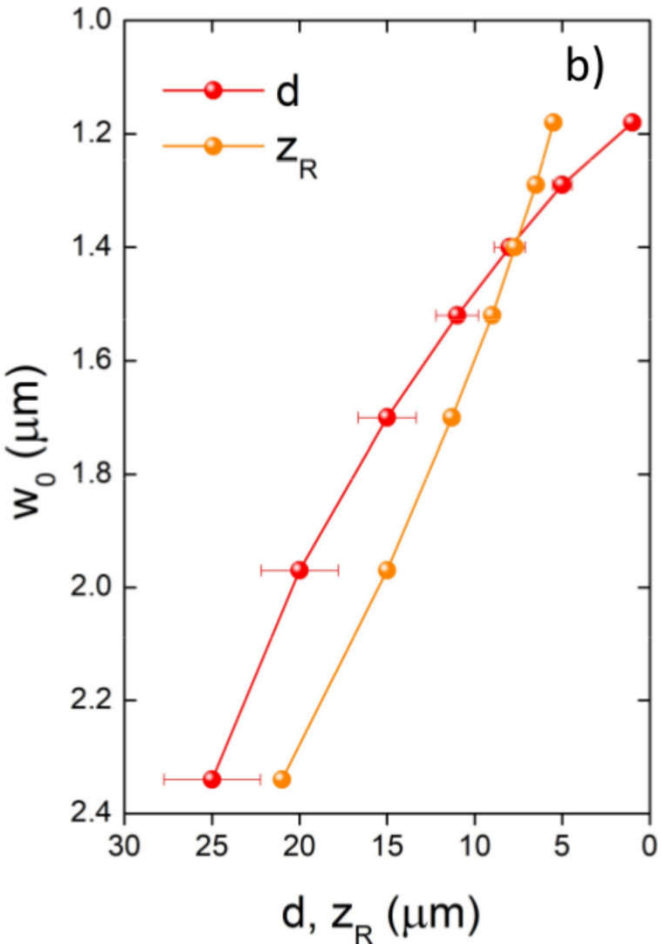

By changing the size, w_0, of the laser beams we can control the distance and binding interaction

Rich spin rotational dynamics regulated by shape

Imaging the XZ plane

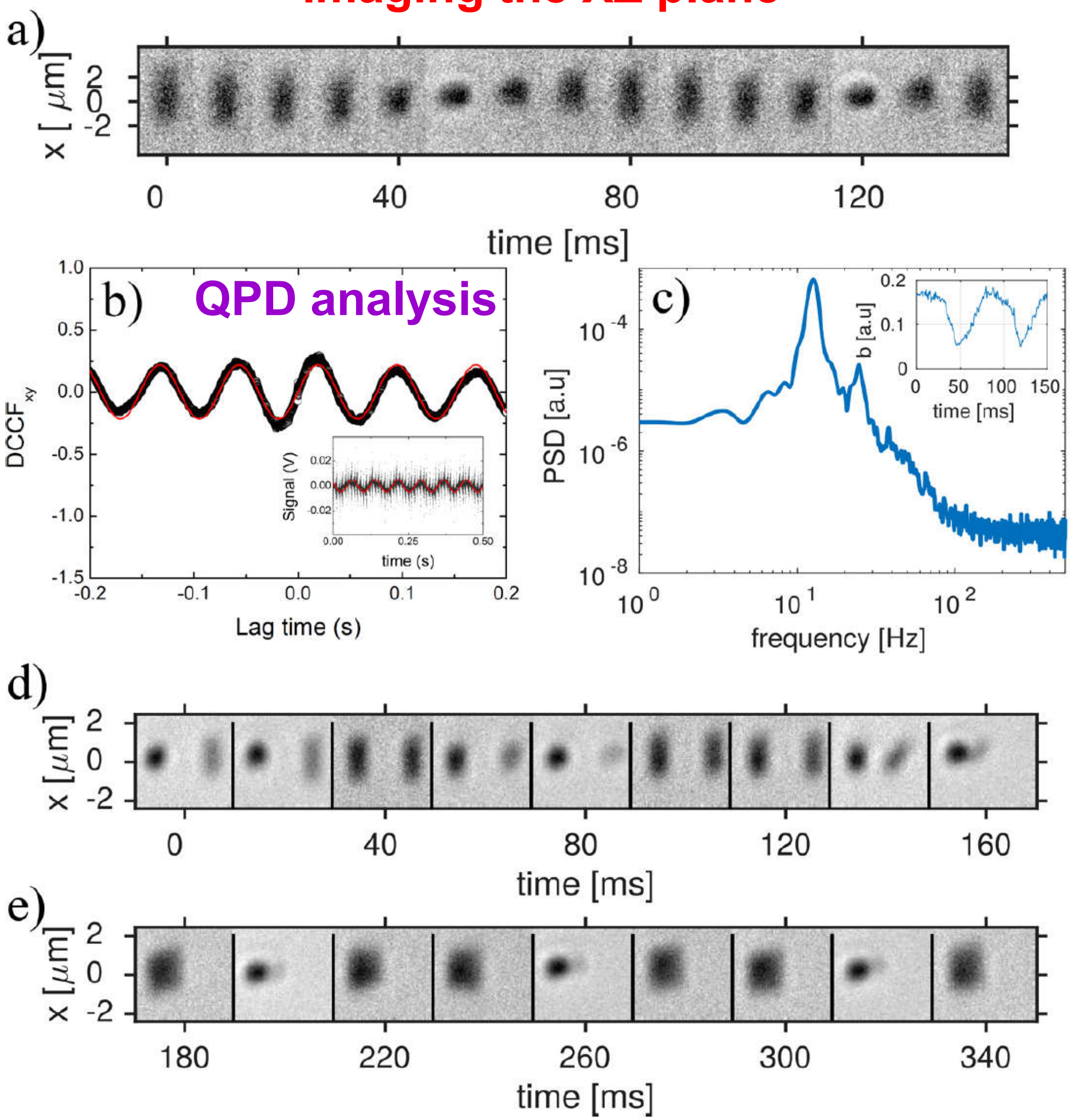

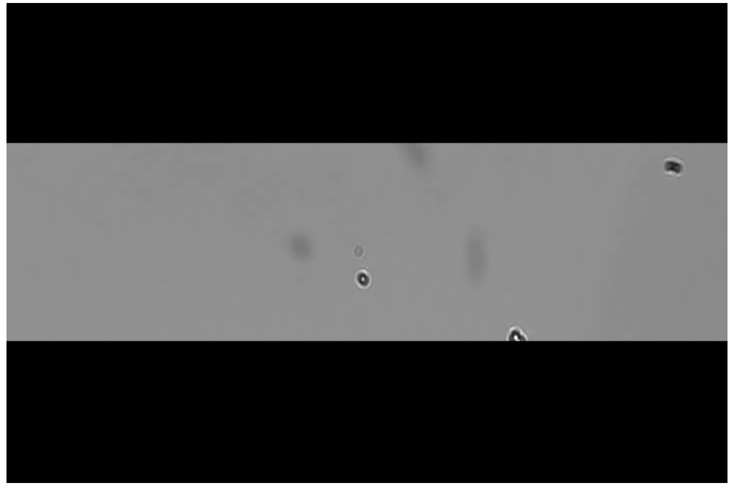

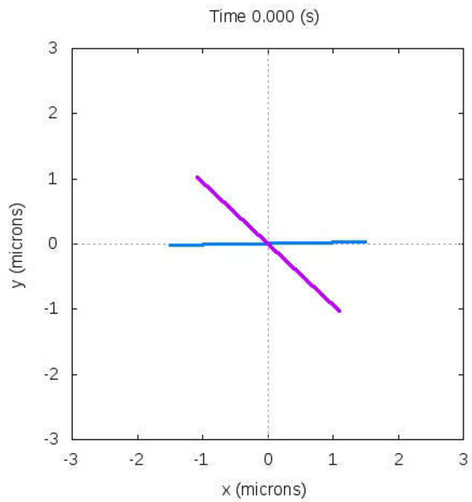

Simulations by S. H. Simpson

Rich orbital rotational dynamics regulated by shape

Imaging the XZ plane

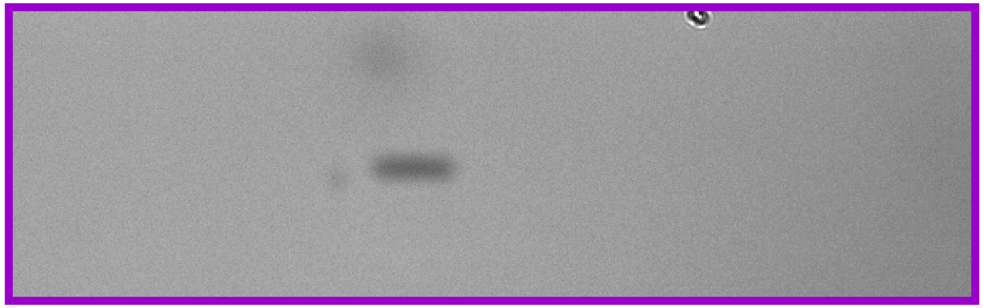

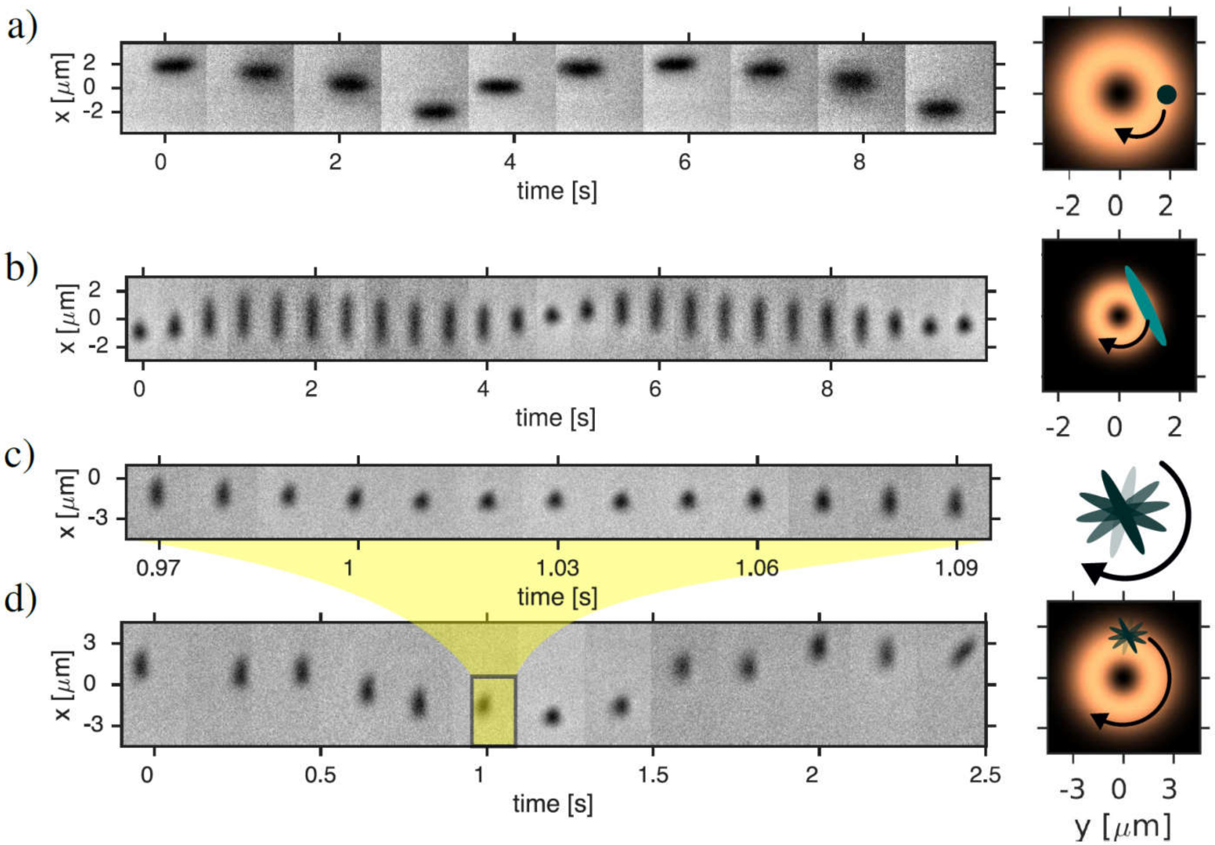

Sim. by S. H. Simpson **XZ**

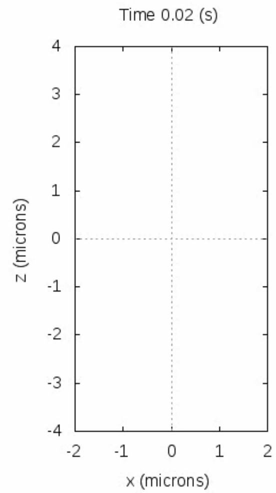

XY

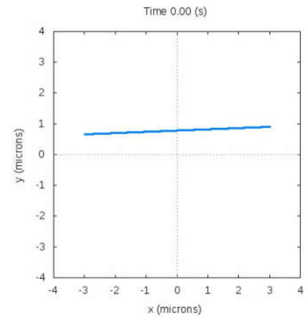

XY

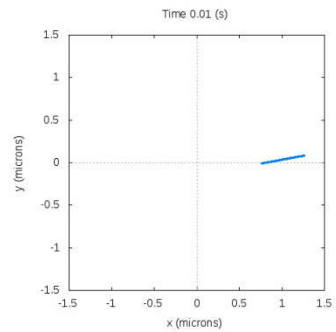

Layered materials

Liquid Phase Exfoliation

Graphene

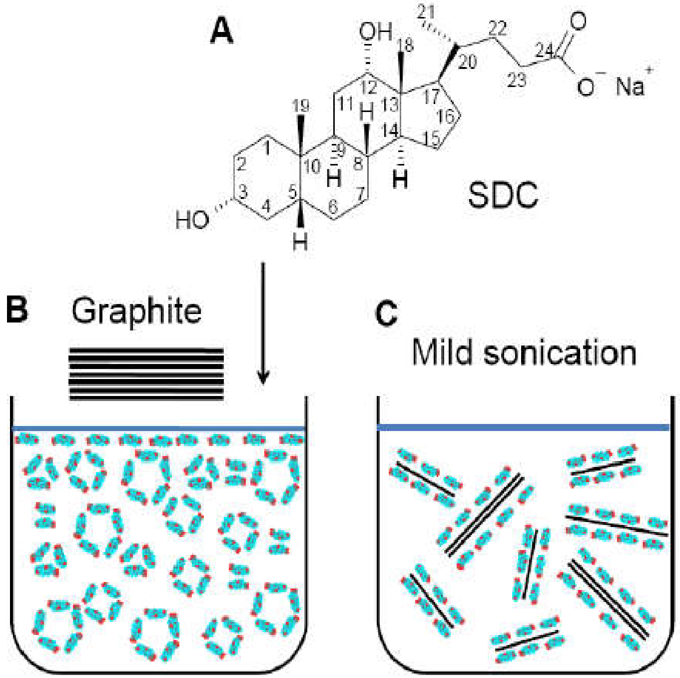

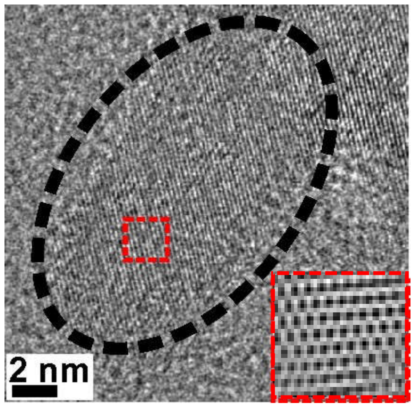

O.M. Maragò et al. ACS Nano **4**, 7515 (2010)

2d Materials

Ultrasonication

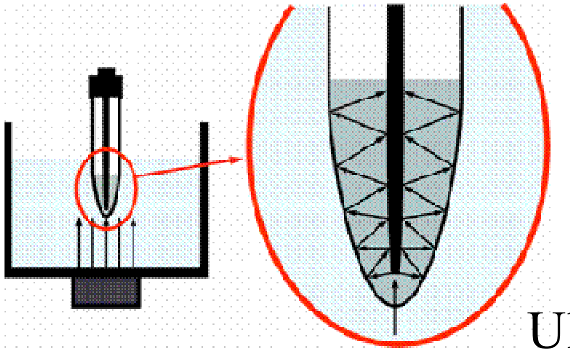

Ultracentrifugation

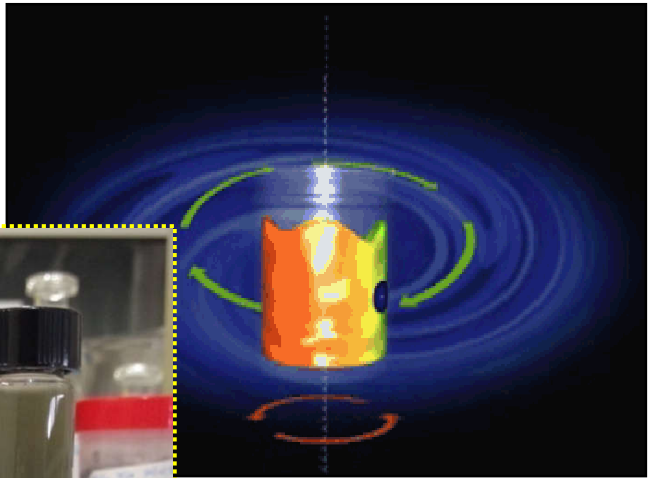

2d Materials Inks

Flexible electronics and textile

Raman Tweezers

- 561nm,633nm,785nm…
- Edge/Notch filter
- Jobin-Yvon Triax 190 spectrometer
- Avalanche photodiode, SPC (Perkin Elmer)

Raman & Photoluminescence inspection of trapped samples

E.g., Inspection of **Graphene** flakes

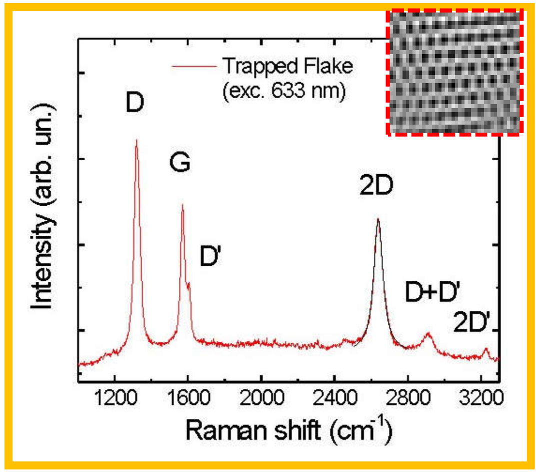

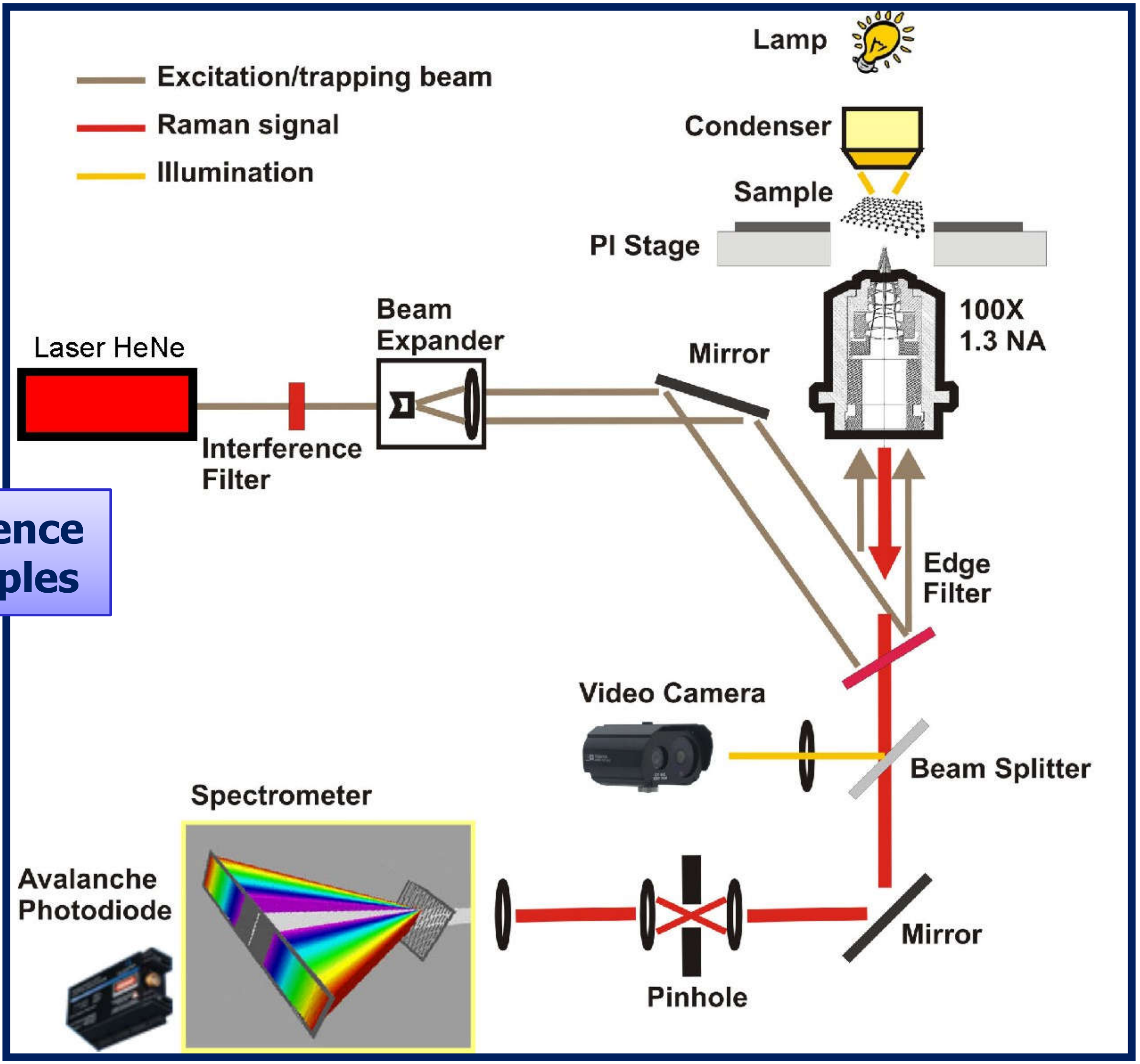

Maragò, et al.,"Brownian Motion of Graphene", *ACS Nano* **4**, 7515 (2010)
Maragò, et al. *Nature Nanotechnology* **8**, 807–819 (2013)

Mechanical effects of light on layered materials

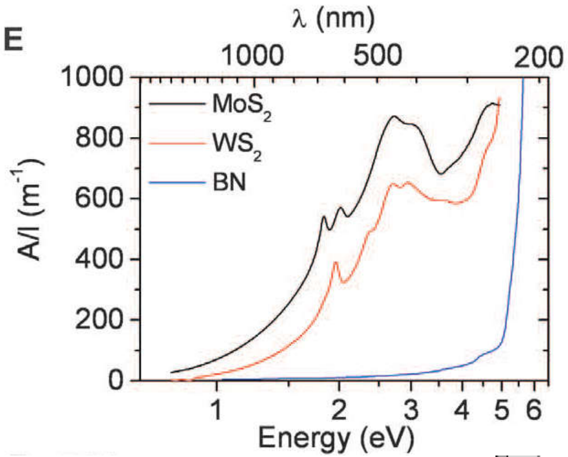

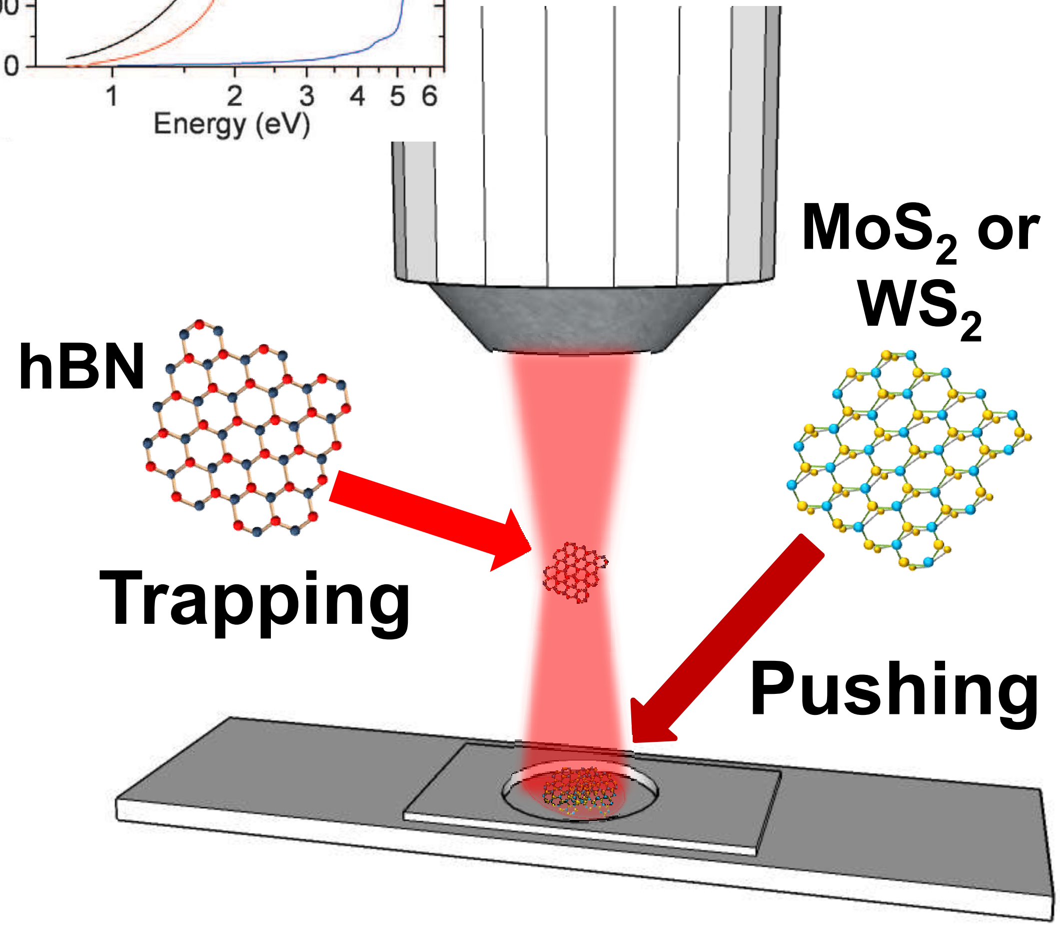

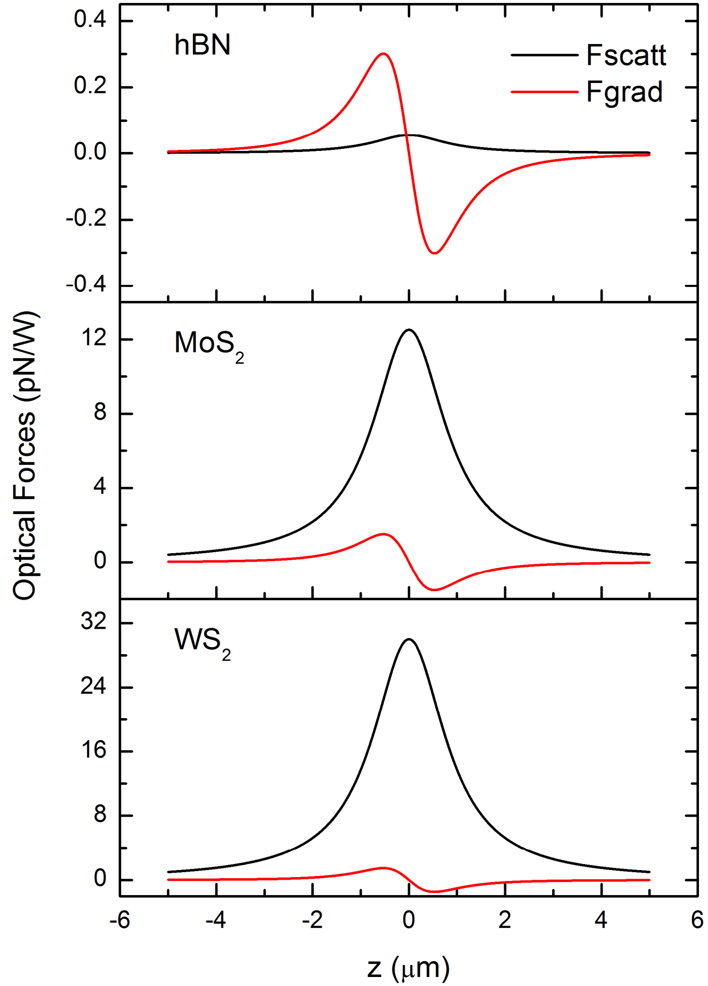

Donato et al., Nanoscale (2018)

RT of hBN flakes

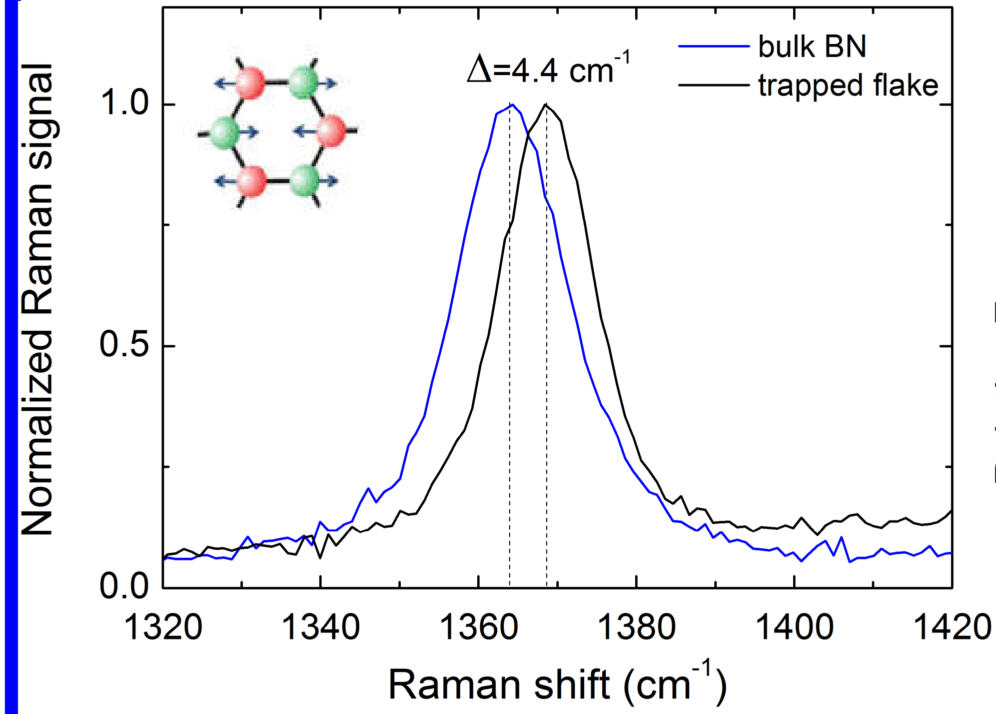

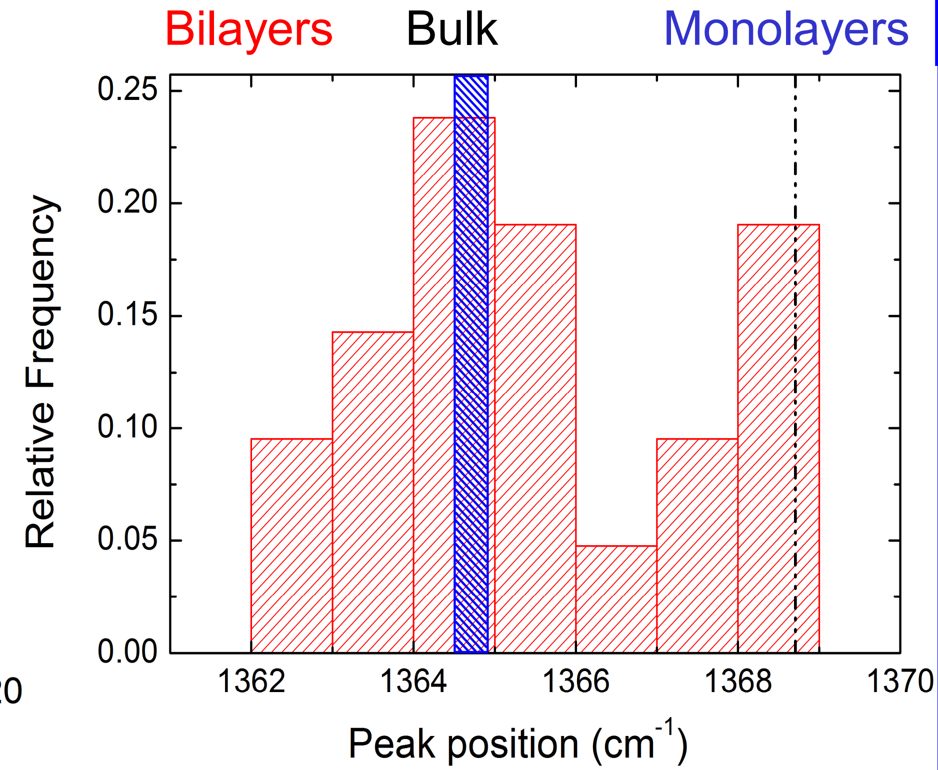

- hBN flakes trapped with **785 & 830 nm laser**
- Trapped flakes have a range of peak positions. The blue-shifted positions (4cm^{-1}) of some peaks (~1370cm^{-1}) suggests that **monolayer flakes** are present in the sample. Presence of **bi-layers** (that should show a 2 cm^{-1} red shift) is also evident.

Donato et al., Nanoscale (2018)

Optical force calibration of hBN

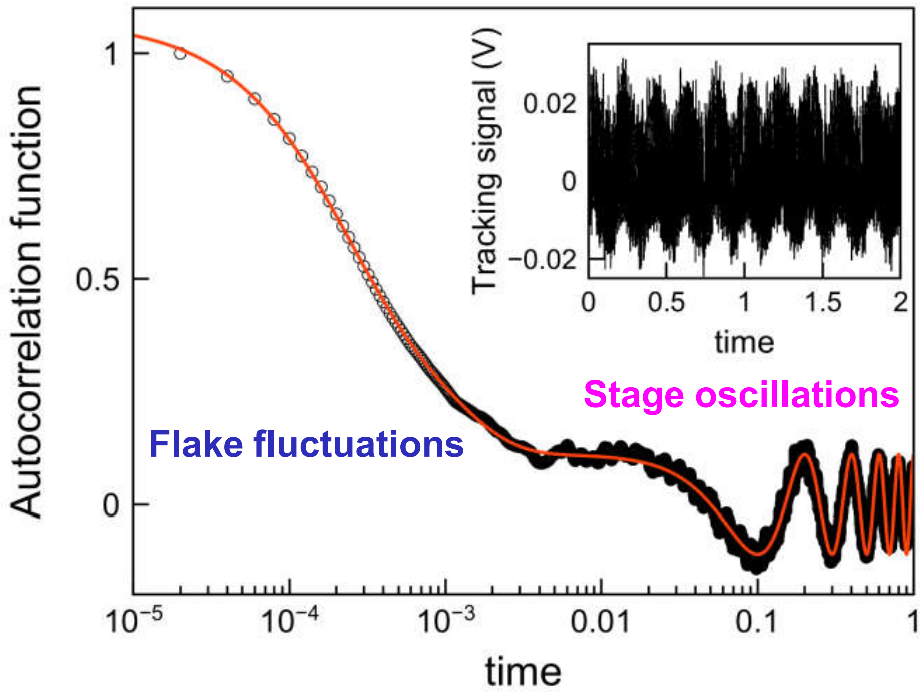

Microscope stage calibration combined with ACFs

Microscope **stage oscillation** yield a sinusoidal modulation of the particle's displacement

$$V_x(t) = x_V(t) + a_V \sin(\omega_{stage} t)$$

All parameters from ACF fitting

Hydrodynamics for a thin disk

$$\gamma_{||} = 8\eta D$$
$$\gamma_{\perp} = \frac{16}{3}\eta D$$
$$\gamma^r = \frac{4}{3}\eta D^3$$

$$C^V{}_{xx}(\tau) = A e^{-\omega_x \tau} + \frac{a_V^2}{2}\cos(\omega_{stage}\tau) = \beta_x^2 \frac{k_B T}{k_x} e^{-\omega_x \tau} + \frac{a_V^2}{2}\cos(\omega_{stage}\tau)$$

ACFs full calibration enable flake size estimates from a simple hydrodynamic model

Donato et al., Nanoscale (2018)

Optical force scaling on hBN

Two-dimensional scaling of optical trapping forces

Polarizability depends on the **area** of the layered particle

Flattening for large flakes (dipole approximatin breaks down)

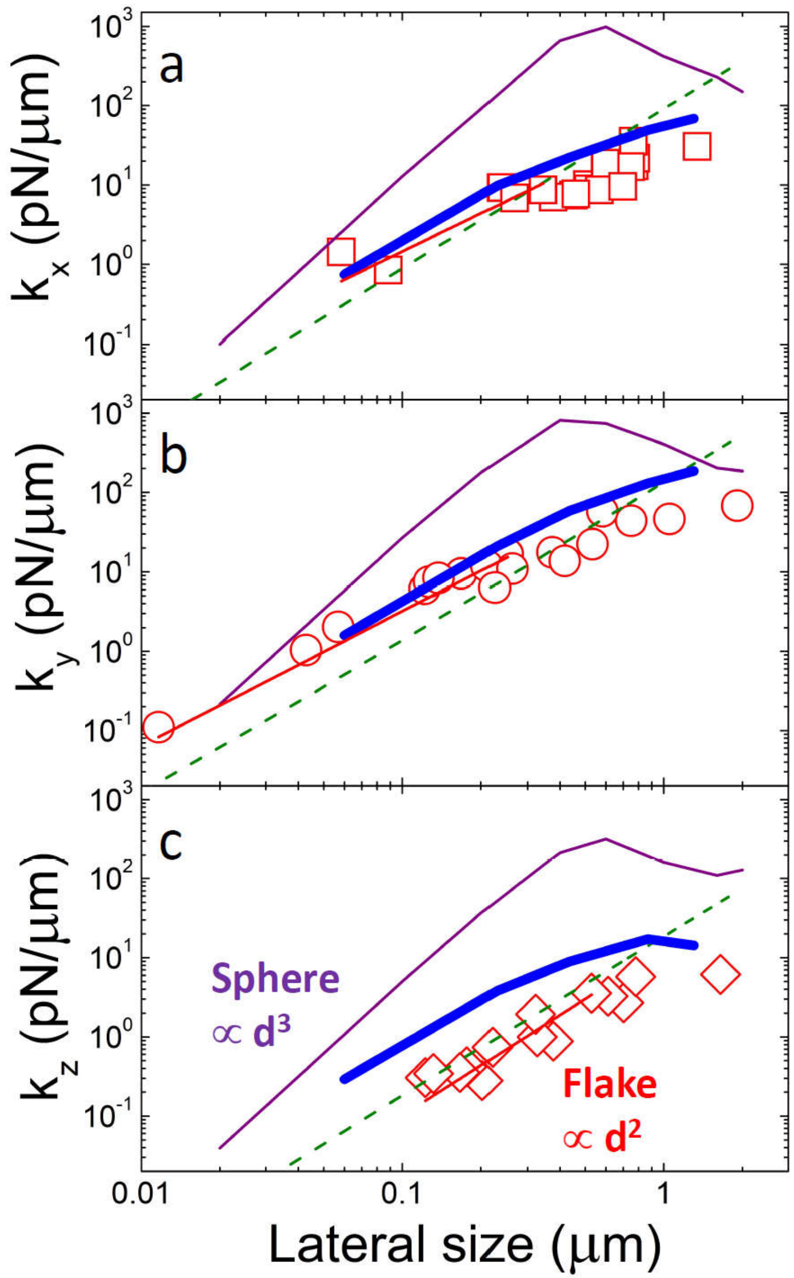

Donato et al., Nanoscale (2018)

Optical force positioning of MoS2 & WS2

Begin pushing

LG-Beam (l=30)

After few minutes

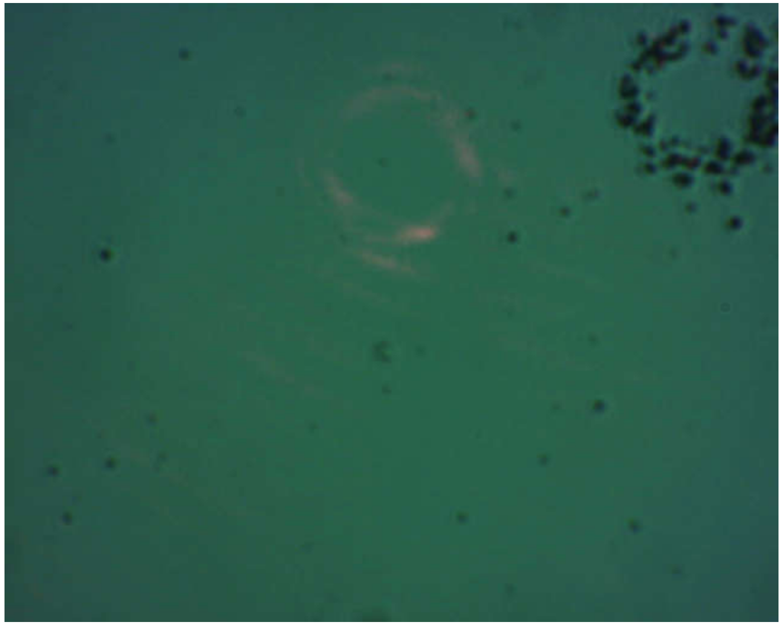

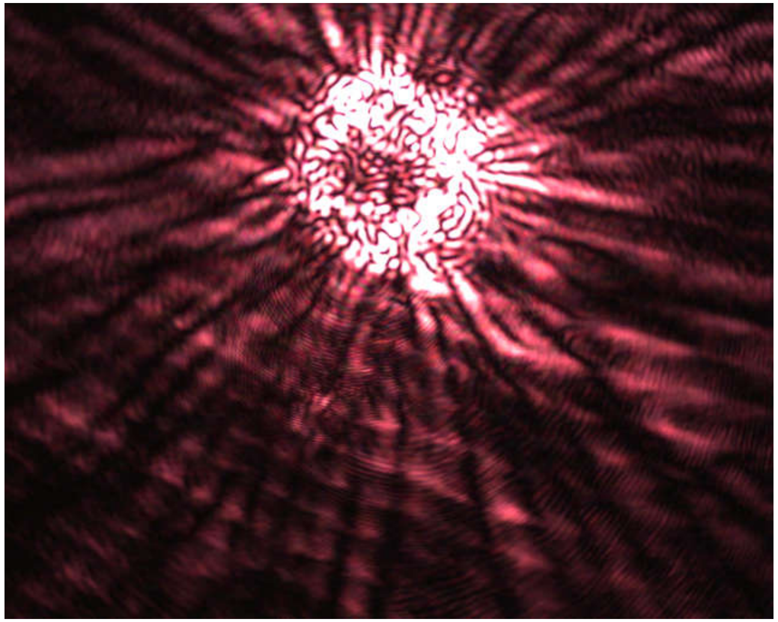

time

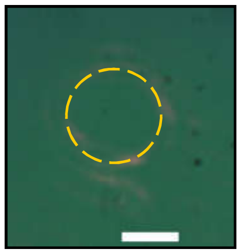

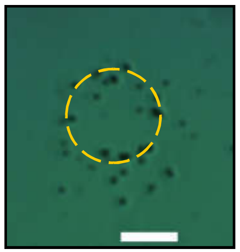

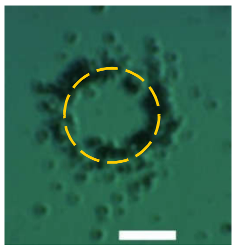

start

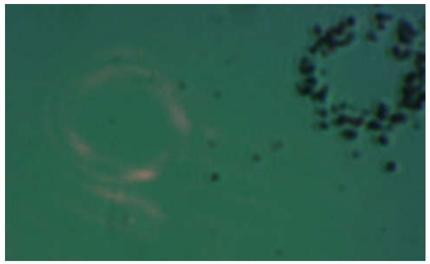

end

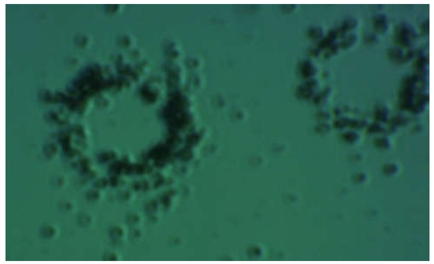

Use proteins (BSA) to glue the structures to a simple glass substrate

Time-evolution of optical force aggregation of MoS2

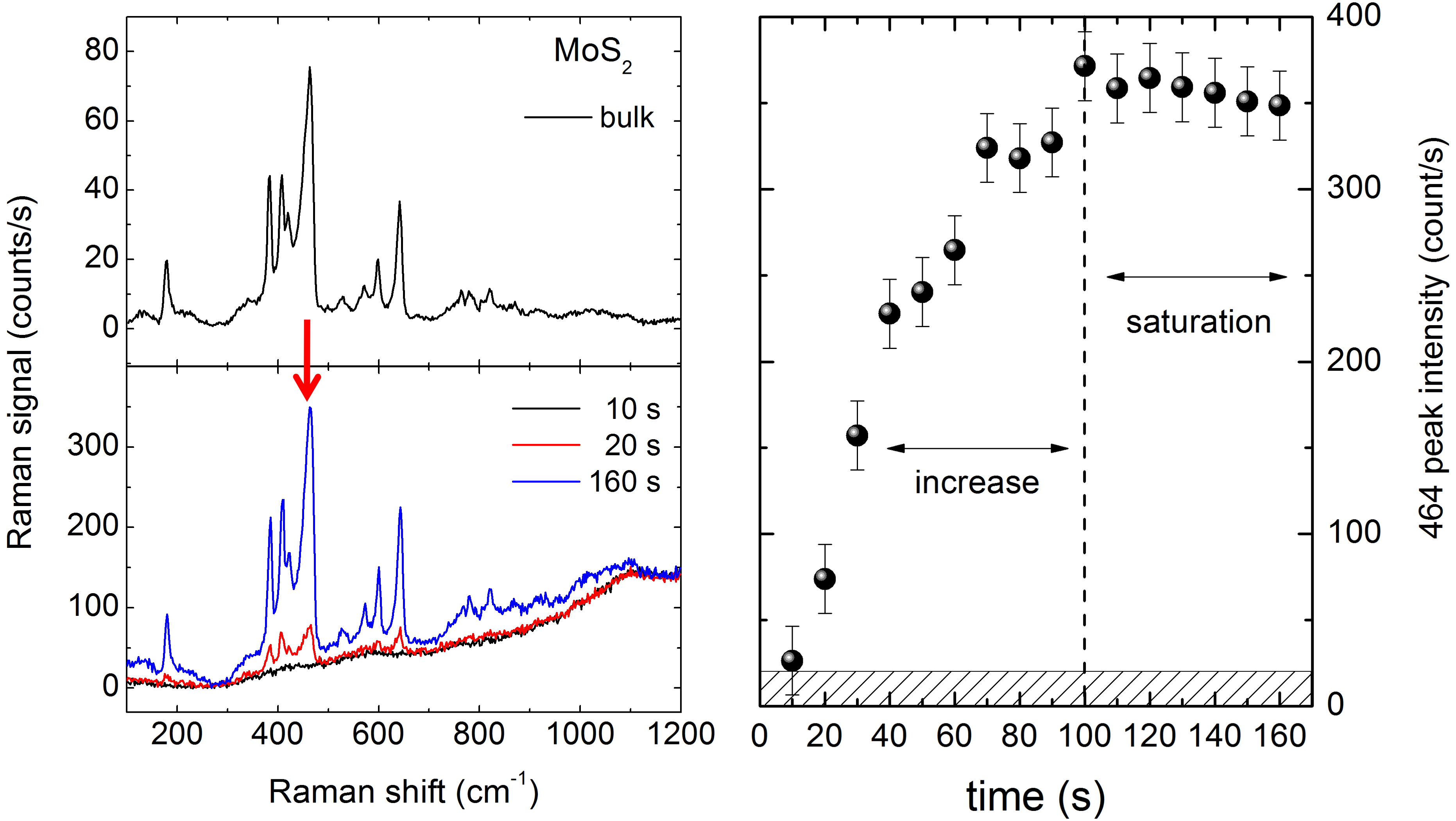

Donato et al., Nanoscale (2018)

Raman Tweezers for Small Microplastics and Nanoplastics Identification in Seawater

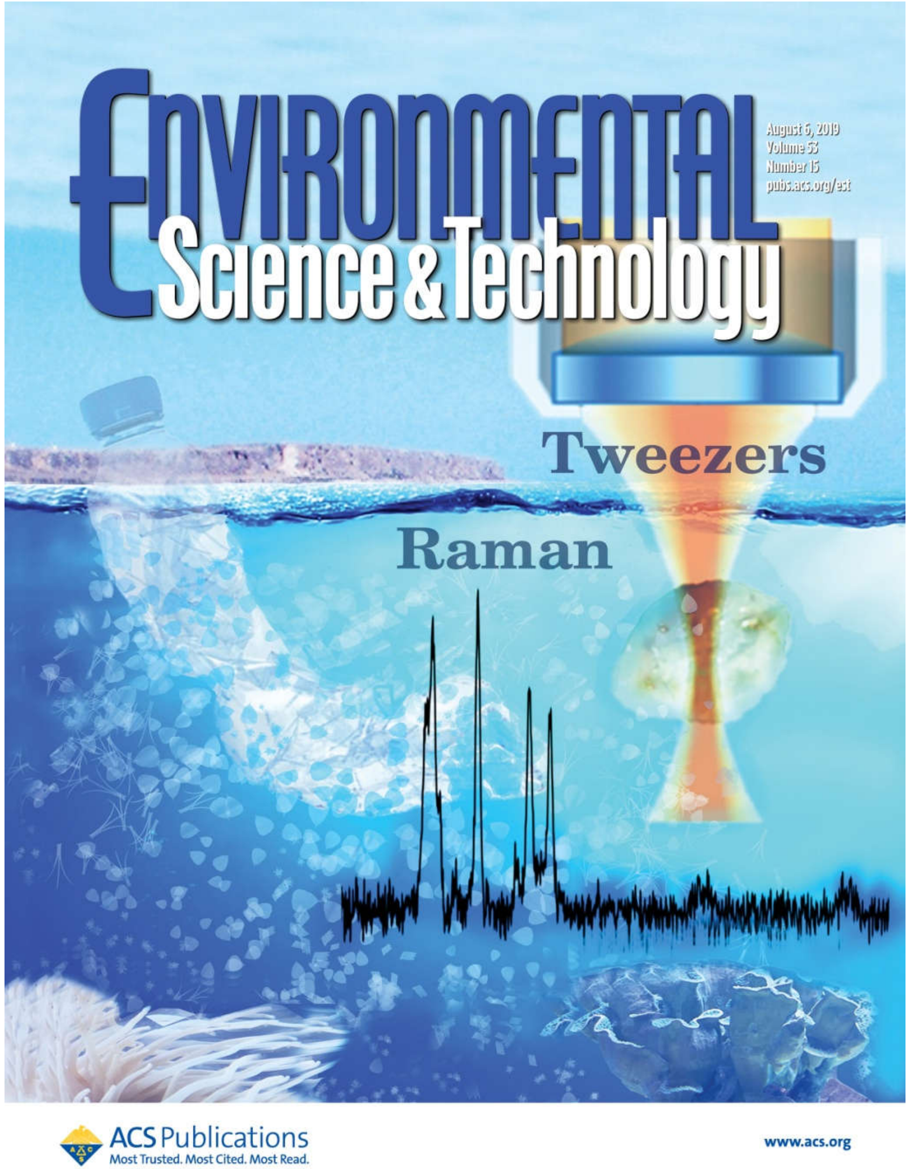

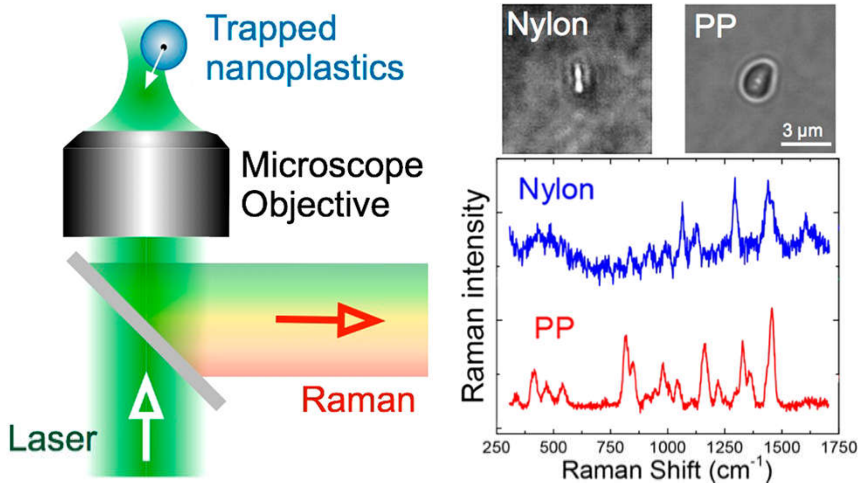

Raman Tweezers permits one to assess the **size and shape** of particles (beads, fragments, and fibers), with spatial resolution only limited by diffraction

Gillibert, R., et al. *Env. Science & Technol.* **53** (2019): 9003.

SERS Tweezers

SERS phenomenology

1. Molecules laying on metal nanoparticles and in their interstices <u>experience an enhanced excitation field</u> due to localized plasmon resonances
2. Molecules will experience an <u>enhancement of the scattered fields</u>

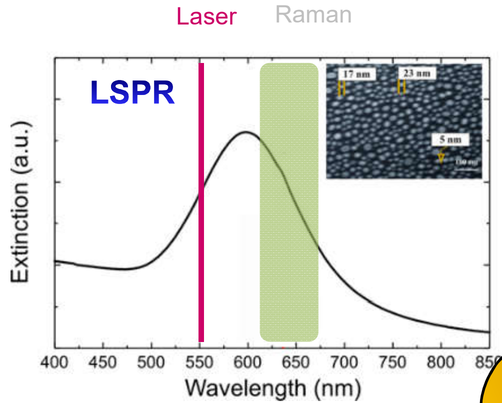

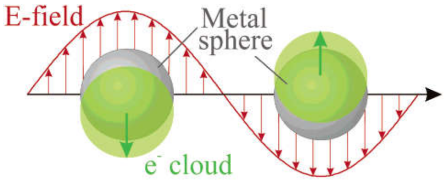

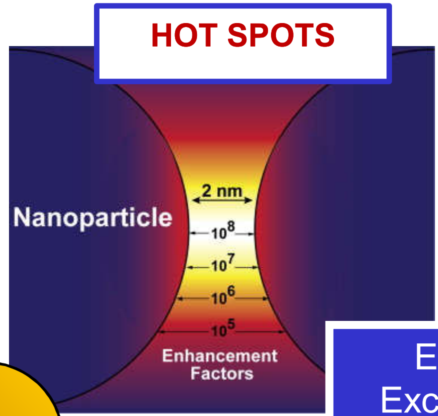

Enhanced Excitation field

$$E_{loc} = \Gamma_{exc}(\lambda_L)E_0$$

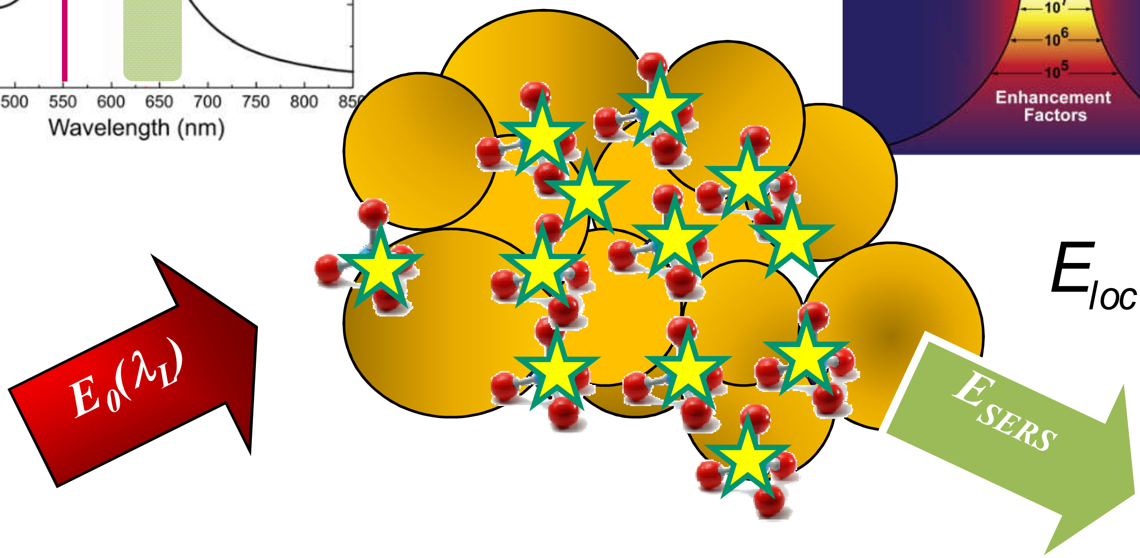

Enhanced Scattering

$$E_{SERS} = \Gamma_{rad}(\lambda_R)E_{Raman}$$

➢ *Fleischman et al., Chem Phys Lett, 26 (1974), p. 123*
➢ *Albrecht MG, Creighton JA, J. Am. Chem Soc., 99 (1977), p. 5215*
➢ *Jeanmaire DL and Duyne RPV, J. Electroanal. Chem, 84 (1977), p.1*
➢ *E.C. Le Ru, P.G. Etchegoin, Phys. Chem. Chem. Phys., 10 (2008), p. 6079*

OT of Au NanoAggregates

V. Amendola

LASiS

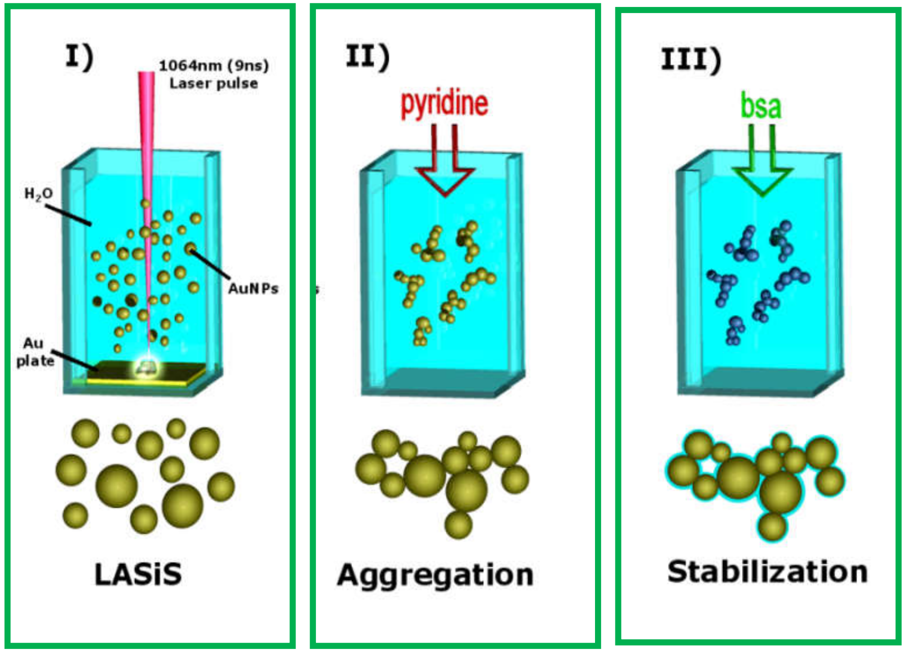

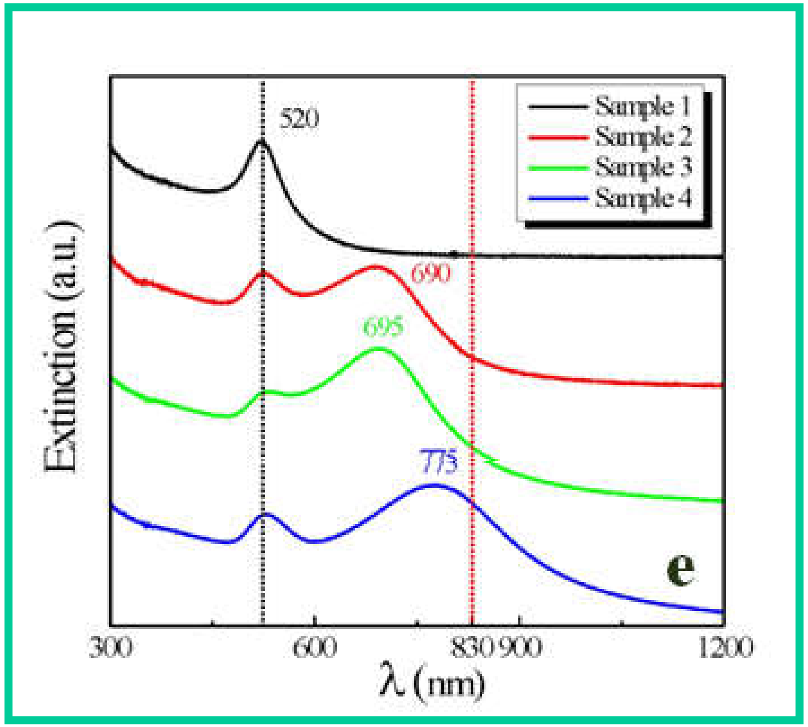

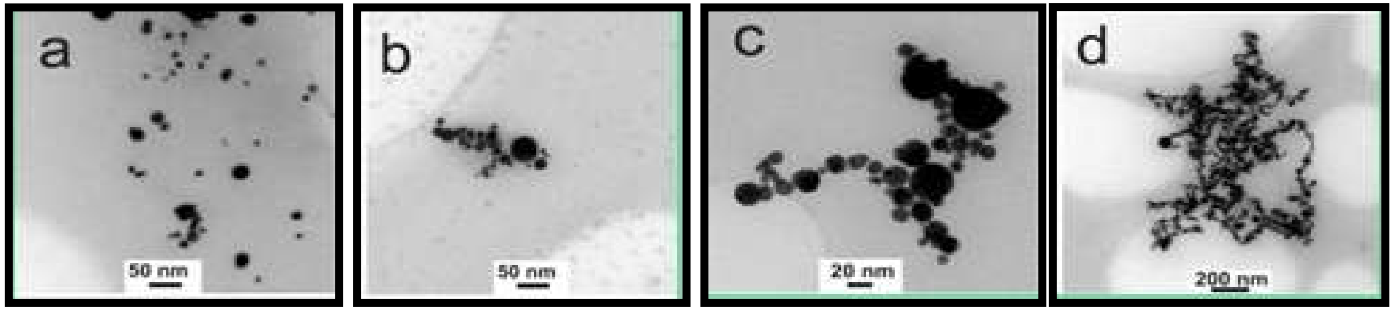

Messina et al., *ACS Nano* **5**, 905 (2011)

Surface-Enhanced Raman Tweezers

V. Amendola

BOVINE SERUM ALBUMIN (BSA)

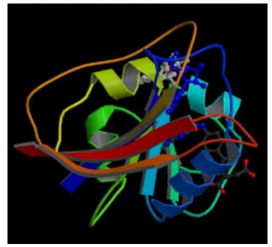

Use the <u>SAME</u> light **to trap and excite** SERS
Trapping wavelength **785nm** > **695nm** MNP Aggregate SPR

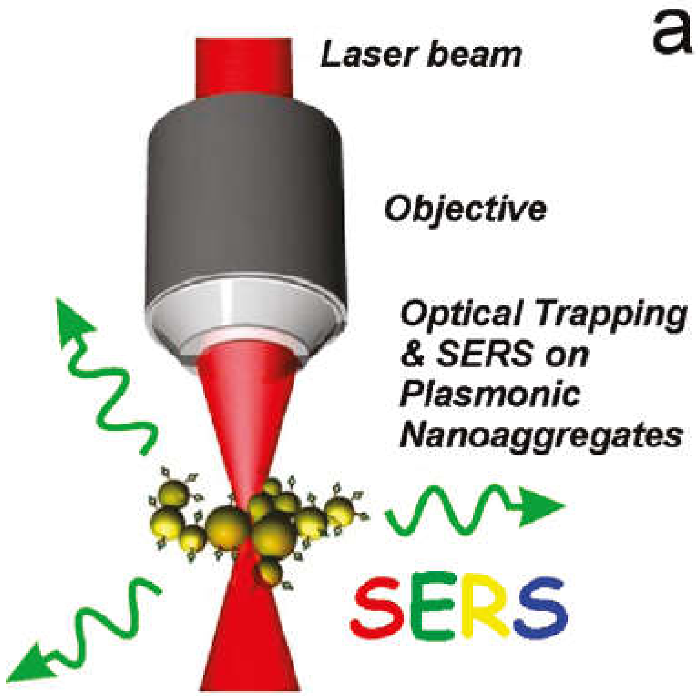

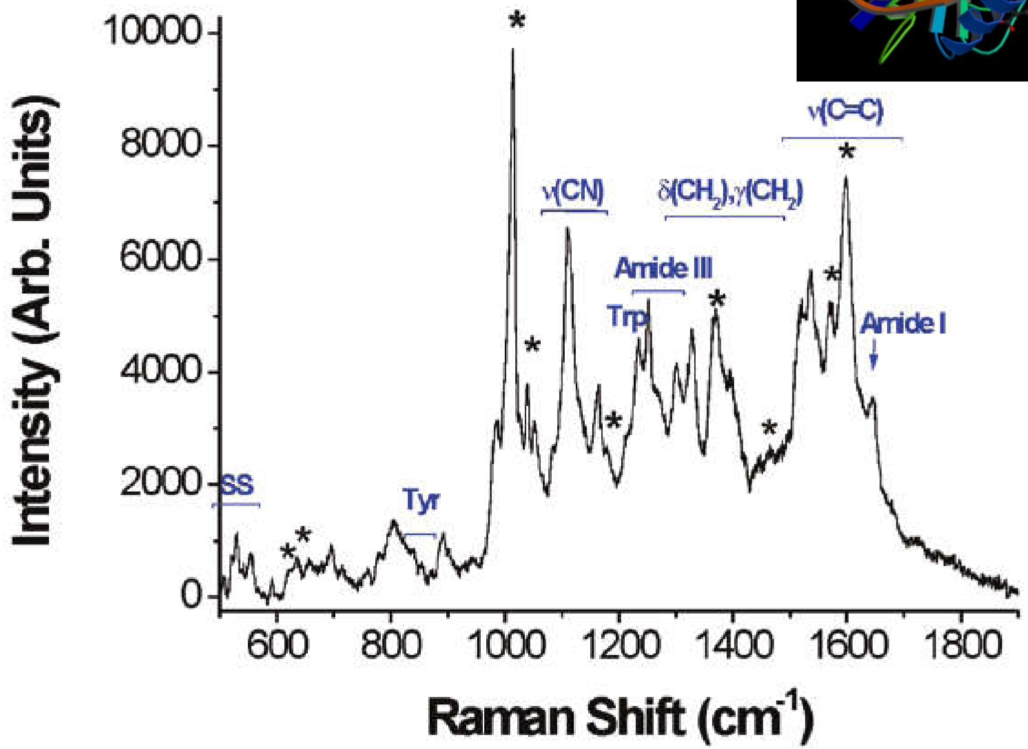

Messina et al., *J Phys Chem C* **115**, 5115 (2011)
Messina et al., ACS Nano **5**, 905 (2011)

The huge electromagnetic field enhancement enables dramatic increase of the vibrational signal of molecules located in the *hot spots*.

A biosensor based on optical forces

Optical forces aggregates plasmonic particles and create **“hot spots”on demand**

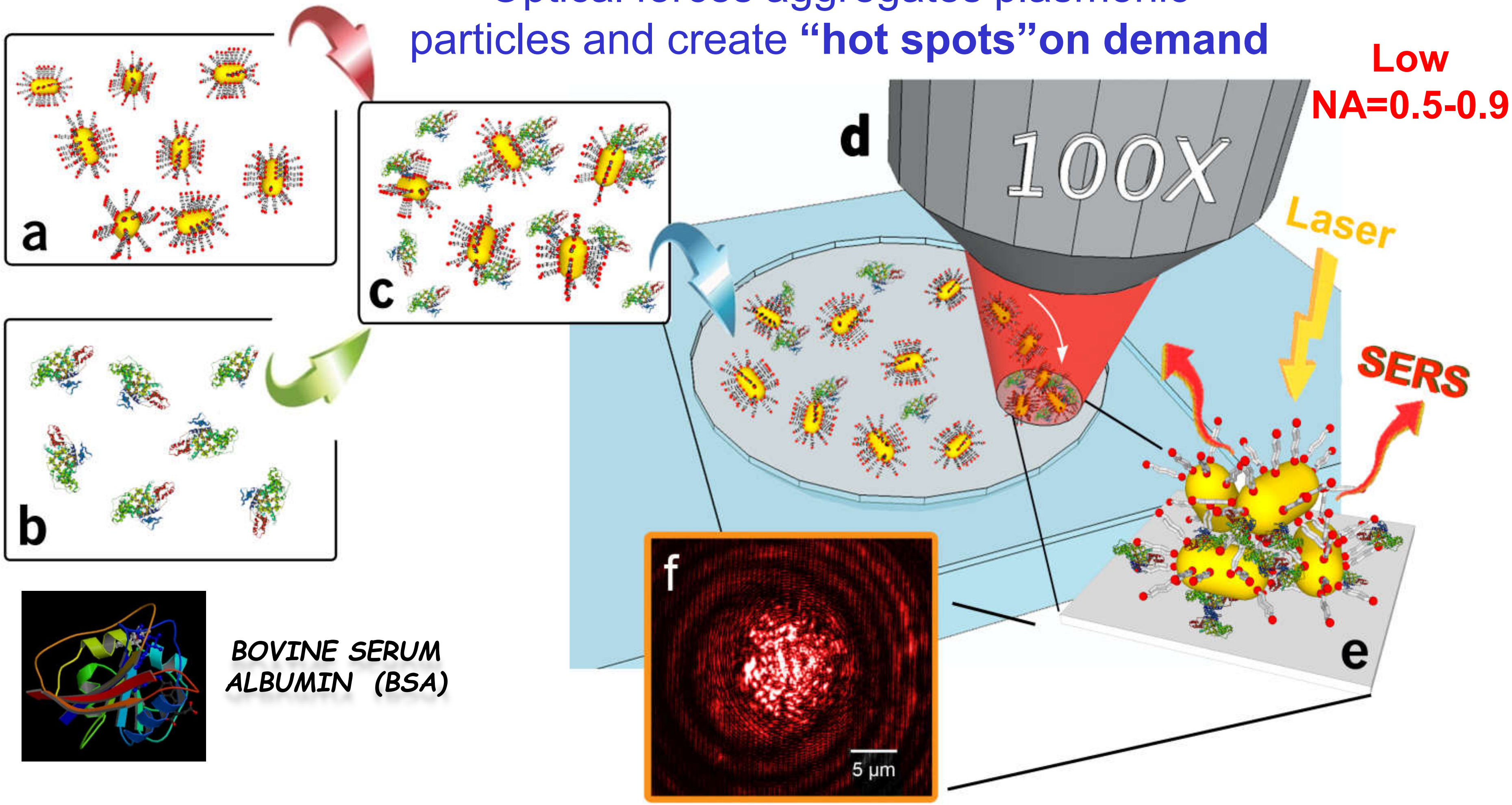

BOVINE SERUM ALBUMIN (BSA)

Use the **SAME** light **to push and excite** SERS, Pushing wavelength **633nm** < **687nm** Nanorods SPR

Proteins (BSA) are detected directly in their **natural (PH)** liquid environment with high sensitivity

B. Fazio, et al., Scientific Reports 6 (2016): 26952

Time evolution of SERS spectra

a. Phe ring breathing
b. Aromatic aminoacids and Amide I
c. CH stretching region

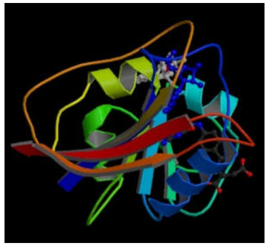

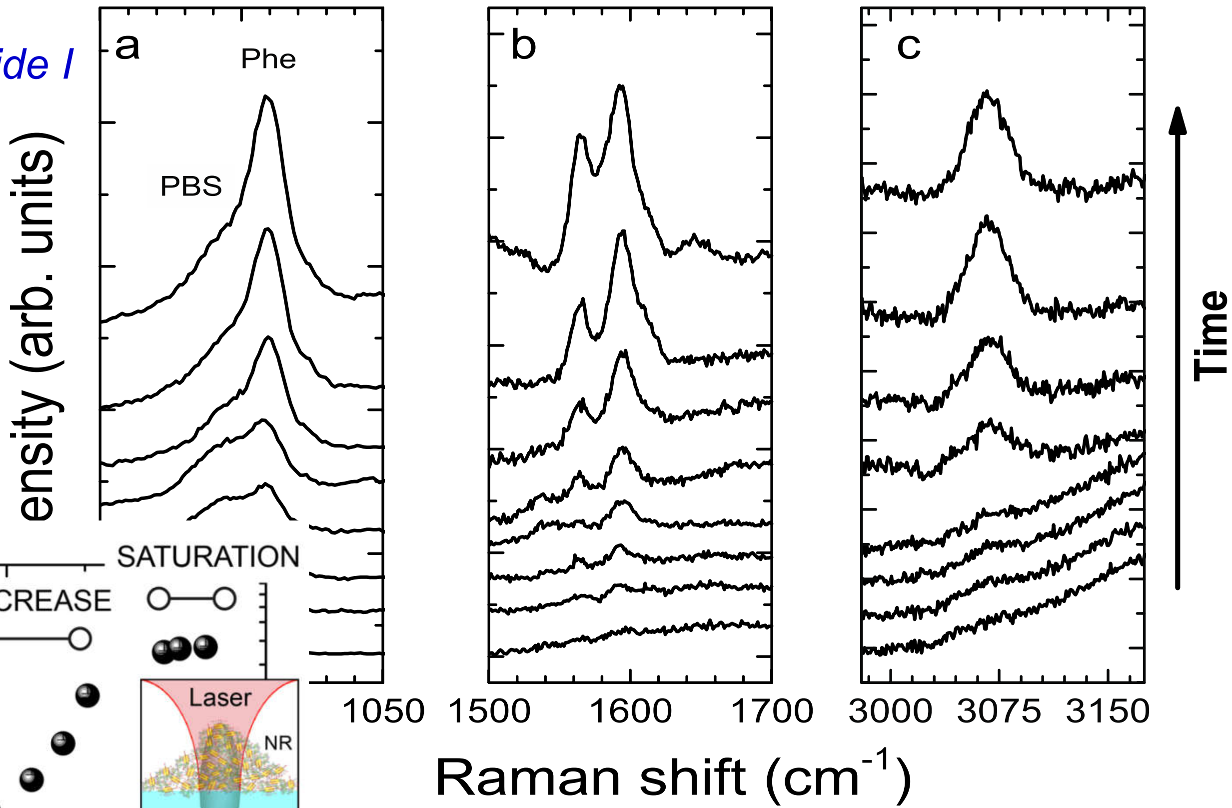

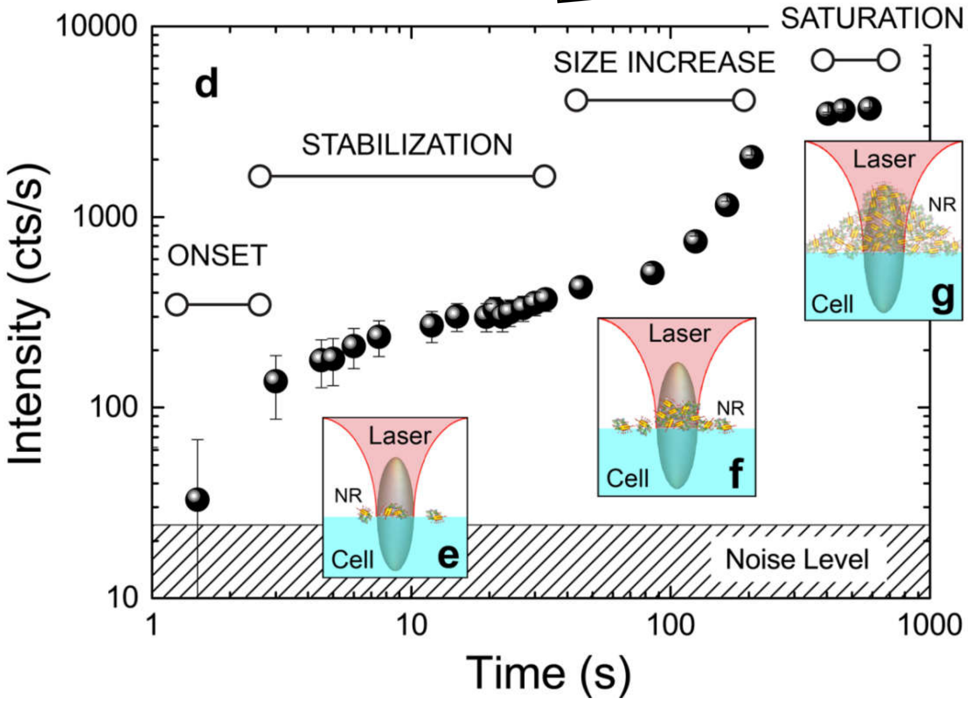

Time evolution of SERS signals can be used to study the dynamics of aggregation.

This depends on wavelength and power.

SERS Detection at low molar concentration

Creation of HOT SPOT region in liquid environment for high sensitive spectroscopy

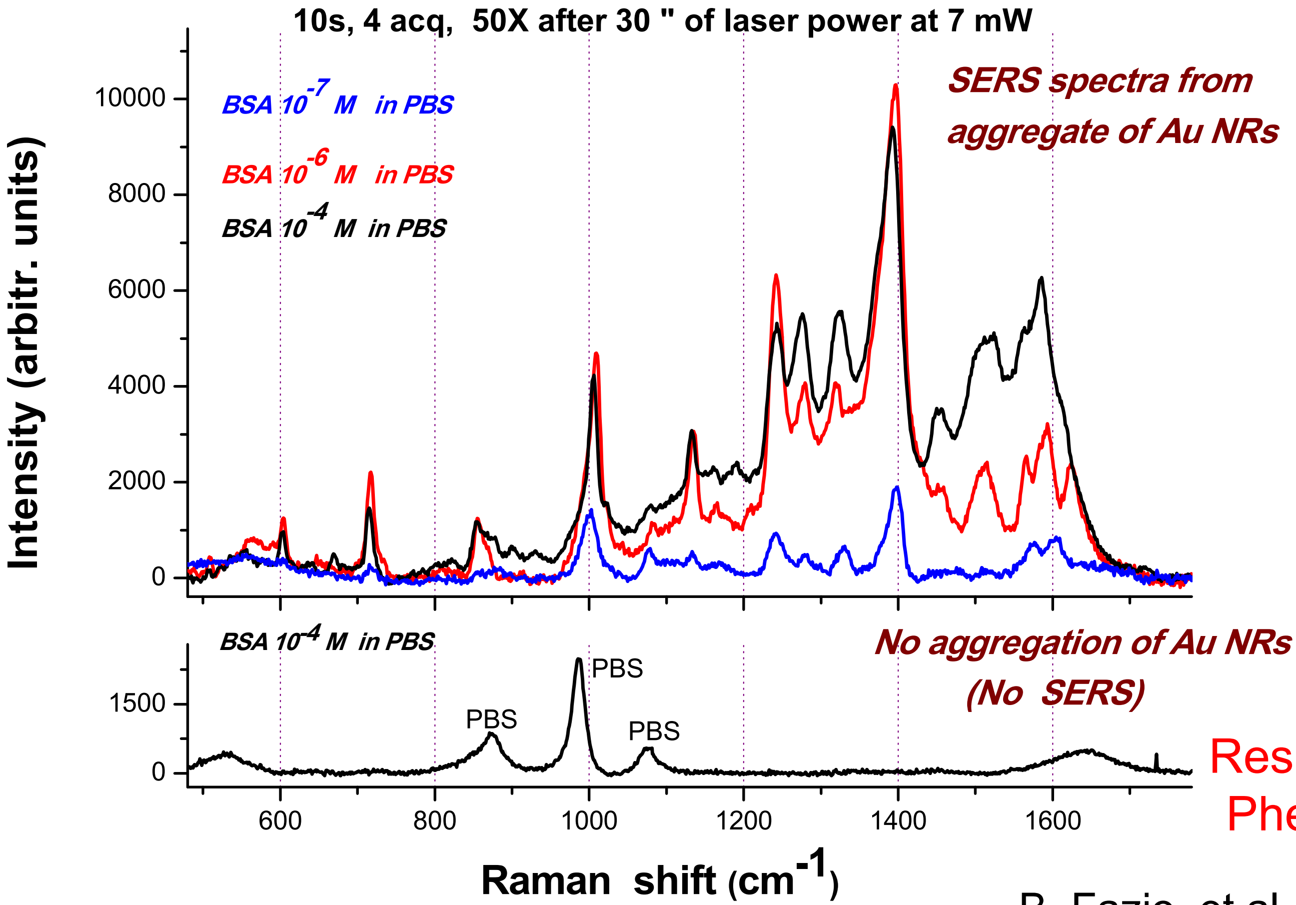

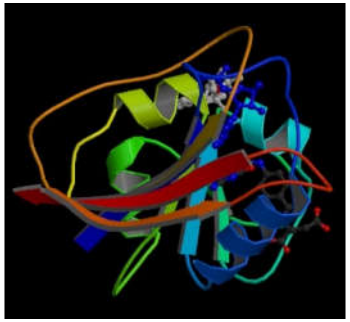

•Detection of **BSA** at concentrations as low as **10^{-7} M**

•Enhancement of BSA Raman scattering by **5 orders of magnitude**

Results also with Lysozyme, Phenylalanine, and Mnsod

B. Fazio, et al., Scientific Reports (2016)

Wavelength dependence

P=4 mW, after 500 s

S. Bernatova, et al., J. Phys. Chem C (2019)

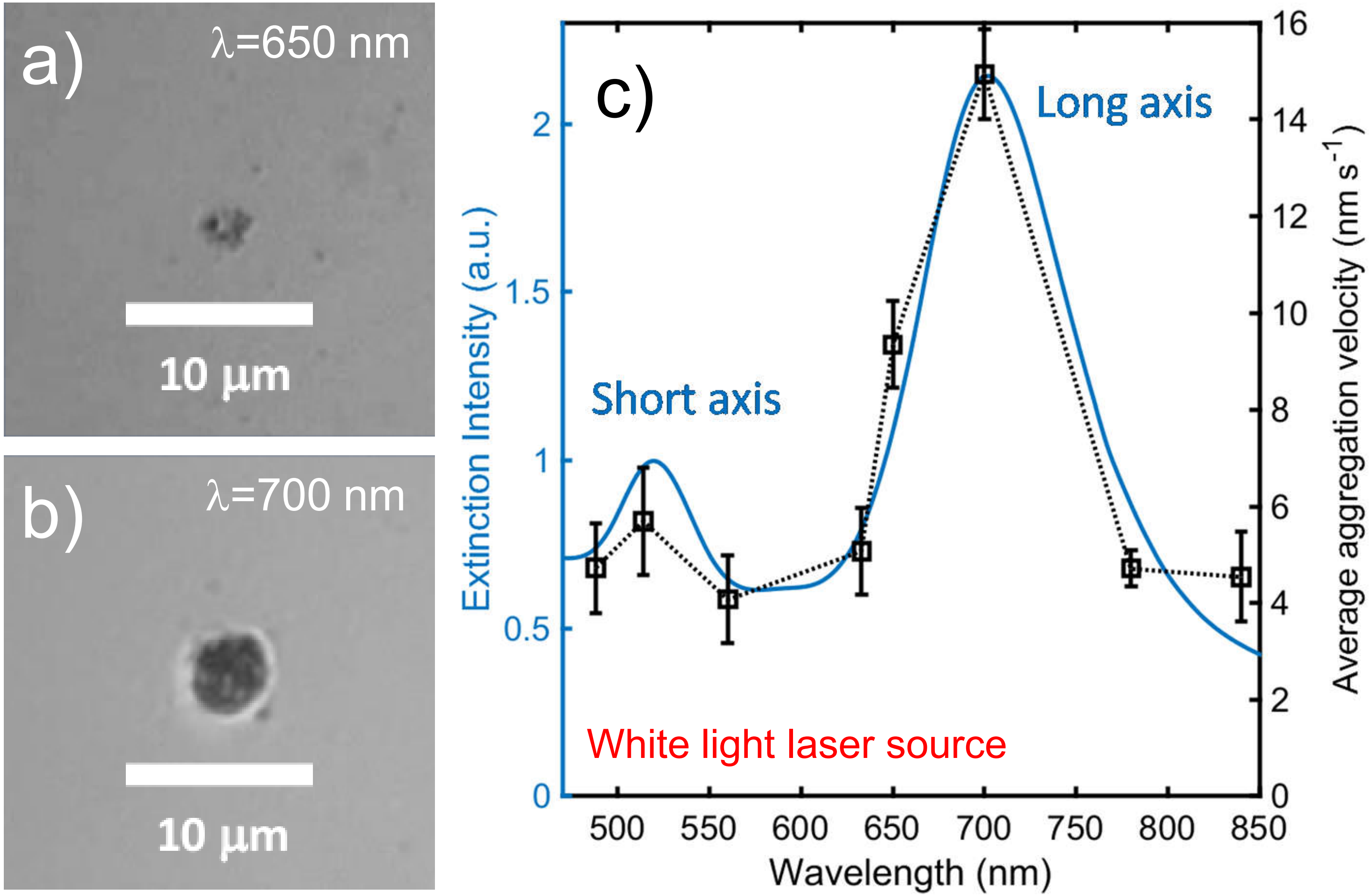

Average velocity of aggregation is estimated in the linear regime (before saturation) as the size of the aggregate divided by the aggregation time

Power dependence of aggregation velocity

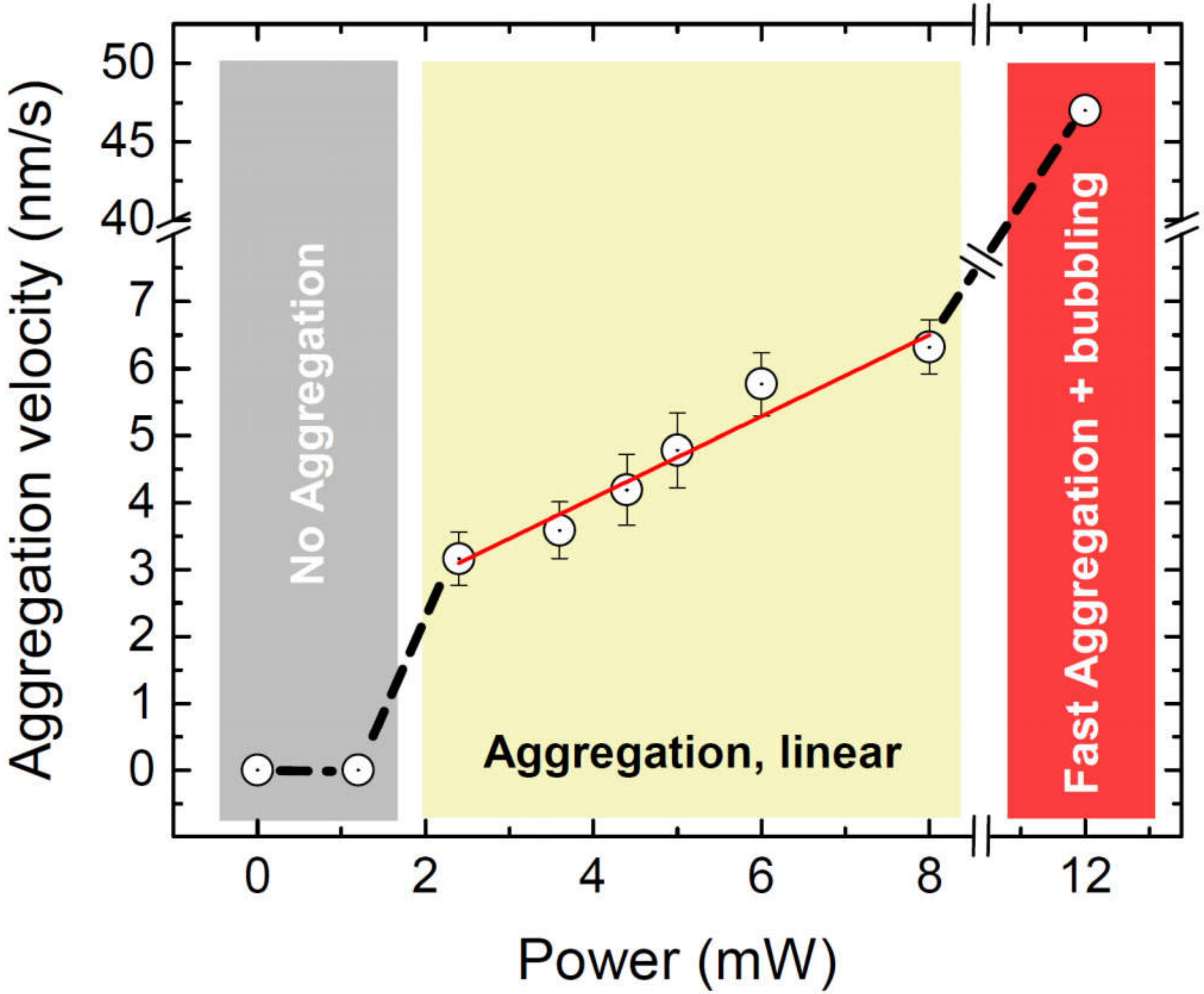

S. Bernatova, et al., J. Phys. Chem C (2019)

Controlled patterning for in situ SERS detection

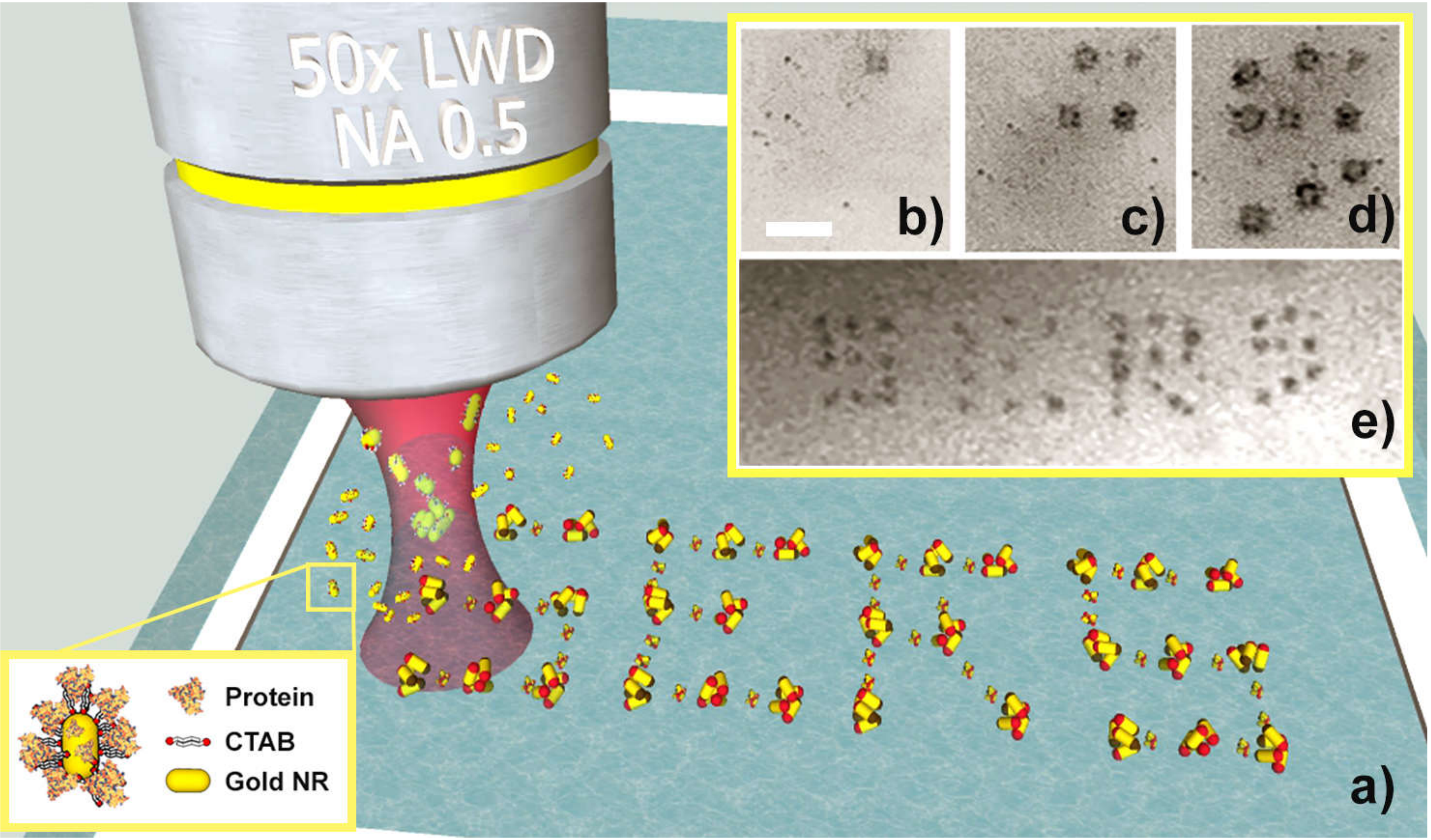

A. Foti et al., Materials **11**, 440 (2018)

Outlook

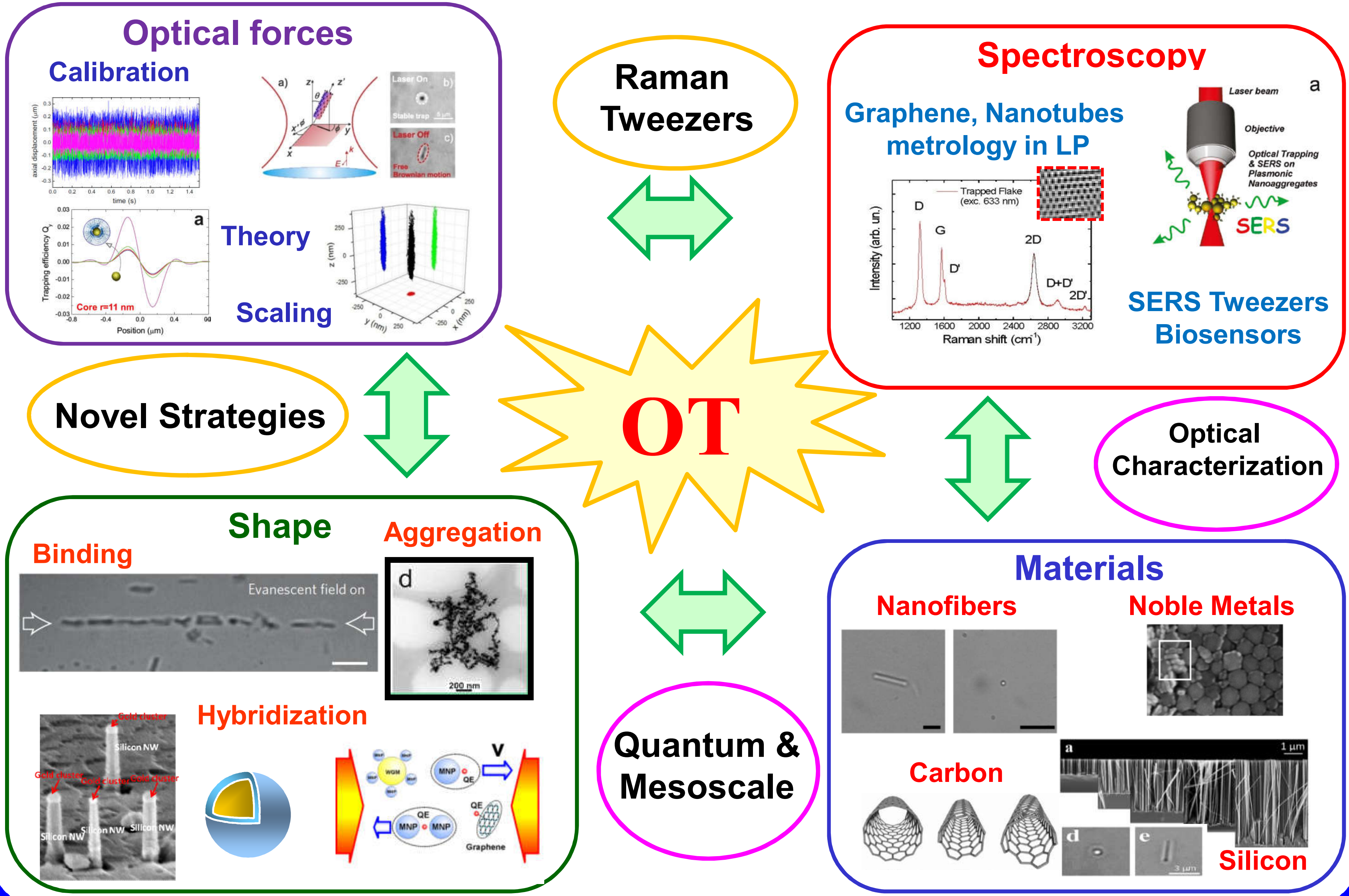
Optical forces
Calibration
Theory
Scaling
Core r=11 nm
Raman Tweezers
Spectroscopy
Graphene, Nanotubes metrology in LP
Trapped Flake (exc. 633 nm)
D
G
D'
2D
D+D'
2D'
Intensity (arb. un.)
Raman shift (cm-1)
Laser beam
Objective
Optical Trapping & SERS on Plasmonic Nanoaggregates
SERS
SERS Tweezers
Biosensors
Novel Strategies
OT
Optical Characterization
Shape
Binding
Evanescent field on
Aggregation
200 nm
Hybridization
Gold cluster
Silicon NW
MNP
QE
WGM
Graphene
V
Quantum & Mesoscale
Materials
Nanofibers
Noble Metals
Carbon
Silicon
1 μm
3 μm

SPACE Tweezers

Optical forces were "born" in SPACE

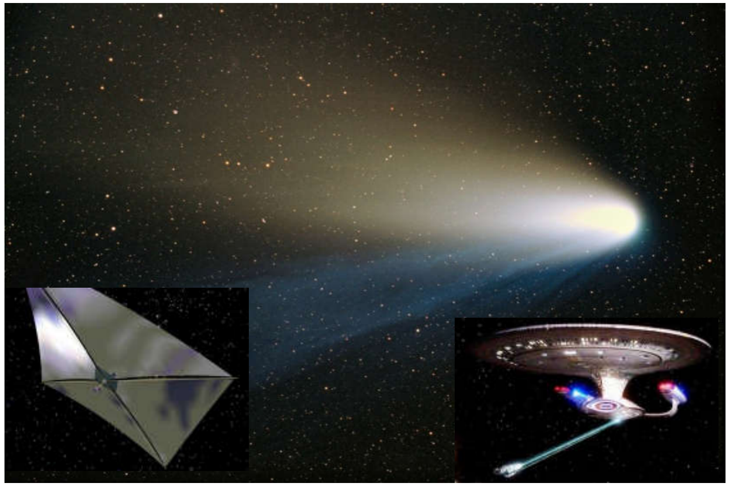

Starshot project for a laser-driven lightsail

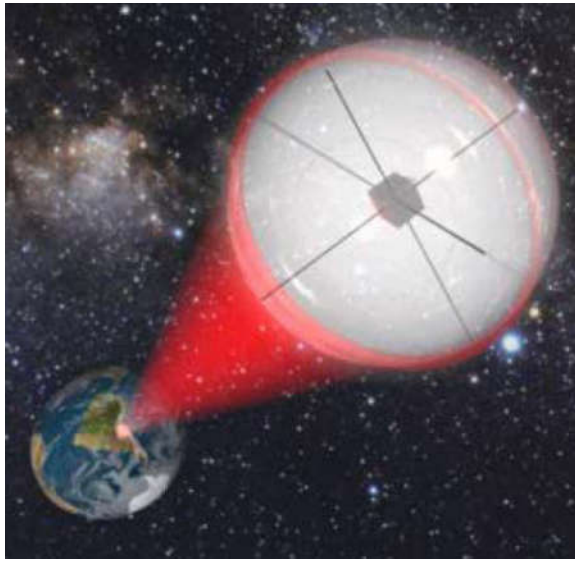

Nanomaterials and nanophotonic design

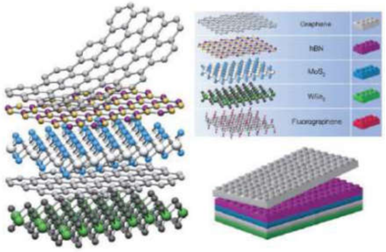

Atwater et al. Nat Mater. (2018)

Bring them back "home"

Trap and investigate **nanoparticulate** matter in space or planetary atmospheres

Sunset from Vulcano, Onofrio M. Maragò

SPACE Tweezers

Optical forces were “born” in SPACE

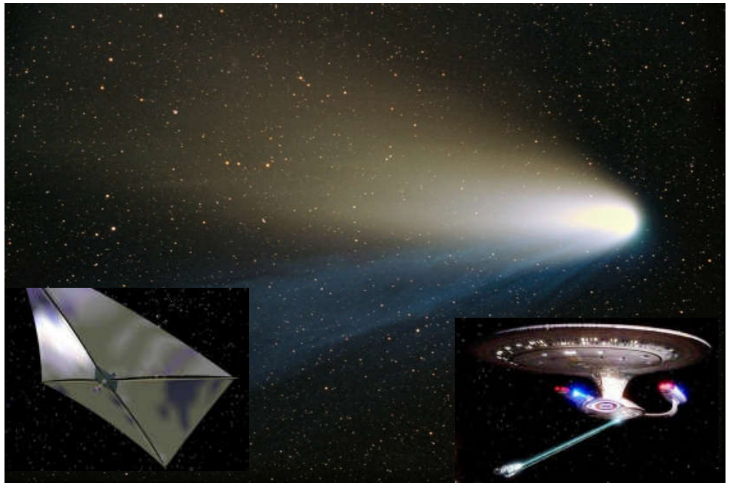

Bring them back “home”

Trap and investigate **nanoparticulate** matter in space or planetary atmospheres

Starshot project for a laser-driven lightsail

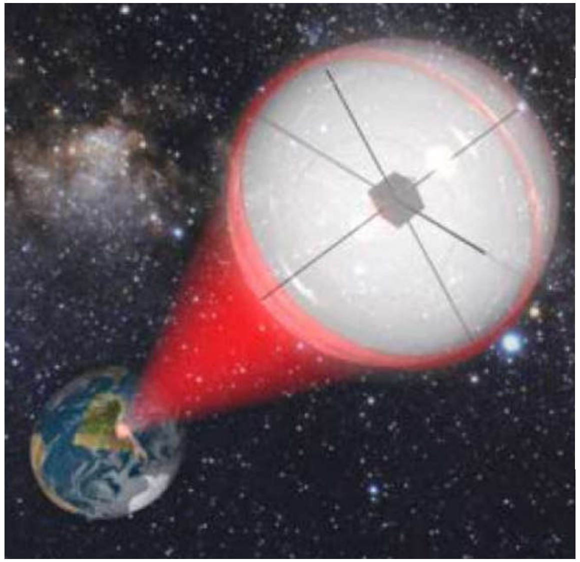

Atwater et al. Nat Mater. (2018)

Nanomaterials and nanophotonic design

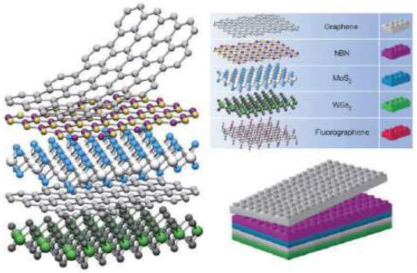

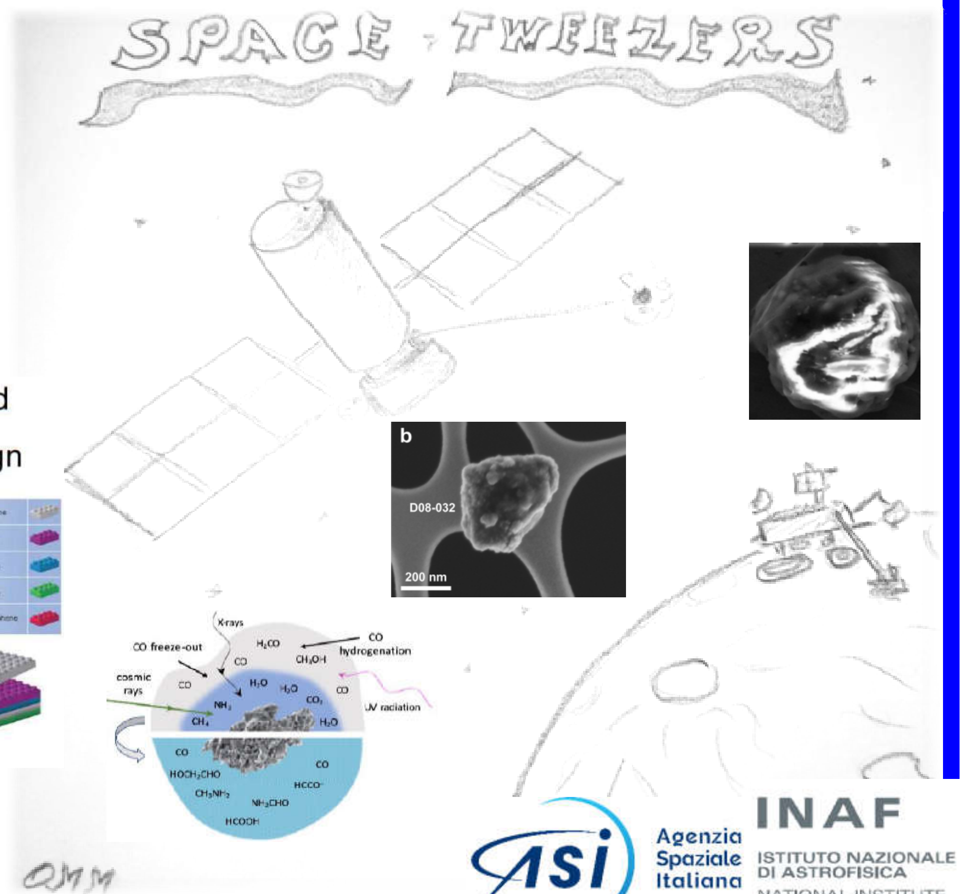

Agenzia Spaziale Italiana
INAF
ISTITUTO NAZIONALE DI ASTROFISICA
NATIONAL INSTITUTE FOR ASTROPHYSICS

Localised surface plasmon

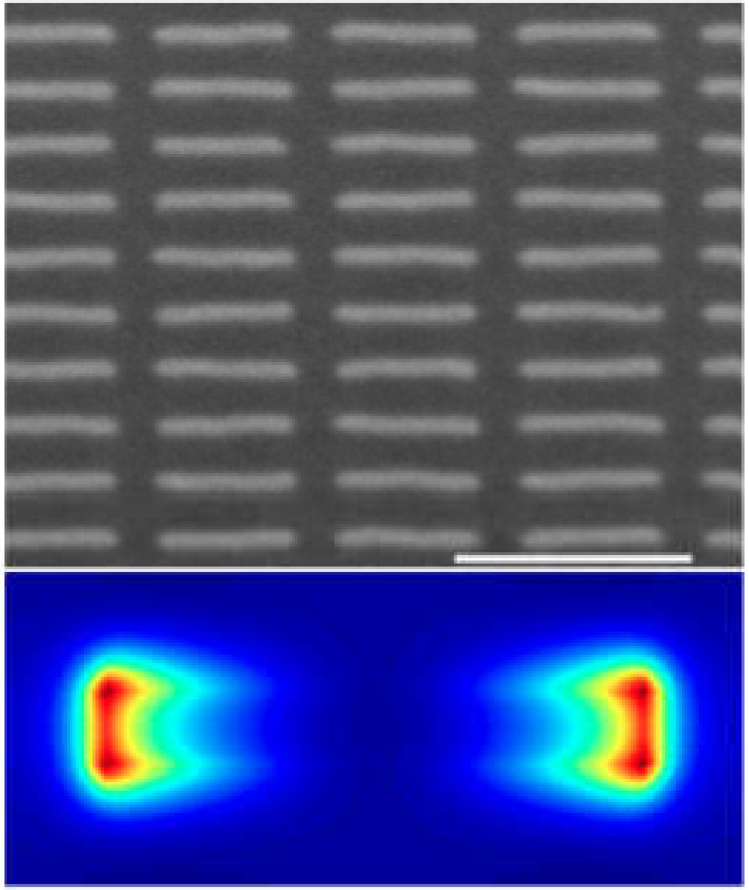

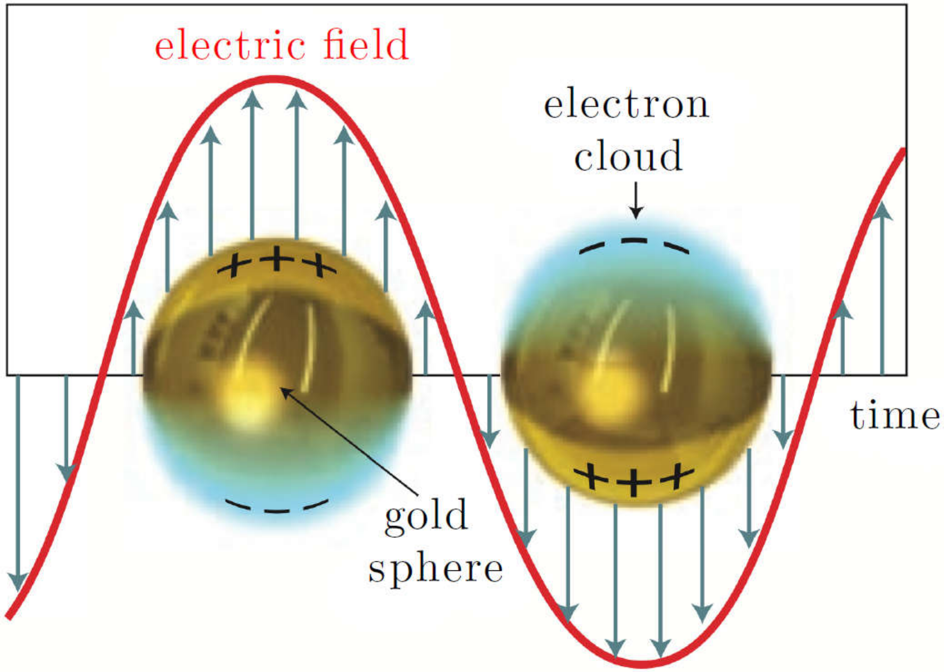

⇒ **Collective oscillation of the electrons inside the nanoparticle**

⇒ **Interaction with light**

Amendola, V., Pilot, R., Frasconi, M., Maragò, O. M., & Iatì, M. A. (2017). **Surface plasmon resonance in gold nanoparticles: a review**. *J. Phys.: Cond. Matt.*, *29*, 203002.

Plasmonic Tweezers

Juan et al., Nat. Photon. **5**,349 (2011); Maragò et al., Nat. Nano. **8**, 807 (2013)

Surface Plasmon Polaritons
Plasmonic landscape (microscale)

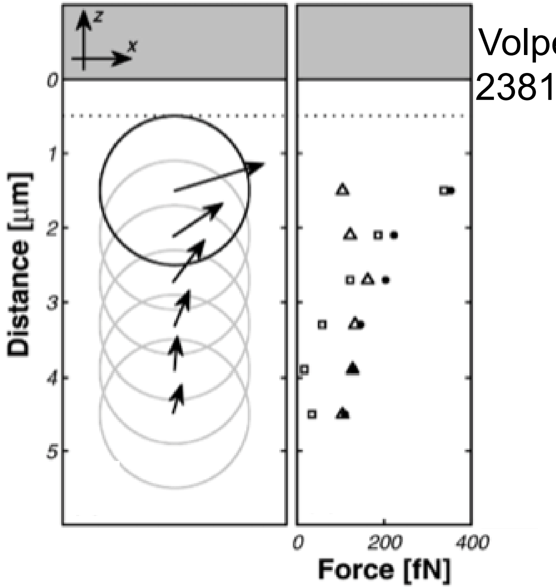

Volpe, PRL 96, 238101 (2006).

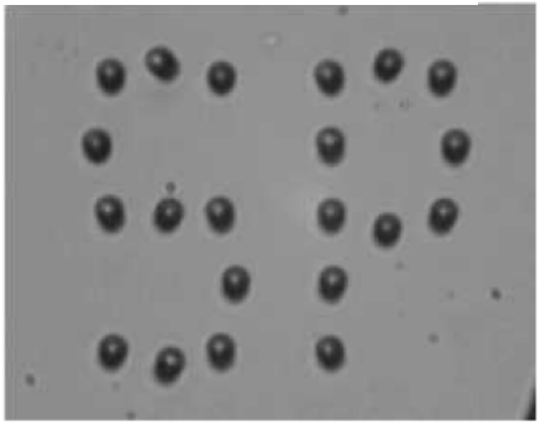

Righini, Nat. Phys. 3, 477 (2007).

Localized Plasmon Polaritons
Nanoantennas (*hot spot* trapping, nanoscale)

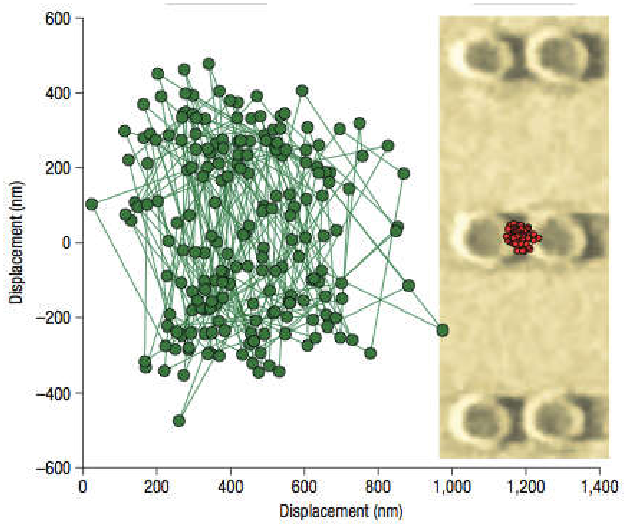

Grigorenko, Nat. Photon. 2, 365 (2008).

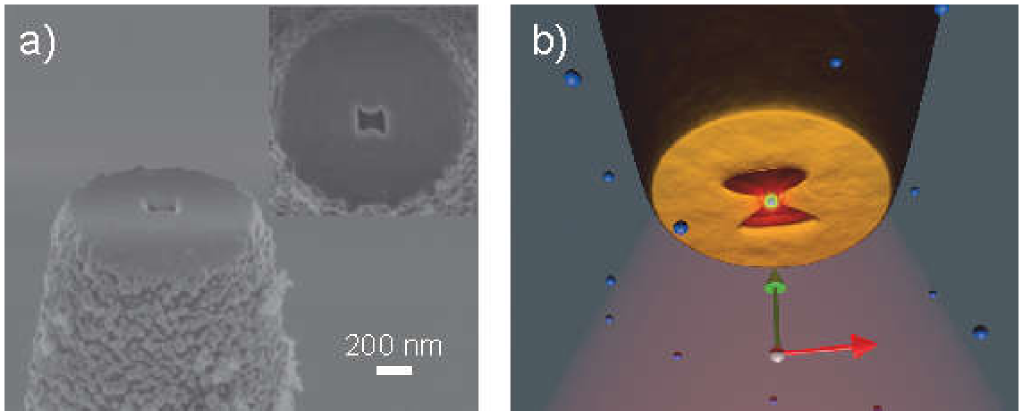

Berthelot, Nat. Nano. 9, 295 (2014).

BSA+Nanorods Extinction

In solution UV spectra
do not change

NRs are aggregated by optical forces
and **glued by plasmonic heating** at the
surface of the sample chamber

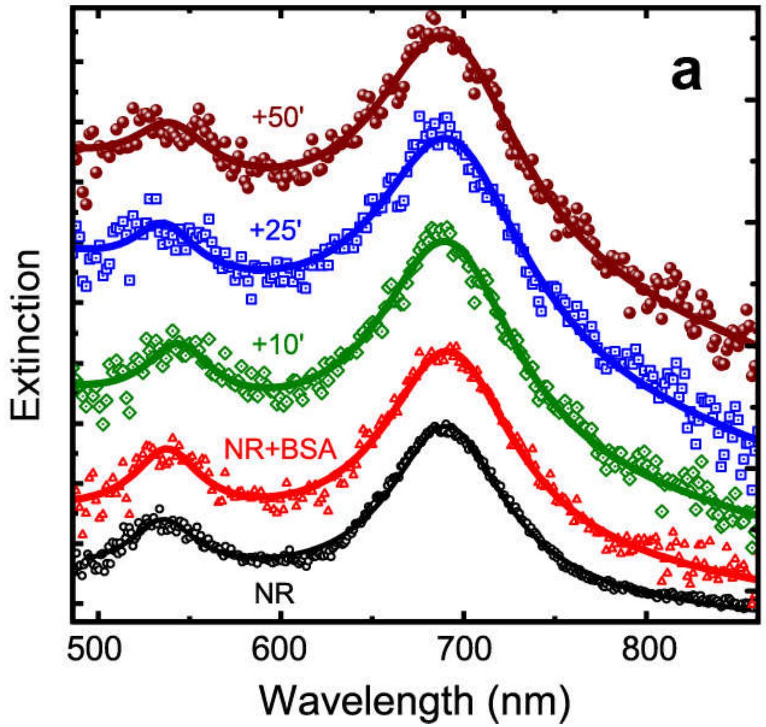

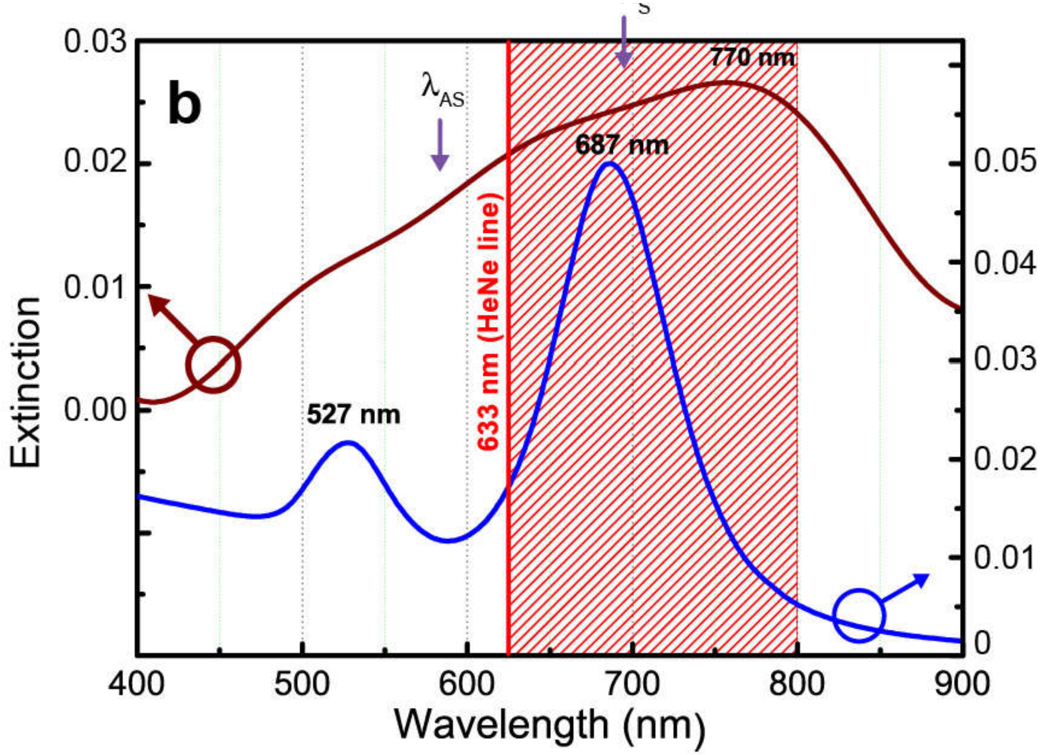

- ✓ **Protein-Nanorods complexes** in solution are composed by **individual NRs surrounded by protein layer.**

- ✓ **Broadening and red-shift** of the plasmon resonance, **nanorods are coupled**. This leads to enhanced fields, and then, SERS amplification of biomolecules spectra.

B. Fazio, et al., Scientific Reports (2016)

Optical Tweezers & Force Sensing

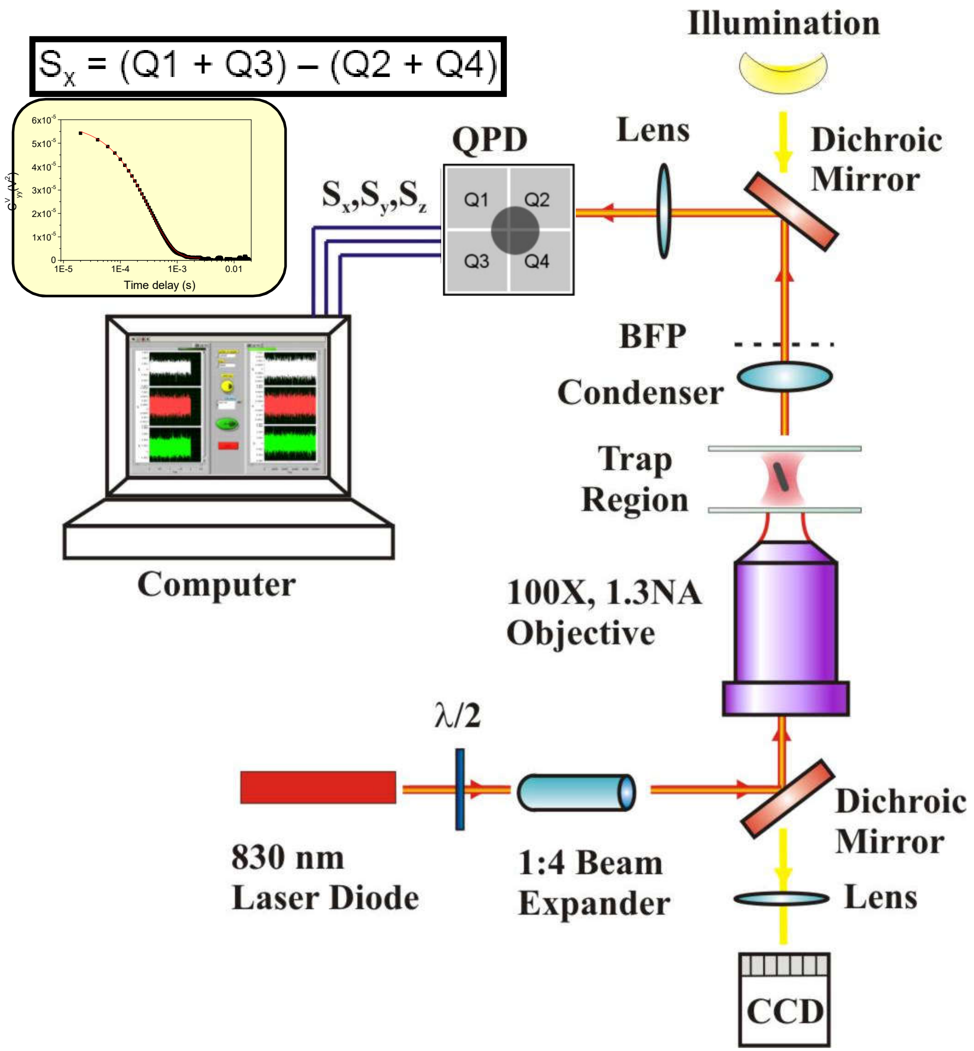

- Standard OT with QPD forward or back detection
- Multiwavelength: **830nm, 785nm**, 633nm, 417nm, **White Light Source**
- Radial Polarizer (arcoptics)
- Piezostage (1nm resolution)
- LC waveplate
- Galvomirrors

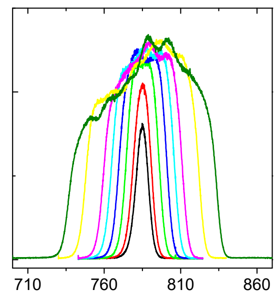

Back focal plane interferometry combined with a QPD is sensitive to Brownian fluctuations

Brownian motion is a key ingredient in Force Sensing with optical tweezers.

NIR light ensures very low water absorption

How do we measure forces?

We measure the interference pattern between scattered and unscattered light in the back focal plane on a QPD. Time evolution is proportional to the particle positional fluctuations.

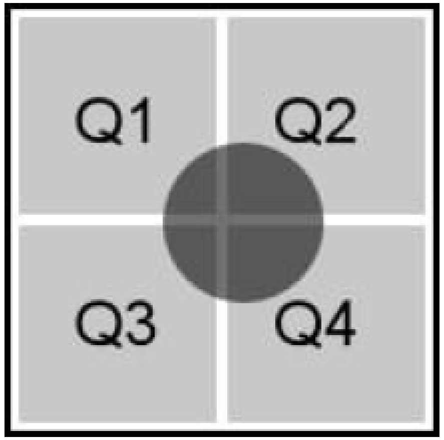

$$S_x = (Q1 + Q3) - (Q2 + Q4)$$

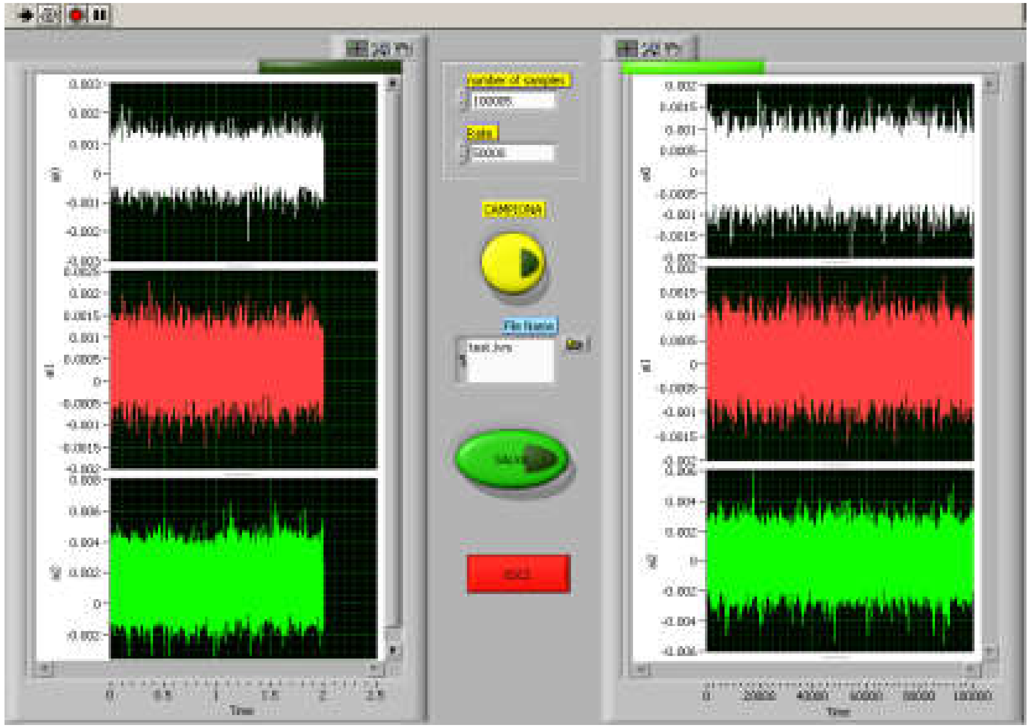

Brownian motion is the key ingredient to calibrate Optical Tweezers.

Brownian Motion for a bead

- Equation of motion of a damped harmonic oscillator subject to a randomly fluctuating force:

$$\cancel{m\frac{\mathrm{d}^2x}{\mathrm{d}t^2}} + \gamma\frac{\mathrm{d}x}{\mathrm{d}t} + \kappa x = \xi(t)$$

Stokes

Trap

- The term ξ(t) describes random (uncorrelated) fluctuations in force with zero mean, i.e.

$$\langle\xi(t)\rangle = 0 \qquad \langle\xi(t+\tau)\xi(t)\rangle = \frac{2k_BT}{\gamma}\delta(\tau)$$

- Equation of motion in the overdamped regime:

$$\gamma\partial_t x(t) = -\kappa x(t) + \xi(t)$$

- Calculate the **autocorrelation** of position fluctuations:

$$C_{xx}(\tau) = \langle x(t)x(t+\tau)\rangle$$

- The solution to which is straightforward:

$$C_{xx}(\tau) = C_{xx}(\tau = 0)\exp(-\omega\tau)$$

$$\boxed{\omega = \frac{\kappa}{\gamma}}$$

Calibration for a bead

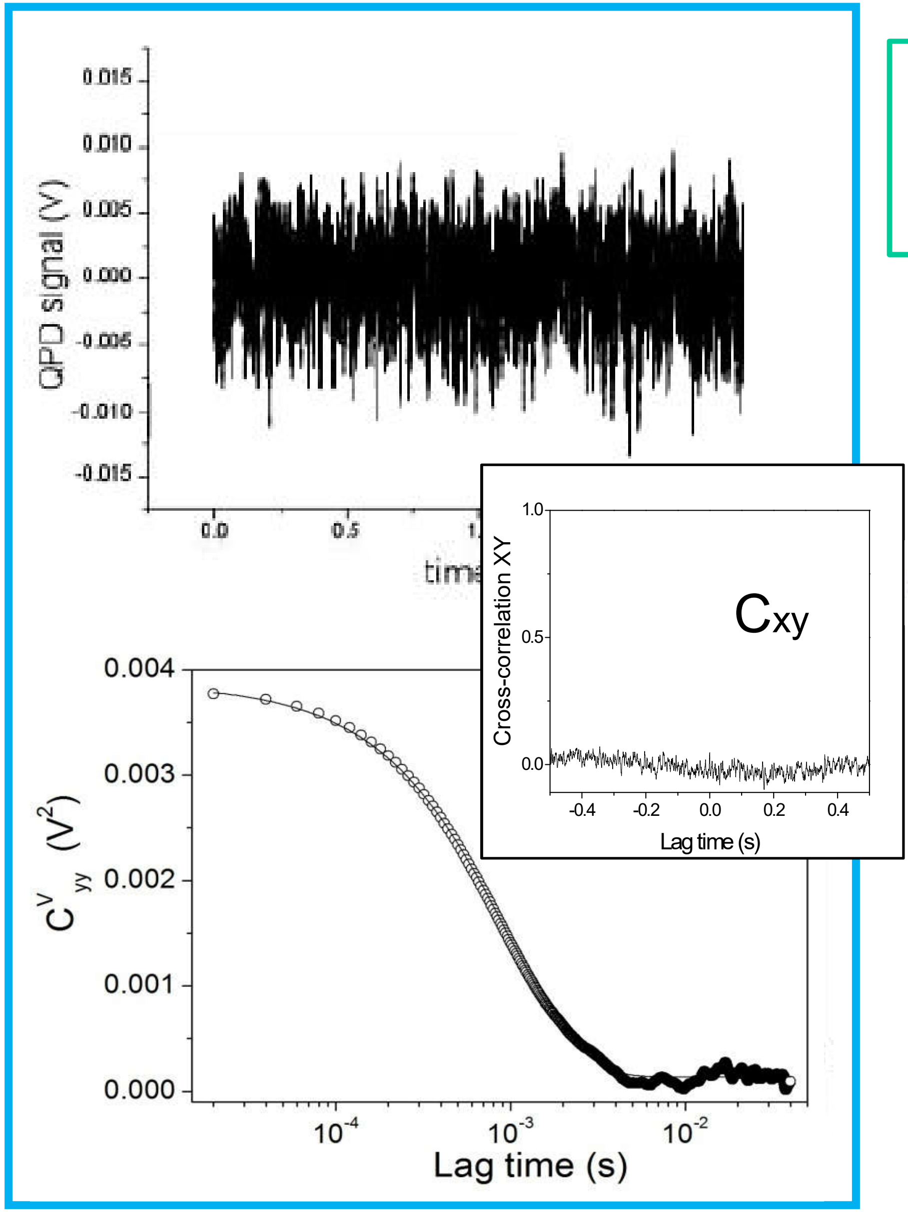

From QPD tracking signals we get Autocorrelation Functions and eventually the Force Constants

$$C_{xx}(\tau) = C_{xx}(0)exp\left(-\frac{\kappa_x}{\gamma}\tau\right)$$

$$C^V_{xx}(\tau) = \langle V_x(t)V_x(t+\tau)\rangle = \beta_x^2 C_{xx}(\tau)$$

$$C^V_{xx}(0) = \beta_x^2 C_{xx}(0) = \beta_x^2 k_B T / k_x$$

Calibration factor

$$\beta_x = \sqrt{\frac{C^V_{xx}(0)\kappa_x}{k_B T}}$$

Different Analysis for the same data

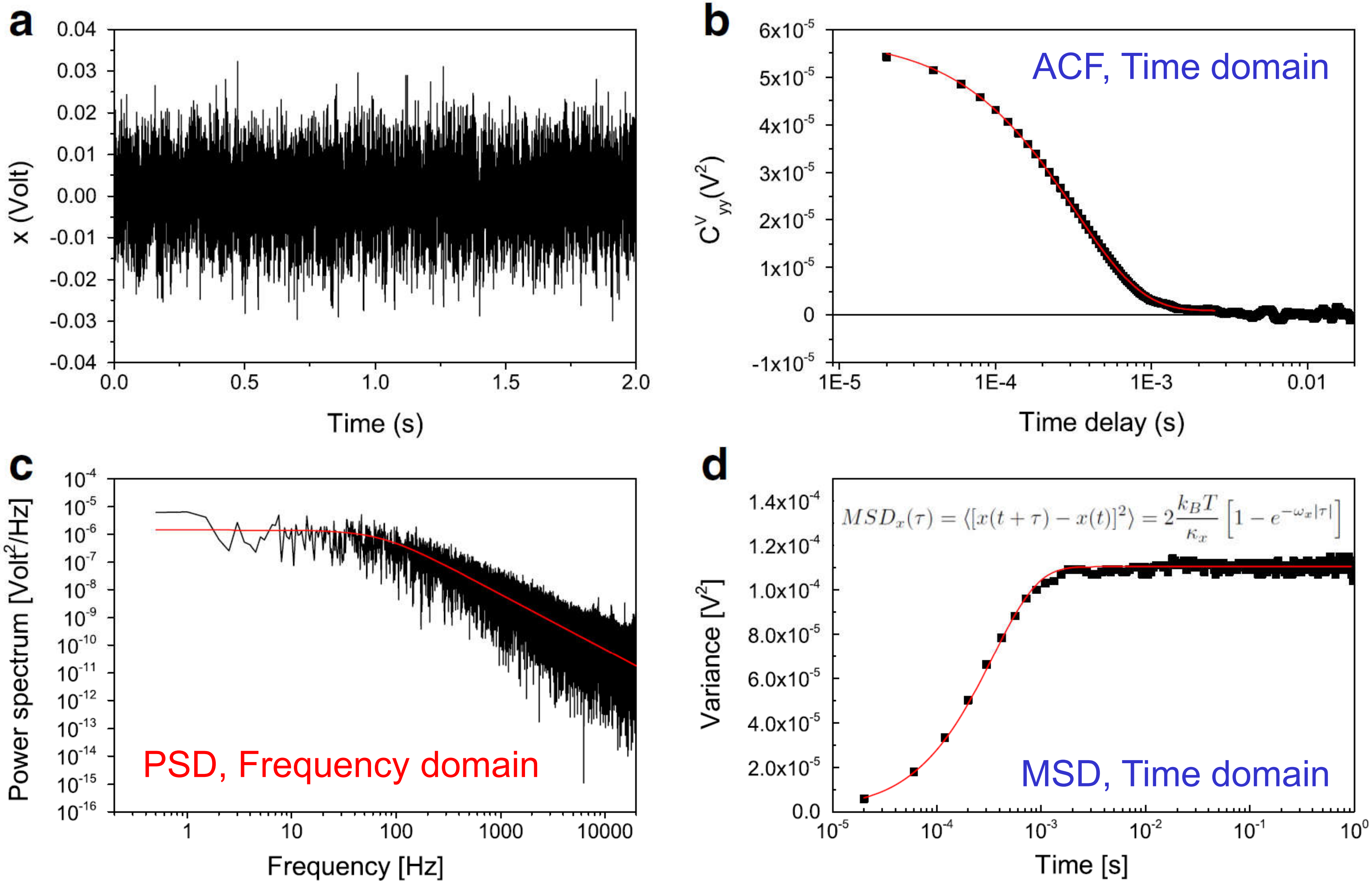

Magazzù et al., *Rendiconti Lincei* **26**S2, 203-218 (2015)

But different methods yield different information on the particle dynamics

Optical trap potential analysis

Dynamics → Probability → Potential

$$\frac{d}{dt}x(t) = -\frac{1}{\gamma}\frac{d}{dx}U(x) + \sqrt{2D}W_x(t)$$

$$\rho(x) = \rho_0 \exp\left[-\frac{U(x)}{k_{\mathrm{B}}T}\right]$$

$$U(x) = -k_{\mathrm{B}}T \log\left[\rho(x)\right] + U_0$$

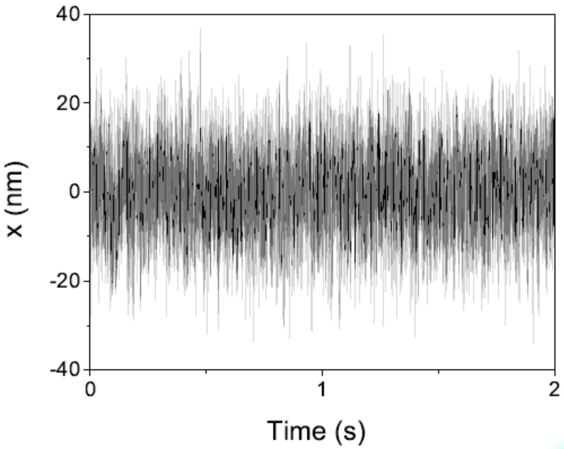

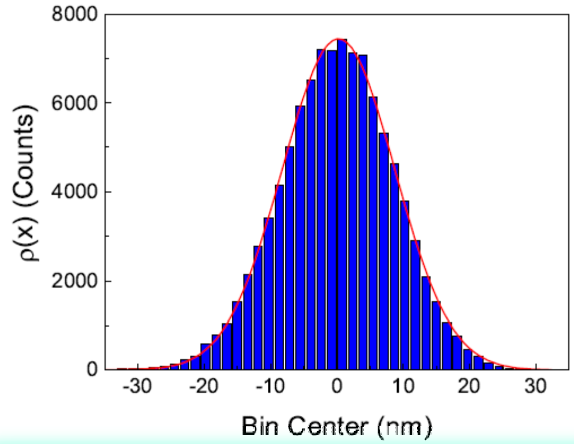

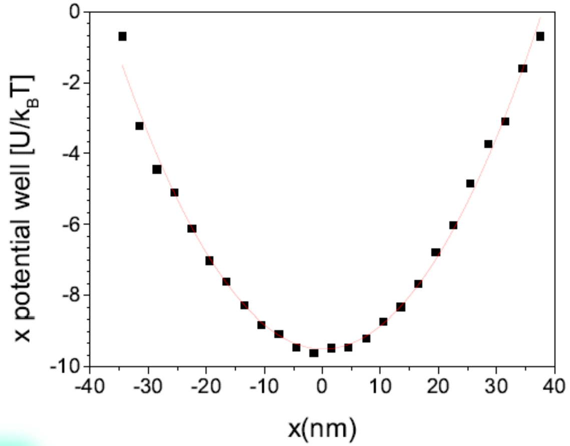

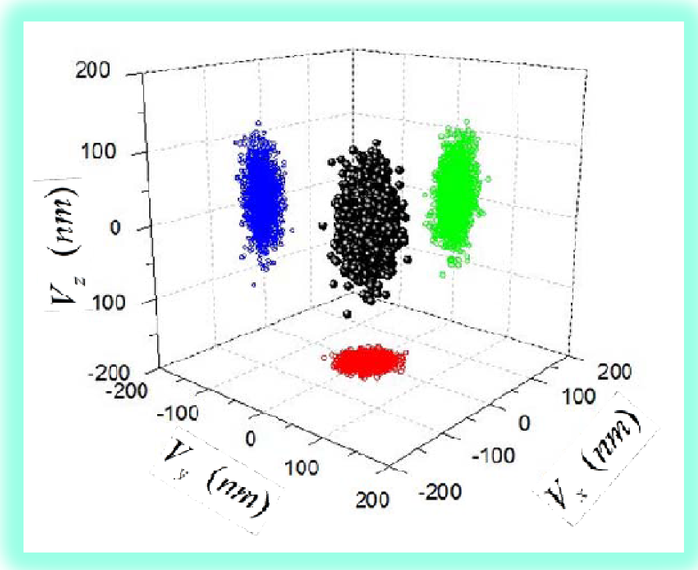

From each signal we can reconstruct the effective trapping potential in 3D

Brownian Motion is more complex

$$\partial_t X_i(t) = -\omega_i X_i(t) + \xi_i(t), \quad i = x, y, z$$
$$\partial_t \Theta_j(t) = -\Omega_j \Theta_j(t) + \xi_j(t), \quad j = x, y$$

From correlation functions we can extrapolate the <u>force</u> and <u>torque</u> constants on the SWNT bundle

$$C_{X_i X_i}(\tau) = \langle X_i(t) X_i(t+\tau) \rangle$$
$$C_{\Theta_j \Theta_j}(\tau) = \langle \Theta_j(t) \Theta_j(t+\tau) \rangle$$

$$\omega_x = \Gamma_\perp k_x,\ \omega_y = \Gamma_\perp k_y,\ \omega_z = \Gamma_{\|} k_z$$
$$\Omega_x = \Gamma_\Theta k_{\Theta_x},\ \Omega_y = \Gamma_\Theta k_{\Theta_y}.$$

Relaxation Frequencies for Translational and Angular Motion

Hydrodynamics of a rod-like nanostructure is embedded in the relaxation frequencies

Surface Plasmon Polaritons and Localized Surface Plasmons

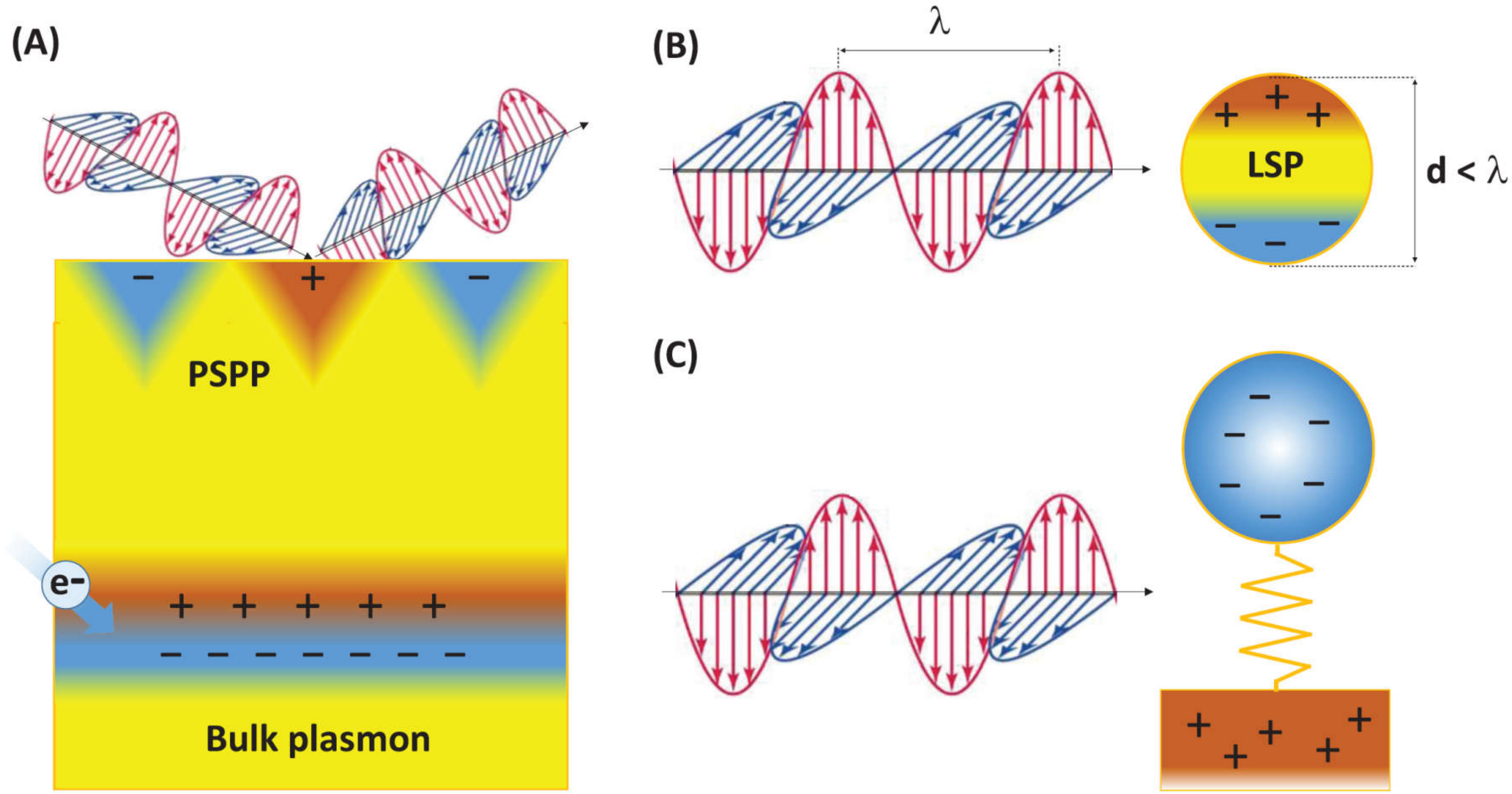

Amendola, V., Pilot, R., Frasconi, M., Maragò, O. M., & Iatì, M. A. (2017). Surface plasmon resonance in gold nanoparticles: a review. *J. Phys.: Cond. Matt.*, *29*(20), 203002.

Plasmonic Mesocapsules

G. Strangi
M. A. Correa-Duarte

Mesocapsule: external porous **Silica** shell **30nm**, internal **AuNPs** with diameters **11nm**. Capsule diameter **1.4 microns**

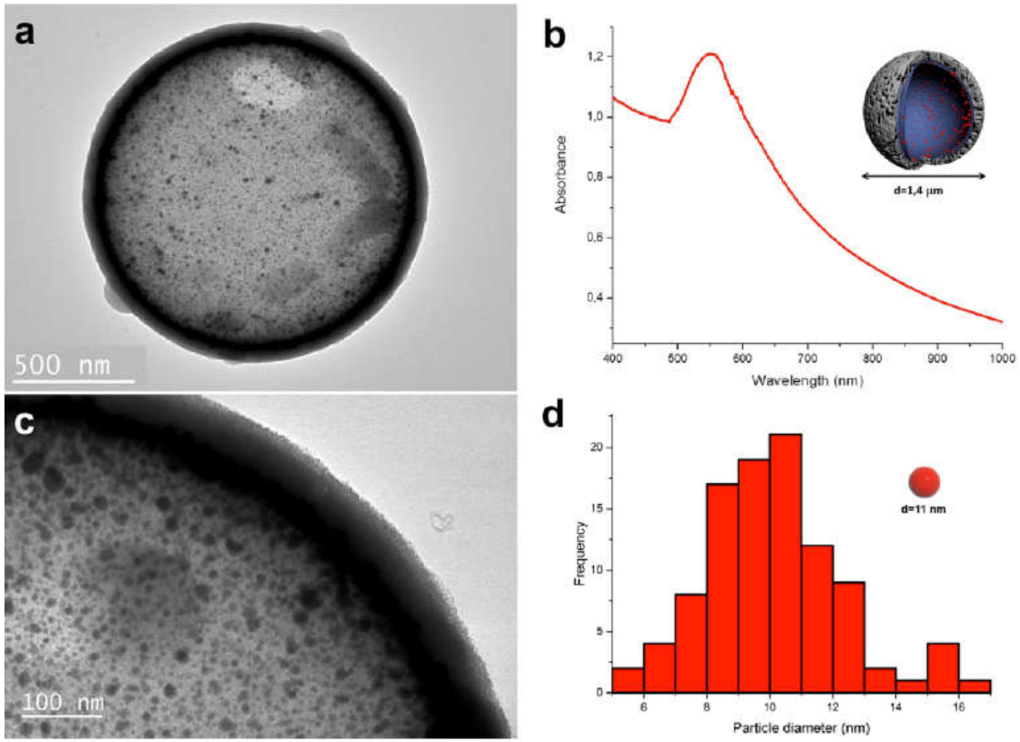

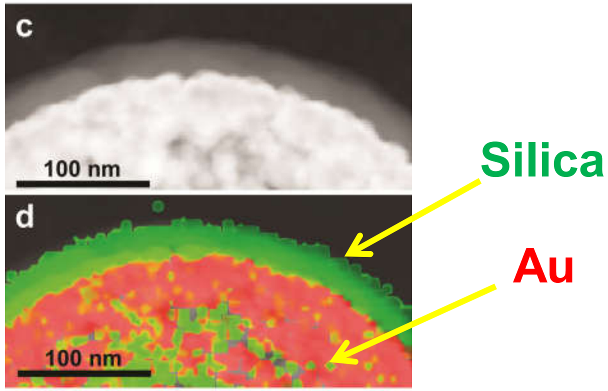

SERS Tweezers
Methylene Blue 10^{-5} M

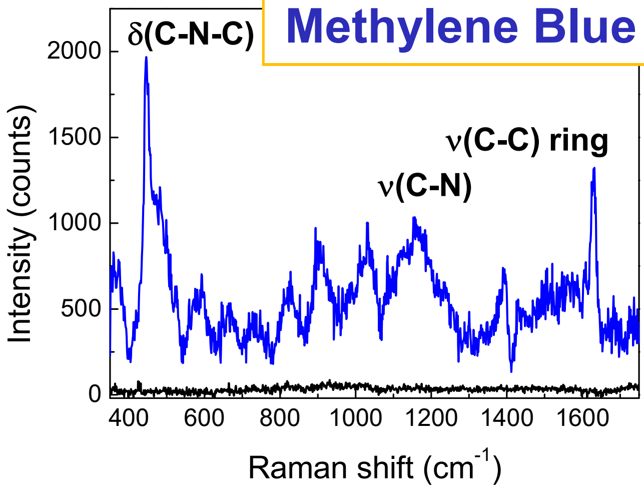

Cargo mesocapsules can be manipulated and activated to release specific molecules in-situ

Spadaro et al. J Phys Chem C (2017)

SERS enhancement due to **AuNPs in the inner walls** of Mesocapsule, that can be reached by MB molecules thanks to the **porosity of the shell**.

Optical Trapping in Dipole Approximation

- Particle size parameter is small, $x = k_m a \ll 1$
- Interaction of electric field of laser with induced dipole in dielectric $\mathbf{p}(\mathbf{r},t) = \alpha_\mathrm{p}\mathbf{E}(\mathbf{r},t)$
- The (harmonic) trapping potential is defined by the incident light intensity

$$\langle \mathbf{F} \rangle_\mathrm{DA} = \underbrace{\frac{1}{2}\frac{n_\mathrm{m}}{c\varepsilon_\mathrm{m}}\Re\{\alpha_\mathrm{p}\}\nabla I(\mathbf{r})}_{\text{Gradient force}} + \cancel{\underbrace{\frac{n_\mathrm{m}}{c}\sigma \cdots (\mathbf{r})}_{\text{Scattering force}}}$$

$$U_\mathrm{dip} = -\underline{p}\cdot\underline{E}$$

$$\underline{F}_\mathrm{grad} \propto \underline{\nabla} I(\underline{r}) = -\kappa_i x_i$$

J. R. Arias-González and M. Nieto-Vesperinas, *JOSA A* (2003)

Counter-propagating Gaussian beam

$$\kappa_\rho^\mathrm{c.p.} = 8\frac{\Re\{\alpha_\mathrm{p}\}}{cn_\mathrm{m}}\frac{I_0}{w_0^2}.$$

$$z_0 = \frac{k_\mathrm{m} w_0^2}{2} \qquad w_0 = 0.5\,\lambda_0/NA$$

$$\kappa_z^\mathrm{c.p.} = 4\frac{\Re\{\alpha_\mathrm{p}\}}{cn_\mathrm{m}}\left(2 - 2k_\mathrm{m}z_0 + k_\mathrm{m}^2 z_0^2\right)\frac{I_0}{z_0^2}.$$

$$I_0 = 2P/\pi w_0^2$$

O. Brzobohatý et. al. *Opt. Exp.* (2015)

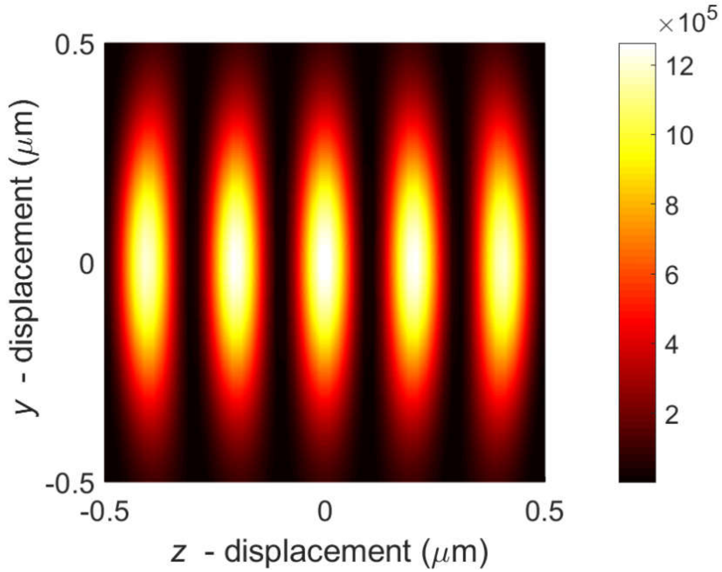

Paolo Polimeno

Resonant gain metal/dielectric nanoshell

Under a pumping threshold, nano-shell shows a stable dipolar field.

$$\bar{\mathbf{p}} = \frac{\alpha_{\mathrm{NUM}}(\varepsilon_1, \varepsilon_2, \varepsilon_3, \rho)}{\alpha_{\mathrm{DEN}}(\varepsilon_1, \varepsilon_2, \varepsilon_3, \rho)} \bar{\mathbf{E}}$$

$$\rho = \frac{a_1}{a_2}$$

a_1 int. radius

a_2 ext. radius

$$\alpha = a_2^3 \frac{(\varepsilon_2 - \varepsilon_3)(\varepsilon_1 + 2\varepsilon_2) + \rho^3(\varepsilon_1 - \varepsilon_2)(\varepsilon_3 + 2\varepsilon_2)}{(\varepsilon_2 + 2\varepsilon_3)(\varepsilon_1 + 2\varepsilon_2) + 2\rho^3(\varepsilon_2 - \varepsilon_3)(\varepsilon_1 - \varepsilon_2)}$$

ε_3 water (solvent) dielectric permittivity

Steady State Gain dielectric permittivity

$$\varepsilon_1 = \varepsilon_b - \frac{G\Delta}{2(\omega - \omega_{21}) + i\Delta} \qquad \Delta = \frac{2}{\tau_2}$$

ε_b dielectric host permittivity

$$G = \Im[\varepsilon_1(\omega_{21})] = -\frac{n\mu^2\tau_2}{3\hbar\varepsilon_0}\tilde{N}$$

Single metallic nanoparticle permittivity (Drude model)

$$\varepsilon_2 = \varepsilon_\infty - \frac{\omega_{pl}^2}{\omega(\omega + 2i\gamma)}$$

In our calculation,

ρ = 0,77 and a_2 = 20 nm

A. Veltri and A. Aradian, *Phy. Rev. B* (2012); A. Veltri et al., *Sci. Rep.* (2016)

The Scattering Problem – Multipole Expansion

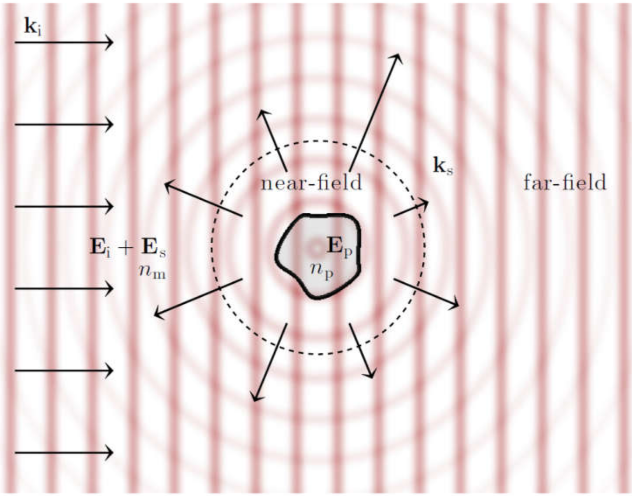

Helmholtz equations

$$(\nabla^2 + n^2 k_v^2)\boldsymbol{E} = 0 \, , \qquad (\nabla^2 + n^2 k_v^2)\boldsymbol{B} = 0$$

Boundary conditions $\quad E_2 = E_i + E_s \quad E_1 = E_p$

$$\hat{\boldsymbol{n}} \times (\boldsymbol{E}_2 - \boldsymbol{E}_1) = 0 \, , \quad \hat{\boldsymbol{n}} \times (\boldsymbol{B}_2 - \boldsymbol{B}_1) = 0$$

Expansion of the incident field

$$\mathbf{E}_i(r, \hat{\mathbf{r}}) = E_i \sum_{l=0}^{\infty} \sum_{m=-l}^{l} W_{i,lm}^{(1)} \mathbf{J}_{lm}^{(1)}(r, \hat{\mathbf{r}}) + W_{i,lm}^{(2)} \mathbf{J}_{lm}^{(2)}(r, \hat{\mathbf{r}})$$

Expansion coefficients

$$\boldsymbol{J}_{lm}^{(1)} = j_l(kr)\boldsymbol{X}_{lm}(\hat{\boldsymbol{r}})$$

Magnetic multipole

$$\boldsymbol{J}_{lm}^{(2)} = \frac{1}{k}\nabla \times \boldsymbol{J}_{lm}^{(1)}$$

Electric multipole

Vector spherical harmonics

$$\boldsymbol{X}_{lm} = [l(l+1)]^{-1/2} \mathrm{L} Y_{lm}$$

F. Borghese, P. Denti, and R. Saija, *Scattering from model non-spherical particles* (Springer, 2007)

The Scattering Problem – Transition Matrix

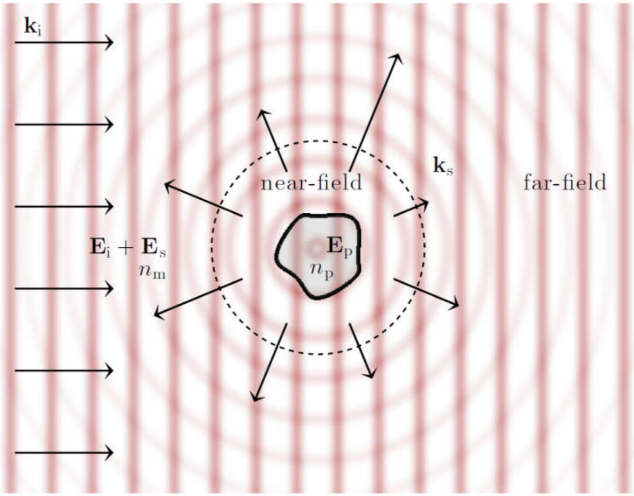

Expansion of the scattered wave

$$\mathbf{E}_s(r,\hat{\mathbf{r}}) = E_i \sum_{l=0}^{\infty} \sum_{m=-l}^{l} A^{(1)}_{s,lm} \mathbf{H}^{(1)}_{lm}(r,\hat{\mathbf{r}}) + A^{(2)}_{s,lm} \mathbf{H}^{(2)}_{lm}(r,\hat{\mathbf{r}})$$

Expansion of the internal field

$$\mathbf{E}_p(r,\hat{\mathbf{r}}) = E_i \sum_{l=0}^{\infty} \sum_{m=-l}^{l} W^{(1)}_{p,lm} \mathbf{J}^{(1)}_{lm}(r,\hat{\mathbf{r}}) + W^{(2)}_{p,lm} \mathbf{J}^{(2)}_{lm}(r,\hat{\mathbf{r}})$$

Boundary conditions

$$\hat{\boldsymbol{n}} \times (\boldsymbol{E}_2 - \boldsymbol{E}_1) = 0$$

$\boldsymbol{E}_2 = \boldsymbol{E}_i + \boldsymbol{E}_s$

$\boldsymbol{E}_1 = \boldsymbol{E}_p$

By imposing the Boundary conditions at the particle surface it is possible to find the relation between the **A** and **W** coefficients

$$A^{(p')}_{s,l'm'} = \sum_{p=1,2} \sum_{l=0}^{\infty} \sum_{m=-l}^{l} T^{(pp')}_{lml'm'} W^{(p)}_{i,lm}$$

$$\mathbf{E}_s = \mathbb{T}\mathbf{E}_i$$

T- Matrix

Borghese et al., J. Math. Phys. (1980); Borghese et al. Aerosol Sci. & Tech. (1984)

ZnO nanowires in 2-beam traps in air and vacuum

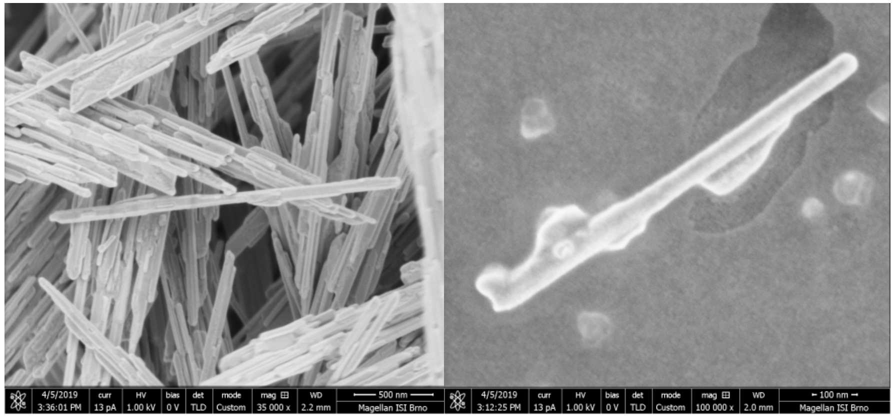

Commercial samples
L=1 micron, d=70 nm

NA=0.5, $w_0 = 2.8\,\mu$m beam waist

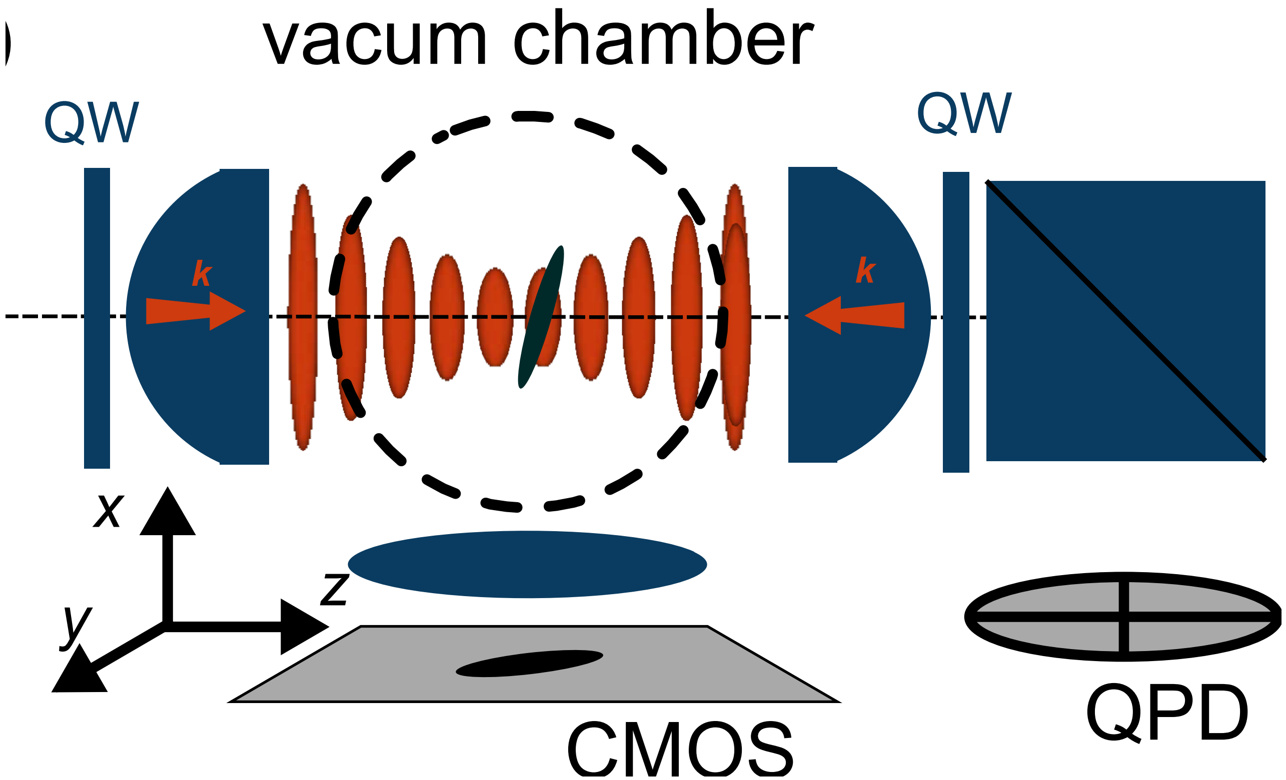

QPD detection of rotational dynamics vs Pressure

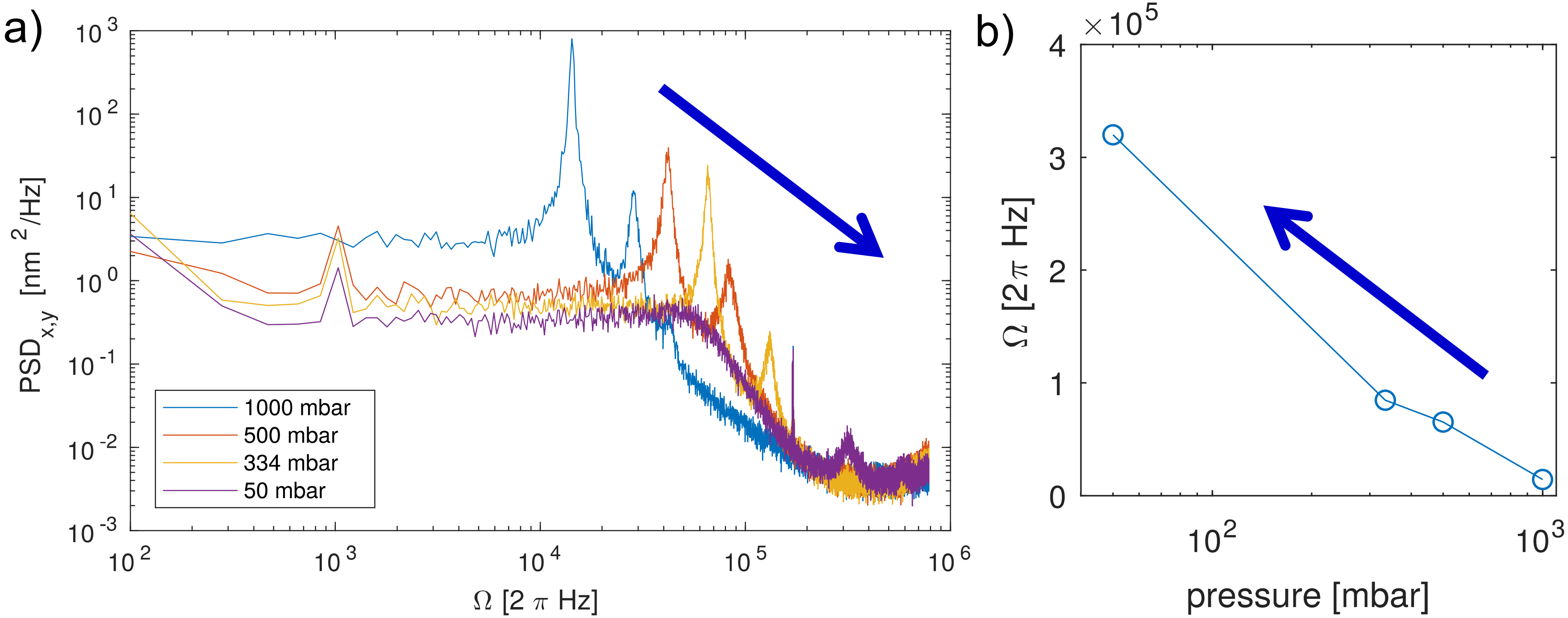

$$\mathrm{PSD}(\Omega) = \frac{k_\mathrm{B}T}{\pi m}\Big[\overbrace{\frac{\Gamma_\mathrm{transl}}{(\Omega_\mathrm{transl}^2-\Omega^2)^2+\Gamma_\mathrm{transl}^2\Omega^2}}^{\text{Translations (background)}} + \sum_i \overbrace{\frac{\Gamma_{\mathrm{rot},i}}{(\Omega_{\mathrm{rot},i}^2-\Omega^2)^2+\Gamma_{\mathrm{rot},i}^2\Omega^2}}^{\text{Rotations}}\Big]$$

Damping decreases with pressure, hence rotational frequency increases

Length controls both transferred torque and damping